1-1-2014

A PDE-based Method for Optimizing Solar Cell Performance

Xiaoxian Liu
University of Pennsylvania, liuxiaox@sas.upenn.edu

A PDE-based Method for Optimizing Solar Cell Performance

Abstract
In this paper, we address the optimal design problem for organic solar cells (OSC). In particular, our focus is to enhance short-curcuit photocurrent by optimizing the donor-acceptor interface. To that end, we propose two drift-diffusion models for organic solar cells, both of which account for the physics of OSC's that charge carriers are mostly generated in the region near the donor-acceptor interface. For the first drift-diffusion model, the generation of charge carriers is translated into a boundary condition across the donor-acceptor interface. We apply the theory of shape optimization to compute the shape gradient functional of the photocurrent. In particular, shape differential calculus is extensively applied in the computation. For the second drfit-diffusion model, we parameterize the donor-acceptor interface as a leve set of a function, i.e. the "phase field function". The dependence of the second drift-diffusion model on the geometry is therefore transformed into its dependence on the phase field function. Such transformation greatly simplifies the sensitivity analysis and leads to an easy-to-implement numerical optimization algorithm. In numerical examples, it is shown that the maximum output power of the optimized solar cell can be increased by a factor of 3. Our analysis and examples in this paper are in two dimensions, but the generelization of both the analysis and numerical optimization to three dimensions is straightforward.

Degree Type
Dissertation

Degree Name
Doctor of Philosophy (PhD)

Graduate Group
Applied Mathematics

A PDE-BASED METHOD FOR OPTIMIZING SOLAR CELL PERFORMANCE

Xiaoxian Liu

A DISSERTATION

in

Applied Mathematics and Computational Sciences

Presented to the Faculties of the University of Pennsylvania in Partial Fulfillment of the Requirements for the Degree of Doctor of Philosophy

2014

Charles L. Epstein, Thomas A. Scott Professor of Mathematics
Supervisor of Dissertation

Charles L. Epstein, Thomas A. Scott Professor of Mathematics
Graduate Group Chairperson

Dissertation Committee:
Cherie R. Kagan, Professor of Material Science and Engineering
Eugene J. Melé, Professor of Physics and Astronomy
Philip T. Gressman, Professor of Mathematics

Acknowledgments

First of all, my special thanks go to my adviser, Dr. Epstein, for his encouragement and patience ever since my first day at Penn. The discussions we had have been absolutely indispensable for my research. This work would not have been possible without his guidance and help along the way.

I thank Dr. Kagan and Dr. Melé for the hours of discussion they spent with me. It has greatly deepened my understanding of semiconductor devices and has made my research experience so much more enjoyable. I also thank everyone in Dr. Kagan's group, especially Dr. Aaron Fafarman, for all the helpful discussions, even on the topics that are completely trivial to them.

I thank Dr. Andreas Klöckner, whom I met when I was a visiting student at the Courant Institute of New York University. Without his help, it would have been so much more difficult to build efficient numerical solvers.

I would like to extend my thanks to all of my fellow AMCS students and other people I have met at Penn. You all have made my life at Penn as vivid as it has been.

I would like to thank my families. They are the dearest people to me. My parents, who are my biggest supporters, help me through many difficulties. I wish I could always make them proud. And to my lovely wife, I just want to say that meeting you is the best thing that has happened to me in the past 5 years.

Finally, I thank the NSF grants DMS-0935165 and DMS-1205851 for supporting my Ph.D. study.

ABSTRACT

A PDE-BASED METHOD FOR OPTIMIZING SOLAR CELL PERFORMANCE

Xiaoxian Liu

Charles L. Epstein

In this paper, we address the optimal design problem for organic solar cells (OSC). In particular, our focus is to enhance short-curcuit photocurrent by optimizing the donor-acceptor interface. To that end, we propose two drift-diffusion models for organic solar cells, both of which account for the physics of OSC's that charge carriers are mostly generated in the region near the donor-acceptor interface. For the first drift-diffusion model, the generation of charge carriers is translated into a boundary condition across the donor-acceptor interface. We apply the theory of shape optimization to compute the shape gradient functional of the photocurrent. In particular, shape differential calculus is extensively applied in the computation. For the second drfit-diffusion model, we parameterize the donor-acceptor interface as a leve set of a function, i.e. the "phase field function". The dependence of the second drift-diffusion model on the geometry is therefore transformed into its dependence on the phase field function. Such transformation greatly simplifies the sensitivity analysis and leads to an easy-to-implement numerical optimization algorithm. In numerical examples, it is shown that the maximum output power of the optimized solar cell can be increased by a factor of 3. Our analysis and examples in this paper

are in two dimensions, but the generelization of both the analysis and numerical optimization to three dimensions is straightforward.

Contents

Chapter 1

Introduction

Organic solar cells (a.k.a.OSCs) have emerged as a promising candidate for future solar cells, mostly due to its low cost to manufacture. However, the efficiency of power conversion of current experimentally available OSCs is barely above 10%, much lower than that of inorganic solar cells [28]. It is therefore important to improve the efficiency of OSCs, which is what we are trying to address in this work.

1.1 Physics of Organic Solar Cells

A typical OSC is comprised of two different organic materials, known as the "donor"(D) and "acceptor"(A). Both donor and acceptor are characterized by their electronic structures, in particular the highest occupied molecular orbital (a.k.a. "HOMO") and the lowest unoccupied molecular orbital (a.k.a. "LUMO"). They are the analog of valence band and conduction band in crystalline inorganic semiconductors such

as silicon.

When light is absorbed by organic polymers, an electron in the HOMO state is excited to reach the LUMO state, and at the same time a hole (regarded as positively charged particle) is created in the HOMO state. Due to the strong Coulomb attraction between the electron and the hole, they are closely bound together. Such bound pairs of electrons and holes are treated as a charge neutral particles called "excitons". This is in contrast to the case of inorganic semiconductors, where the Coulomb potential between electrons and holes is so weak that electrons and holes are effectively treated as free particles after photo excitation.

Excitons are essentially an excited electronic state and they have, on average, finite life time. Before their decay, excitons move inside either donor or acceptor by diffusion. Excitons can also dissociate into free electrons and holes. The key feature of the exciton dissociation is that it mainly takes place near the donor-acceptor interface. Hence, it is not surprising that the performance of OSC's is greatly influenced by its morphology, i.e. the spatial distribution of donor material and acceptor material. Once excitons arrive at the DA interface, due to the difference in the energy levels of LUMO and HOMO, electrons and holes tend to stay in their energetically favorable states, which leaves the electron in the acceptor and the hole in the donor. The diagram in Figure 1.1 demonstrates such a process.

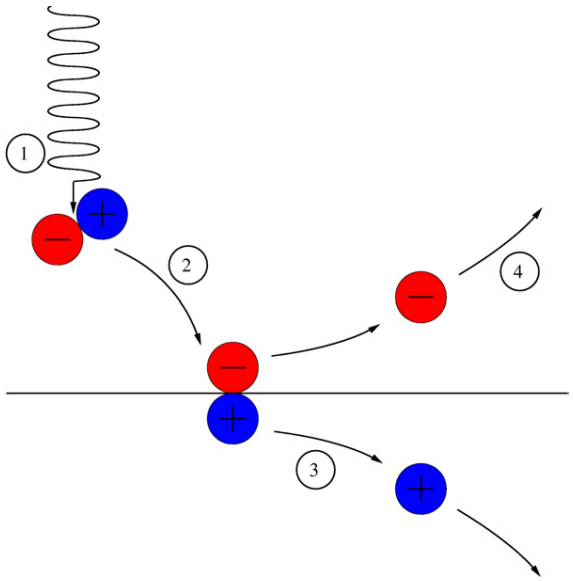

Figure 1.1: Exciton dissociation and charge transport near donor-acceptor interface. The diagram is extracted from the paper [6].

1.2 Mathematical Modeling of Semiconductor Devices

1.2.1 A hierachy of existing models

There are a family of mathematical models for the transport properties of semiconductors [22, 18]. They can be roughly divided into two categories: microscopic models and macroscopic models. Microscopic dynamics of electrons can be modeled either classically by the Liouville's equation or quantum mechanically by Schrödinger's equation or the density matrix operator. To address the dynamics of a large collection of electrons in semiconductors, one needs to derive the Boltzmann

equation based on those microscopic models. Nonetheless, it is computationally costly to use either microscopic models or the Boltzman equation, however accurate they are, and it leads to the need for macroscopic models. In contrast, the macroscopic models of semiconductors are concerned with macroscopic quantities, such as electrical potential and spatial densities of charge carriers. In terms of computational cost, they are more accessible than Boltzmann equation.

1.2.2 Drift-diffusion model for organic solar cells

The mathematical model that we use in this work is based on the *drift-diffusion equations*, a macroscopic PDE model. Conventional drift-diffusion equations include a Poisson's equation for the electrical potential and reaction-diffusion equations for the density functions of electrons and holes. It has proved successful on modeling semiconductor devices in the past few of decades; in fact, it can be formally derived from the Boltzmann equation under certain assumptions [22]. Questions on the existence and uniqueness of such system are now well understood [21, 22, 17].

For OSC's, one needs to extend the conventional drift-diffusion model by adding a reaction-diffusion equation for excitons. Furthermore, as pointed out in Sec. 1.1, it is essential to include the dependence of reaction rates on the morphology of OSC's. A few drift-diffusion models for OSCs have been proposed in previous works [1, 19, 5, 6, 12, 11, 3]. In particular, [1, 19] proposed one-dimensional drift-diffusion models for bipolar OSCs. Two-dimensional models were proposed in [5, 6, 11, 3];

The influence of morphology of OSC's on its performance is investigated from a computational point of view. Mathematical analysis of drift-diffusion equations in OSCs was first addressed in [12].

1.3 Optimal Morphology

1.3.1 What is optimal morphology?

In the aforementioned works on drift-diffusion models for OSC's, much emphasis has been given to the modeling of physical parameters such as carrier mobilities, dissociation rate of excitons, and recombination rate of electrons and holes. These results laid the groundwork for the drift-diffusion model for OSC's, but the quest for optimal morphology was not resolved.

In [5, 6], an optimal design was postulated. By numerically solving the drift-diffusion equations, it is observed that OSC's with such "optimal" design exhibits better performance than those with planar D-A interface. However, such "optimality" is not defined with mathematical rigor; in fact, it's not clear whether the postulated design can be further optimized. In this work, it is our goal to uncover the optimality condition on morphology. In other words, we would like to improve what intuitions are capable of by mathematical analysis.

1.3.2 Optimal control with drift-diffusion equations

The first work on optimal design with drift-diffusion model is [15]. Unlike the approach of band structure engineering, the authors of this paper view the *dopant density* as a *control function* and introduced the optimal control theory to semiconductor design. The same authors gave a summary of the optimal design with drift-diffusion model in [16]. Furthermore, [27] extended the optimal control framework to quantum drift-diffusion model.

Our analysis and computation in this work is similar to [15] in that it is also an application of the optimal control theory on the drift-diffusion model. However, the specific optimization problem is quite different from that in [15]. On the one hand, the drift-diffusion model of organic semiconductors is very different from its counterpart for conventional semiconductors. On the other hand, the control function is not explicitly present in the model: since the goal is to identify the optimal geomtry of the donor-acceptor interface, our control must be the geometry itself or a representation of the geometry. Therefore, our primary goal is to formulate the drift-diffusion model in such a way that its dependence on the geometry is "easily" tractable.

We also note that, the idea of geometric optimization may also be applicable to conventional semiconductors. In fact, we can transform the work of [15] to a geometric optimization problem if we require the dopant density to have the

following form

$$C = C_p \mathbf{1}_p + C_n \mathbf{1}_n \tag{1.3.1}$$

where $C_{p,n}$ are the constants of dopant densities and $\mathbf{1}_{p,n}$ are the indicator functions of the p-side and n-side of a PN junction, respectively. Unlike [15], the interest here is the optimal indicator function $\mathbf{1}_p$ and $\mathbf{1}_n$, i.e. the optimal layout of materials for a PN junction. Even though the generation of electrons and holes are not strongly associated with the interface of a PN junction, we expect the dependence of solutions on the layout of C through the drift-diffusion model.

1.4 Two Drift-Diffusion Models for the Optimal Design of Organic Solar Cells

1.4.1 The first drift-diffusion model: sharp donor-acceptor interface and shape optimization

As pointed out in Section 1.1, most of the free charge carriers are generated in a very narrow neighborhood of the donor-acceptor interface. The width of such region is only a few percent of the dimension of the whole solar cell. When it comes to mathematical modeling, it makes sense to take the limit of zero-width for the interfacial region which leads to our first drift-diffusion model where all the reactions between excitons, electrons, and holes are assumed to take place strictly

on the interface. By taking this limit, one can focus on the geometry of the interface and analyze its influence on the performance of the solar cell.

Once such limit is taken, the optimal design problem falls into the regime of shape optimization, which is prevalent in such fields as structural optimization in mechanical engineering. We introduce the theory of shape differential calculus and then apply it to the shape optimization problem of our first drift-diffusion model. As is shown later, although shape optimization is conceptually easy, the analysis of shape optimization is in general harder than ordinary optimization problems. Statement of the first drift-diffusion model and the shape optimization analysis of it can be found in Chapter 3 -5.

1.4.2 The second drift-diffusion model: phase field method

A few difficulties arise in the shape optimization approach above. First of all, the formulations of the adjoint equations and the shape gradient functional are very complicated and appear to be difficult for both analytical and computational purposes. Also, optimal shapes are in general expected to be very complex. Explicit parametrization of D-A interface leads to several difficulties in computation. For instance, it is difficult to handle topological change via explicit parametrization of shape boundary. Furthermore, one needs to resolve the issue of remeshing for each updated shape.

These difficulties can be easily resolved by the level set method, where the

interface is assumed to be the level set of some function defined on the whole domain. Such a viewpoint leads us to the second drift-diffusion model. To be specific, we first introduce a level set function called the "phase field function" ϕ. Given any phase field function ϕ, we can write down the drift-diffusion equations whose dependence on the geometry is expressed by the dependence of all the modeling parameters on ϕ. For example, if we have a Poisson equation with a diffusivity coefficient D,

$$-\nabla \cdot (D\nabla y) = f$$

its formulation, based on level set function, is

$$-\nabla \cdot (D(\phi)\nabla y) = f(\phi)$$

Such an approach provides certain convenience for our purpose. On the one hand, the adjoint equations and the gradient functional for this phase field model are much simpler, compared with the adjoint equations and shape gradient in the approach of shape optimization. On the other hand, the numerical implementation of the phase-field method is much easier: instead of updating the geometry for each step and remeshing the whole domain, we can solve the equations on a **fixed** rectangular grid without the overhead of remeshing, and the evolution of shape is handled by updating the phase field function.

1.5 Summary of Later Chapters

In Chapter 2, we start by introducing the theory of optimal control with PDE constraints, which is the standard method of solving optimization problems for PDE's and used in both drift-diffusion models.

From Chapter 3 to Chapter 5, we concentrate on the first drift-diffusion model and the shape optimization problem. For completeness, useful results of shape differential calculus are introduced in Chapter 4. We conclude Chapter 5 by computing the shape gradient functional of photocurrent.

Chapter 6 and 7 are dedicated to the second drift-diffusion model based on the phase field method. In Chapter 6, we introduce the second drift-diffusion model and apply sensitivity analysis to it. In particular, we compute the phase-field gradient functional G and state an optimization algorithm based on the Allen-Cahn equation. In Chapter 7, we provide details of the numerical methods for solving each partial differential equation of the optimization algorithm, and conclude the chapter with examples of optimal design using the phase-field method.

Chapter 2

Optimal Control with PDE Constraints

Before entering the details of optimal design of organic solar cells, let us briefly review the mathematics of optimal control of partial differential equations, which is applied repeatedly in later chapters. The purpose is to present a high-level introduction to optimal control so that later chapters are more accessible to the readers. Therefore, we focus on the formulation of optimal control in a PDE setting and its sensitivity analysis; we do not worry about the mathematical topics such as the existence and even uniqueness of optimal solution, albeit their importance is evident. Many references are available on the theory of optimal control of PDE's, for example [20, 26].

2.1 Statement of an Optimal Control Problem of Partial Differnetial Equations

To define an optimal control problem, we need to introduce the basic concepts of functional analysis. Let V and U be two Banach spaces. We keep the convention that V is the space of *state functions* or *state variables* and U is the space of *control functions* or *control variables*; both concepts are made clear later.

A bounded linear functional $l : V \mapsto \mathbb{R}$ is a linear function that maps all elements in V to the set of real numbers. The vector space of bounded linear functionals on a Banach space is called its dual space. The dual spaces of V and U are denoted as V^* and U^*, respectively. We assume both V and U are *reflexive*, meaning $(V^*)^* = V$ and $(U^*)^* = U$. The action of a functional $l \in V^*$ on a function $y \in V$ is often written as

$$l(y) =< l, y >_{(V^*,V)} \in \mathbb{R} \tag{2.1.1}$$

It looks very much like an inner product on a Hilbert spaces. In fact, if V is a Hilbert space, that is, a Banach space with an inner product structure, V^* can be identified with V, and (2.1.1) is indeed an inner product.

Let $y \in V$ be our *state variable* and $u \in U_{ad} \subset U$ be our *control variable*. U_{ad} is a closed subset of U, and is called the *admissible* subset of U; we are only interested in the control functions in U_{ad}. The relationship between y and u is determined by the so-called *state equation*, which may consist of more than one PDE. On an

abstract level, we can formally write this PDE model as

$$A(y) = B(u) \tag{2.1.2}$$

where $A : V \mapsto V^*$ and $B : U_{ad} \mapsto V^*$ are two operators that map y and u to the same element in V^*. Note that $A(y) = B(u)$ does not have to be linear PDE's; both A and B can possibly depend on y and u, and in such case we have a nonlinear PDE model. We always assume the equation $A(y) = B(u)$ is well defined for $\forall u \in U_{ad}$. Alternatively, we can define a solution operator $S : U \mapsto V$ such that $y = S(u)$ is the solution to $A(y) = B(u)$.

An analogy in linear algebra may help to understand the dry statements so far. Concretely, one can think of V as a finite-dimensional Eucledian space $\mathbb{R}^n$: V is the space of column vectors, and V^* is the space of row vectors (dual of column vectors). The pairing between V and V^* is simply the dot product of Eucledian space. The same analogy holds for U. Our state variable y and control variable u are column vectors living in V and U, respectively. The operators A and B are represented as n-by-n and n-by-m matrices, respectively. In other words, the finite-dimensional analogue of our PDE model $A(y) = B(u)$ is a system of algebraic equations.

Having defined *state variable* and *control variable* and the function spaces they belong to, we are ready to formulate an optimal control problem with PDE constraints. Let $J : V \times U \mapsto \mathbb{R}$ be a cost functional of our optimal control problem, which is supposed to be minimized by convention. We further assume that J is a

smooth function of y and u. The corresponding optimal control problem with PDE constraints can be formulated as

$$\min_{u \in U_{ad}} J[y(u), u] \tag{2.1.3}$$

$$\text{where} \qquad A(y) = B(u) \tag{2.1.4}$$

2.2 Sensitivity Analysis of Optimal Control Problems

The purpose of sensitivity analysis is to understand how the state function y and the cost functional J are affected by changef to control function u. To this end, we need to introduce the notion of Gâteaux differentiability and Fréchet differentiability in function space. We let $u \in U$ and $y(u) \in V$ be two elements in two Banach spaces.

Definition 2.2.1 (Directional derivative)**.** The first variation of the state function $y(u)$ in the direction of $u_1 \in U$ is

$$y'(u; u_1) \stackrel{d}{=} \lim_{t \to 0^+} \frac{y(u + tu_1) - y(u)}{t} \tag{2.2.1}$$

if the limit exists in V and $u + tu_1 \in U_{ad}$ for $\forall t \in [0, \epsilon)$ $(\epsilon > 0)$.

Definition 2.2.2 (Gâteaux differentiable)**.** Suppose the directional derivative $y'(u; u_1)$ exists for $\forall u \in U_{ad}, \forall u_1 \in U$. If there exists a continuous linear operator $M_G : U \mapsto V$ such that

$$y'(u; u_1) = M_G\, u_1 \tag{2.2.2}$$

for all admissible $u_1 \in U$, then the map $y(u) : U_{ad} \mapsto V$ is Gâteaux differentiable at u and the linear operator M_G is the Gâteaux derivative of $y(u)$.

Definition 2.2.3 (Fréchet differentiable)**.** $y(u)$ is Fréchet differentiable at u if there exist a continuous linear map $M_F : U \mapsto V$ such that

$$\lim_{\|u_1\|_U \to 0} \frac{\|y(u+u_1) - y(u) - M_F u_1\|_V}{\|u_1\|_U} = 0 \tag{2.2.3}$$

for $\forall u_1 \in U$. The Fréchet derivative of $y(u)$ at u is therefore defined to be the operator M_F.

Remark 2.2.4 (Gâteaux derivative v.s. Frêchet derivative). Fréchet differentiability is a stronger requirement: Gâteaux differentiability only guarantees differentiability in the sense of *linear* purturbation, whereas Fréchet differentiable defines uniform differentiability for all possible ways of taking the limit. If a function is Fréchet differentiable, then it is Gâteaux differentiable and its Fréchet derivative is also its Gâteaux derivative; the reverse is in general false.

Remark 2.2.5 (Notation on derivatives). For our purpose, we shall mostly work with Gâteaux derivative; sometimes it's even sufficient to only look at directional derivatives for all the admissible directions. Therefore we make the following convention

$$\text{Directional derivative:} \qquad y'(u; u_1) \text{ or } y' \tag{2.2.4}$$

$$\text{Gâteaux derivative:} \qquad \frac{\partial y}{\partial u} \tag{2.2.5}$$

Now we are in place to introduce the sensitivity of state equation $A(y) = B(u)$ and the cost functional J. We shall assume $y(u)$ is always Gâteaux differentiable with respect to u and $J(y, u)$ is Gâteaux differentiable with respect to both y and u. Then, formally, we have

- Sensitivity of the state equation $A(y) = B(u)$

  The directional derivative $y'(u; u_1)$ satisfies the following *linear* equation

  $$A_y \; y'(u; u_1) = B_u u_1 \tag{2.2.6}$$

  Here A_y is the formal derivative of A with respect to y, which is a *linear* operator, and we have similar assertion on B_u

- Sensitivity of the cost functional $J[y(u), u]$

  By the chain rule, it is easy to obtain the sensitivity of J with respect to u

  $$J'[y(u), u; u_1] = < \frac{\partial J}{\partial y}, y'(u; u_1) >_{V^*,V} + < \frac{\partial J}{\partial u}, u_1 >_{U^*,U} \tag{2.2.7}$$

  where $\frac{\partial J}{\partial y}$ and $\frac{\partial J}{\partial u}$ are the Gâteaux derivative of J with respect to y and u; they are apparently functionals in V^* and U^*, respectively.

2.3 First-order Optimality Condition

For optimal control problem, one is often interested in the optimality condition for J as a function of u. Thus the sensitivity of J in y, i.e. $\frac{\partial J}{\partial y} \in V^*$ needs to be "translated" to the sensitivity in u. This can be achieved by the method of

adjoint equations, and the most convenient way of deriving the adjoint equations is by forming the Lagrangian functional $\mathcal{L}$.

We first define the *adjoint* of a linear operator. Let $A : V \mapsto U$ be a bounded linear operator. We also let l be a linear functional in U^* and let y be a vector in V. Then we can define the *adjoint operator* $A^* : U^* \mapsto V^*$

$$< l, Ay >_{(U^*,U)} = < A^* l, y >_{(V^*,V)} \tag{2.3.1}$$

Now we let $p \in V$ and then construct the *Lagrangian* functional $\mathcal{L}$ as

$$\mathcal{L}(y, u, p) = J(y, u) - < A(y) - B(u), p >_{(V^*,V)} \tag{2.3.2}$$

The function p is the so-called *Lagrange multiplier* or *adjoint variable*. Note that although $\mathcal{L}$ is in general a nonlinear functional of y and u, it is linear in the adjoint variable p.

Now $\mathcal{L}(y, u, p) : V \times U_{ad} \times V \mapsto \mathbb{R}$ is a smooth function in y,u,and p, and therefore we can consider its sensitivity with respect to the control variable u. Since p does not depend on u, we have

$$\begin{aligned} \mathcal{L}'(y, u, p; u_1) = & < \frac{\partial J}{\partial y}, y'(u; u_1) >_{V^*,V} + < \frac{\partial J}{\partial u}, u_1 >_{U^*,U} \\ & - < A_y y'(u; u_1) - B_u u_1, p >_{V^*,V} \\ = & < \frac{\partial J}{\partial y} - A_y^* p,\ y'(u; u_1) >_{V^*,V} \\ & + < \frac{\partial J}{\partial u} + B_u^*\, p, u_1 >_{U^*,U} \end{aligned} \tag{2.3.3}$$

$\mathcal{L}'$ is apparently linear in $y'(u; u_1)$ and u_1. Furthermore, we have the freedom of choosing the adjoint variable $p \in V$ at our convenience. In particular, if we define

the *adjoint equation* in V^*

$$A_y^* p = \frac{\partial J}{\partial y} \tag{2.3.4}$$

we end up with

$$\begin{aligned}
\mathcal{L}'(y,u,p;u_1) &= < \frac{\partial J}{\partial u} + B_u^*\, p, u_1 >_{U^*,U} \\
&= < \frac{\partial J}{\partial u}, u_1 >_{U^*,U} + < B_u u_1,\ p >_{V^*,V} \\
&= < \frac{\partial J}{\partial u}, u_1 >_{U^*,U} + < A_y\, y'(u;u_1),\ p >_{V^*,V} \\
&= < \frac{\partial J}{\partial u}, u_1 >_{U^*,U} + < A_y^* p,\ y'(u;u_1) >_{V^*,V} \\
&= < \frac{\partial J}{\partial u}, u_1 >_{U^*,U} + < \frac{\partial J}{\partial y},\ y'(u;u_1) >_{V^*,V} \\
&= J'(y,u;u_1)
\end{aligned} \tag{2.3.5}$$

i.e. we have recovered the sensitivity of J and have effectively defined the *gradient functional* of J with respect to u by

$$G(y,u,p) = \frac{\partial J}{\partial u} + B_u^* p \in U^* \tag{2.3.6}$$

which is the main purpose of our sensitivity analysis. Thus we can summarize the first-order optimality condition: if y and u solves the *state equation* $A(y) = B(u)$ and p solves the *adjoint equation* $A_y^* p = \frac{\partial J}{\partial y}$ then the necessary first-order optimality condition at (y,u) is

$$J'(y,u;u_1) =< G(y,u,p), u_1 >_{U^*,U} \ \geq 0 \tag{2.3.7}$$

$$\text{where} \qquad G(y,u,p) = \frac{\partial J}{\partial u} + B_u^* p \tag{2.3.8}$$

for all the admissible $u_1 \in U$.

An important observation is that the method of adjoint equation does not only help us identify the optimality condition, but also helps to compute the *gradient functional* G, which in turn provides analytical tools for numerical methods of solving for some optimal control $\bar{u}$.

Remark 2.3.1 (Formulation of Lagrangian functional). Previously we formulate the Lagrangian functional as in (2.3.2). In fact, for equality constraints (such as PDE's), we can form a Lagrangian differently, i.e.

$$\mathcal{L}(y, u, \eta) = J(y, u) + \langle A(y) - B(u), \eta \rangle \tag{2.3.9}$$

The only difference is that we use "+" instead of the "-" in (2.3.2). This of course leads to a different adjoint equation, but it's easy to see the two adjoint variables have the simple relationship $\eta = -\xi$. One can use either (2.3.2) or (2.3.9) to compute the optimality condition.

2.4 Example: Optimal Control of Poisson Equation

Let Ω be a connected domain in $\mathbb{R}^2$ whose boundary is Lipschitz. We consider the following optimization problem

$$\min_{u \in L^2(\Omega)} J = \int_\Omega \frac{1}{2}(y - y_d)^2 \tag{2.4.1}$$

$$\text{where} \quad -\nabla^2 y = u \quad \Omega \tag{2.4.2}$$

$$y = 0 \quad \partial\Omega$$

where y_d is a known function in $L^2(\Omega)$. The PDE is a simple Poisson's equation with homogeneous Dirichlet boundary condition in $\mathbb{R}^2$. Our goal is to identify the first order optimality condition of J with respect to the control u.

We let both the space of control functions U and the space of state functions V to be the Sobolev space $L^2(\Omega)$. Basic theory of PDE tells us, for a given $u \in L^2(\Omega)$, we have a unique state solution $y \in H_0^1(\Omega) \subset L^2(\Omega)$. We further let $p \in H^1(\Omega) \subset L^2(\Omega)$ be the Lagrange multiplier and write the Laplace equation in its weak form

$$\int_\Omega \nabla y \cdot \nabla p - \int_{\partial\Omega} \frac{\partial y}{\partial \nu} p = \int_\Omega u\, p \tag{2.4.3}$$

We then form the Lagrangian functional as

$$\mathcal{L}(y, u, p) = \int_\Omega \frac{1}{2}(y - y_d)^2 - \int_\Omega \nabla y \cdot \nabla p + \int_{\partial\Omega} \frac{\partial y}{\partial \nu} p + \int_\Omega u\, p \tag{2.4.4}$$

Note that in principle we should obtain the weak form of the PDE first and then

form the Lagrangian functional, because the classical solution to $-\nabla^2 y = u$ does not exist in general when u only has L^2 regularity.

To apply sensitivity analysis to the state equation, we proceed by formally taking directional derivatives on (2.4.3) as well as the Dirichlet boundary condition in the direction of $u_1 \in L^2(\Omega)$. After an integration by parts, we end up with the following boundary value problem

$$-\nabla^2 y' = u_1 \qquad \Omega \tag{2.4.5}$$

$$y' = 0 \qquad \partial\Omega \tag{2.4.6}$$

It's not hard to show that there is a unique solution $y'(u; u_1) \in H_0^1(\Omega) \subset L^2(\Omega)$. One can even make one step further to show that $y(u)$ is in fact Gâteaux differentiable in $V = H_0^1(\Omega)$ with respect to $u \in L^2(\Omega)$.

Next we compute the directional derivative of $\mathcal{L}$. For $\forall u_1 \in U$,

$$\mathcal{L}'(y, u, p; u_1) = \int_\Omega (y - y_d) y'(u; u_1) - \int_\Omega \nabla p \cdot \nabla y'(u; u_1) + \int_{\partial\Omega} \frac{\partial y'(u; u_1)}{\partial \nu} p + \int_\Omega p\, u_1 \tag{2.4.7}$$

By applying integration by parts to the first line of the right hand side we obtained the *adjoint equation* for p

$$-\nabla^2 p = y - y_d \qquad \Omega \tag{2.4.8}$$

$$p = 0 \qquad \partial\Omega \tag{2.4.9}$$

Note that the adjoint equation above shows that p is in fact also a function in $H_0^1(\Omega) \subset L^2(\Omega)$.

Finally, we summarize the sensitivity of J with respect to the control variable u

$$J'(y,u;u_1) =< p, u_1 >_{L^2(\Omega)}= \int_\Omega p\ u_1 \tag{2.4.10}$$

where the gradient functional is simply

$$G = p \in L^2(\Omega) \tag{2.4.11}$$

The necessary optimality condition for an unconstrained problem is simply $G = 0$. Hence for this simple problem, we have

$$p^* = 0 \tag{2.4.12}$$

where p^* is the adjoint function in $H^1(\Omega)$ corresponding to the optimal solution y^*. Since p^* must satisfy the adjoint equation, it is easy to see that the optimal solution is

$$y^* = y_d \tag{2.4.13}$$

in $L^2(\Omega)$, and the minimum value for cost functional J is 0.

2.5 Overture to Optimal Design of Organic Solar Cells

Conceptually, it is not hard to translate the optimal design problem of organic solar cells into the framework of optimal control with PDE constraints. Suppose our cost functional is the short-circuit current J and the system is modeled by the

drift-diffusion equations whose solution is denoted as y, Then we can view the donor-acceptor interface Γ as the "control variable" which affects the value of J through the drift-diffusion equations. But the subtle question here is how to represent the geometry?

In later chapters, we present two views of the geometry of organic solar cells, which leads to two different versions of the drift-diffusion model.

- Drift-diffusion model 1: zero-width donor-acceptor interface (cf. Chapter 3 -5)

  In the first model, we take a *shape optimization* approach and view the donor-acceptor interface as a zero-width boundary between the two materials. By defining proper boundary conditions on Γ, we effectively define the map from Γ to y. To find the optimality condition of Γ, we need to understand the sensitivity of y with respect to Γ. To this end, we need to introduce tools of *shape differential calculus*.

- Drift-diffusion model 2: phase-field method (cf. Chapter 6 - 7)

  The second drift-diffusion model is based on a level-set approach. We introduce the *phase field function* ϕ as a level set function and the level set defined by $\phi = 0.5$ is assumed to be the donor-acceptor interface Γ; in other words, we replace Γ by ϕ as the *control*. As a result, all the parameters and coefficients of the drift-diffusion model depend on ϕ, and thus we have made the dependence of drift-diffusion equations on the domain explicit in the PDE's. It turns out

that the numerical implementation of this approach is rather straightforward as we show in Chapter 7.

Chapter 3

First Drift-Diffusion Model: zero-width interface

In this section, we introduce the drift-diffusion equations that are used to model organic solar cells. A few papers have been published on drift-diffusion model in organic solar cells. For example, see [1, 6, 11]. In these works, specific models for carrier mobilities and the dissociation rates of excitons have been discussed. Although the modeling of such physical parameters is of fundamental importance, the focus of this paper is to understand the influence of shape on the carrier transport properties. Thus we only make some general and reasonable assumptions on these physical parameters.

In what follows, we introduce the geometry of the device first. And then we explicitly state our drift-diffusion model for organic solar cells, including physical

assumptions and mathematical formulations.

3.1 Geometry of organic solar cells: zero-width interface

Organic solar cells are made up of two materials, known as the *donor* and the *acceptor*. We use "1" to indicate the donor phase and "2" to indicate the acceptor phase. A two-dimensional example is given in 3.1

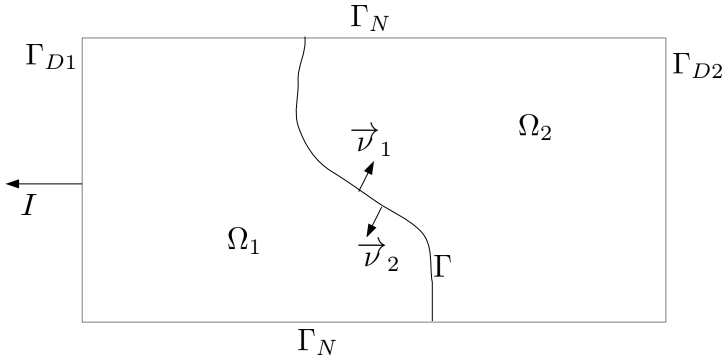

Figure 3.1: Two dimensional structure of an organic solar cell

- **domain**

  Let $\Omega \in \mathbb{R}^d$, $d = 2, 3$ be a rectangular open region. Let $\Omega_1 \subset \Omega$ and $\Omega_2 \subset \Omega$ be two smooth open subregions such that $\overline{\Omega} = \overline{\Omega}_1 \cup \overline{\Omega}_2$ and $\Omega_1 \cap \Omega_2 = \emptyset$.

- **exterior boundaries**

  Let $\partial\Omega_1$ and $\partial\Omega_2$ be the boundary of Ω_1 and Ω_2, respectively. In addition, we require a side of Ω is part of $\partial\Omega_1$, denoted as Γ_{D1} and another disconnected side is part of $\partial\Omega_2$, denoted as Γ_{D2}. From a physical perspective, Γ_{D1} and Γ_{D2} are two contacts connected to different electrodes; apparently they must be disconnected, because otherwise the two contacts are short-circuited. We also define $\Gamma_N = \partial\Omega \backslash (\Gamma_{D1} \cup \Gamma_{D2})$. It represents the parts of the boundary where a zero flux boundary condition or a periodic boundary condition is defined.

- **interface**

  We define the interface as $\Gamma = \partial\Omega_1 \cap \partial\Omega_2$. Γ is supposed to be smooth, but it does not have to be connected.

We use ν to denote outward normal vector for the whole domain. On the interface Γ, we use $\nu_{\mathbf{1,2}}$ for the outward normal vector for $\Omega_{1,2}$, respectively.

3.2 Drift-diffusion equations

For solar cells, we're interested in the stationary case where the photo current and voltage do not change in time. Hence we focus on the stationary drift-diffusion

equations, where we solve for the following unknowns:

ψ	Electric potential
n	Electron density
p	Hole density
u	Exciton density

We first describe the basic assumptions of the model and then state the boundary value problem explicitly.

3.2.1 Assumptions

- **Reactions**

  Symbolically, we use (e^-, h^+) for excitons and e^- and h^+ for electrons and holes. We assume there are only 3 reactions that need to be addressed in the model.

  1. All the incoming photons (light) are converted to excitons (e^-, h^+) with rate Q. Here Q is a function of spatial variables, but it does not depend on the design of OSCs.

  2. There is a bi-directional reaction between excitons and free carriers: excitons may dissociate into free electrons and holes, and electrons and holes can also recombine to form excitons. We use f for the net production rate of free carriers, i.e. f is the rate of exciton dissociation *minus* the rate of carrier recombination.

3. Excitons have a chance to decay into other forms of energy, which do not lead to the formation of charge carriers any more. We assume its rate takes the intuitive form $d_u u$, where $\tau_u = 1/d_u$ has the physical meaning of average lifetime of excitons.

All three reactions are summarized in the table below.

Type of Reaction	Reaction Rate
light $\longrightarrow (e^-, h^+)$	Q
$(e^-, h^+) \rightleftharpoons e^- + h^+$	f
$(e^-, h^+) \longrightarrow$ thermal energy + ...	$d_u u$

Remark 3.2.1. *Omission of "triplet excitons"*

In principle, there are two types of excitons that need to be considered: the "singlets" (spin 0) and the "triplets" (spin 1). In the previous models such as [6, 11], it was pointed out that carrier recombination can lead to the formation of both "singlets" and "triplets", and yet it is the "singlets" that are of interest. Therefore, in these models we have

$$\text{Net conversion of singlet excitons:} \qquad ku - \alpha\gamma np$$

$$\text{Net production of charge carriers:} \qquad ku - \gamma np$$

where k is the dissociation coefficient of excitons, γ is the recombination coefficient of charge carriers, and α is the fraction of singlets produced by carrier recombination; α is typically set to be $1/4$ to reflect the spin statistics.

In this work, we do not differentiate between the "singlets" and "triplets" for simplicity, i.e. we use f for both the net conversion rate of excitons to carriers and the net production rate of carriers; cf. Section 3.2.2. The presence of "triplets" can be enforced by a modification of the boundary value problems in Section 3.2.2, but we choose not to do so for simplicity.

- **Zero-width interface**

  The physics of organic solar cells indicates that the reactions among electrons, holes, and excitons mainly take place near the donor-acceptor interface. The width of this "active" region is relatively small compared with the dimension of the device. In this paper, we take the limit of this width going to 0. In other words, all reactions are assumed to take place strictly on the interface. In mathematical terms, this is simply translated to a boundary condition on the interface as shown in Section 3.2.2. Such an assumption was also made in [11], where it is referred to as a "coarse-grained" model.

3.2.2 Boundary value problems of organic solar cells

The drift-diffusion equations stated below have been nondimensionalized as in [21] and [22]. As mentioned in Section 3.1, we use subscripts "1" for quantities associated with $\overline{\Omega}_1$ and "2" for quantities associated with $\overline{\Omega}_2$. In particular, if a is defined in both $\overline{\Omega}_1$ and $\overline{\Omega}_2$, a_1 denotes its restriction to $\overline{\Omega}_1$ and a_2 denotes its restriction to $\overline{\Omega}_2$. We apply this convention for subscripts only when there is a possibility of confusion,

e.g. quantities defined on the interface Γ.

- **ψ-equation**

$$-\lambda^2\nabla\cdot(\epsilon\nabla\psi) = p - n \qquad \Omega_1\cup\Omega_2 \tag{3.2.1}$$

$$\psi = \psi_D \qquad \Gamma_{D1}\cup\Gamma_{D2} \tag{3.2.2}$$

$$\frac{\partial\psi}{\partial\nu} = 0 \qquad \Gamma_{N1}\cup\Gamma_{N2} \tag{3.2.3}$$

$$\begin{cases} \psi_1 = \psi_2 \\ \frac{\partial\psi_1}{\partial\nu_1} + \frac{\partial\psi_2}{\partial\nu_2} = 0 \end{cases} \qquad \Gamma \tag{3.2.4}$$

where $\lambda > 0$ is a constant due to nondimensionalization and ϵ is the relative permittivity of the materials.

- **n-equation**

$$\begin{cases} \nabla\cdot\mathbf{F}_n = 0 \\ \mathbf{F}_n = -\mu_n(\nabla n - n\nabla\psi) \end{cases} \qquad \Omega_1\cup\Omega_2 \tag{3.2.5}$$

$$n = n_D \qquad \Gamma_{D1}\cup\Gamma_{D2} \tag{3.2.6}$$

$$\mathbf{F}_n\cdot\nu = 0 \qquad \Gamma_{N1}\cup\Gamma_{N2} \tag{3.2.7}$$

$$\begin{cases} n_1 = n_2 \\ \mathbf{F}_{n1}\cdot\nu_1 + \mathbf{F}_{n2}\cdot\nu_2 = -f \end{cases} \qquad \Gamma \tag{3.2.8}$$

where μ_n is the mobility of electrons. [1]

[1] From here on, any Euclidean vector $\overrightarrow{F}$ (such as a flux quantity) is denoted by a letter in its **bold face**, i.e. **F**

- **p-equation**

$$\begin{cases} \nabla \cdot \mathbf{F}_p = 0 \\ \mathbf{F}_p = -\mu_p(\nabla p + p\nabla\psi) \end{cases} \qquad \Omega_1 \cup \Omega_2 \tag{3.2.9}$$

$$p = p_D \qquad \Gamma_{D1} \cup \Gamma_{D2} \tag{3.2.10}$$

$$\mathbf{F}_p \cdot \nu = 0 \qquad \Gamma_{N1} \cup \Gamma_{N2} \tag{3.2.11}$$

$$\begin{cases} p_1 = p_2 \\ \mathbf{F}_{p1} \cdot \nu_1 + \mathbf{F}_{p2} \cdot \nu_2 = -f \end{cases} \qquad \Gamma \tag{3.2.12}$$

where μ_p is the mobility of holes.

- **u-equation**

$$\begin{cases} \nabla \cdot \mathbf{F}_u = Q - d_u u \\ \mathbf{F}_u = -\mu_u \nabla u \end{cases} \qquad \Omega_1 \cup \Omega_2 \tag{3.2.13}$$

$$u = u_D \qquad \Gamma_{D1} \cup \Gamma_{D2} \tag{3.2.14}$$

$$\mathbf{F}_u \cdot \nu = 0 \qquad \Gamma_{N1} \cup \Gamma_{N2} \tag{3.2.15}$$

$$\begin{cases} u_1 = u_2 \\ \mathbf{F}_{u1} \cdot \nu_1 + \mathbf{F}_{u2} \cdot \nu_2 = f \end{cases} \qquad \Gamma \tag{3.2.16}$$

where μ_u is the mobility of excitons.

Remark 3.2.2. Continuity of quantities on Γ

In the boundary value problems above, we assume ψ, n, p, u to be continuous across

the interface Γ. Furthermore, we assume $\nabla\psi$, i.e. the (negative) electric field, to be continuous across Γ.

Remark 3.2.3. It is evident that excitons, electrons and holes are only coupled through the reactions on Γ defined as f.

3.2.3 Modeling of parameters

Given that our interest is in the shape sensitivity analysis of the drift-diffusion model, we do not specify the particular formulations for each parameter except for their dependence on the following quantities:

- spatial variables x
- the unknowns ψ, n, p, u and their gradients
- geometric quantities such as the normal vector ν_1 and the mean curvature H_1 of the interface Γ

Hence, following the discussion in [1], [6], and [11], we make the following assumptions on the parameters in our drift-diffusion model:

Parameter	Dependence
permittivity ϵ	x
electron mobility μ_n	x, $\nabla\psi$
hole mobility μ_p	x, $\nabla\psi$
exciton mobility μ_u	x
photo generation Q	x
exciton decay coefficient d_u	x
exciton conversion rate f	x, $\nabla\psi$, ν_1 and H_1 of interface Γ

The functional dependence on each parameter is assumed to be smooth enough to take derivatives.

Remark 3.2.4. Observations

1. All parameters have an explicit dependence on the spatial variable x. This reflects the fact that the material properties of donor and acceptor are in general different.

2. The carrier mobilities $\mu_{n,p}$ also depend on the electric field $-\nabla\psi$, which reflects the nonlinear dependence of current density on electric field (e.g. saturation of carrier velocities).

3. The reaction rate f is assumed to have complex dependence on other quantities. The models in [1, 6, 11] are all included by our assumption on f,

but the assumption we make on f is more general in the sense that we have also included its dependence on geometric properties of Γ such as the mean curvature.

Chapter 4

Shape Differential Calculus

To find the optimality condition for the photo current, we need to understand how the solution to drift-diffusion equations varies with respect to the change of the morphology of solar cells, i.e. the "shape". In this chapter, we give a brief introduction to the *shape differential calculus*, which is the theoretical tool needed to analyze shape dependence of a function or a functional on its domain of definition. Shape differential calculus is itself an active research field, therefore we only introduce the basic concepts and necessary results needed in later chapters [1].

In particular, Section 4.1 and 4.2 contain results for any fixed smooth domain in $\mathbb{R}^d$, whereas Section 4.3, 4.4 and 4.5 deal with results related to domain transformation.

[1] All of the materials in this chapter can be found in the books [24, 7] and the articles [9, 14, 30].

4.1 Tangential Differential Calculus

Let Ω be an open region in $\mathbb{R}^d$ and $\Gamma = \partial\Omega$ be its boundary of class C^2. We also let U represent arbitrary neighborhood of Γ.

We let ν be the unit normal vector field on Γ and $\bar{H} = \frac{1}{d-1}\sum_i H_i$ to be the *mean curvature* of Γ, where H_i's are the *principal curvatures* of Γ. For convenience, we also define

$$H = (d-1)\bar{H} = \sum_i H_i \tag{4.1.1}$$

which is just the mean curvature multiplied by the constant $d-1$. [2]

Definition 4.1.1 (Tangential gradient, [24] Definition 2.53)**.** Let an element $h \in C^2(\Gamma)$ be given and let $\tilde{h}$ be an extension of h, $\tilde{h} \in C^2(U)$ and $\tilde{h}|_\Gamma = h$. Then the tangential gradient of h is

$$\nabla_\Gamma h = \nabla\tilde{h}|_\Gamma - \frac{\partial\tilde{h}}{\partial\nu}\nu \tag{4.1.2}$$

Definition 4.1.2 (Tangential divergence, [24] Definition 2.52)**.** Let $\mathbf{V} \in C^1(\Gamma;\mathbb{R}^d)$ be a given vector field on Γ and $\tilde{\mathbf{V}}$ be its smooth extension to an open neighborhood of Γ, U. Then the tangential divergence of $\mathbf{V}$ is

$$\mathrm{div}_\Gamma\mathbf{V} = (\mathrm{div}\tilde{\mathbf{V}} - \left\langle D\tilde{\mathbf{V}}\cdot\nu, \nu\right\rangle_{\mathbb{R}^d})|_\Gamma \tag{4.1.3}$$

Note if h and $\mathbf{V}$ in the above definitions are defined not only on Γ but also in Ω, their extensions to U are naturally given by themselves. It can be shown that $\nabla_\Gamma h$ and $\mathrm{div}_\Gamma\mathbf{V}$ are independent of the choice of extension (cf. [24], Prop. 2.51).

[2] Therefore we use "mean curvature" for both H and $\bar{H}$ since they only differ by a constant.

We also define the *Laplace-Beltrami operator* Δ_Γ of $h \in C^2(\Gamma)$

$$\Delta_\Gamma h \stackrel{d}{=} \mathrm{div}_\Gamma(\nabla_\Gamma h) \tag{4.1.4}$$

It can be shown that these definitions of tangential differentials can be extended to larger function space such as the Sobolev spaces on Γ, $H^1(\Gamma)$. From Section 2.20-2.22 in [24], we have the *tangential Green's formula*

Proposition 4.1.3. *Let* $\mathbf{V} \in H^1(\Gamma; \mathbb{R}^d)$. *Define the tangential component of* $\mathbf{V}$ *as*

$$\mathbf{V}_\tau = \mathbf{V} - \langle \mathbf{V}, \nu \rangle_{\mathbb{R}^d} \nu \tag{4.1.5}$$

Then the tangential divergence of $\mathbf{V}$ *is given by*

$$div_\Gamma(\mathbf{V}) = div_\Gamma(\mathbf{V}_\tau) + H \langle \mathbf{V}, \nu \rangle_{\mathbb{R}^d} \tag{4.1.6}$$

And we have the "tangential Green's formula"

$$\int_\Gamma \left[f \; div_\Gamma(\mathbf{V}) + \nabla_\Gamma f \cdot \mathbf{V} \right] d\Gamma = \int_\Gamma H f \mathbf{V} \cdot \nu \, d\Gamma \tag{4.1.7}$$

In particular, if $\langle \mathbf{V}, \nu \rangle_{\mathbb{R}^d} = 0$, *then we have the simple results*

$$\int_\Gamma \left[f \; div_\Gamma(\mathbf{V}) + \nabla_\Gamma f \cdot \mathbf{V} \right] d\Gamma = 0 \tag{4.1.8}$$

Remark 4.1.4. Note that the proposition 4.1.3 is valid only when Γ is the boundary of a region Ω. If Γ is only part of the boundary of an open region (like the donor-acceptor interface of an organic solar cell), $\Gamma \Subset \partial\Omega$, there are also integrals on the boundary of Γ in the formula 4.1.7, i.e. $\int_{\partial\Gamma}$. The formula 4.1.7 maintains its validity by assuming $\mathbf{V} = 0$ on $\partial\Gamma$.

4.2 Signed Distance Function

It is useful to define the *signed distance function* for Ω with boundary Γ.

$$b(x) = \begin{cases} \text{dist}(x, \Gamma) & x \in \mathbb{R}^d - \Omega \\ 0 & x \in \Gamma \\ -\text{dist}(x, \Gamma) & x \in \Omega \end{cases} \tag{4.2.1}$$

where $\text{dist}(x, \Gamma) = \inf_{y \in \Gamma} |x - y|$. In other words, Γ is the zero level set of its signed distance function $b(x) = 0$.

Signed distance function $b(x)$ has many good properties (cf. [7] Chapter 5 and 8). Some useful facts about the signed distance function are summarized below:

- If Γ is smooth, then b is smooth in a neighborhood of Γ
- On Γ, $\nabla b|_\Gamma = \nu$
- $|\nabla b(x)|^2 = 1$
- $\Delta b|_\Gamma = H$, i.e. the laplacian of b at $x \in \Gamma$ is its mean curvature at x.

Signed distance function is convenient for certain calculations of geometric properties. An example is a calculation of the normal derivative of mean curvature $\frac{\partial H}{\partial \nu} = \partial_\nu (\Delta b)|_\Gamma$ on Γ in [9], which we include below

Lemma 4.2.1 (Lemma 3.2 in [9])**.** *The normal derivative of the mean curvature of a surface Γ of class C^3 is given by*

$$\partial_\nu H = -\sum_i H_i^2 \tag{4.2.2}$$

where H_i denote the principal curvatures of the surface. For a two-dimensional surface in 3d, this is equal to

$$\partial_\nu H = -(H_1^2 + H_2^2) = -(H^2 - 2H_G) \tag{4.2.3}$$

where $H_G = H_1 H_2$ is the Gauss curvature.

4.3 Speed Method

Speed method is a method of constructing continuous domain transformation. Let $\Omega \subset \mathbb{R}^d$ be the usual open region of interest. Let T_t be a continuous transformation on Ω parametrized by a fictitious time $t \geq 0$, i.e. $\Omega_t = T_t(\Omega)$. Equivalently, $\forall x \in \Omega$, $x_t = T_t(x)$ at $\forall t > 0$ and $T_0(x) = x$. Furthermore, we let $D \subset \mathbb{R}^d$ to be a "holdall" such that $\Omega_t \subset D$ for all $t > 0$ and D is not changed by the T_t, i.e.

$$T_t(D) = D, \qquad \forall t \geq 0$$

Such a transformation can be generated by a velocity field $\mathbf{V} : \mathbb{R}^d \to \mathbb{R}^d$ in such a way that the trajectory of $T_t(X), 0 \leq t < \epsilon$ for $\forall X \in \Omega$ solves the following initial value problem ([24] Sec.2.9):

$$\begin{cases} \frac{d}{dt} x(t, X) = \mathbf{V}(t, x(t, X)) \\ \qquad\qquad x(0, X) = X \end{cases} \tag{4.3.1}$$

Note that if $\mathbf{V}$ is smooth enough, then the smoothness of Ω is preserved by the tranformation generated by B: if Ω is of class C^k and $\mathbf{V} \in C^k(\mathbb{R}^d; \mathbb{R}^d)$, then Ω_t is

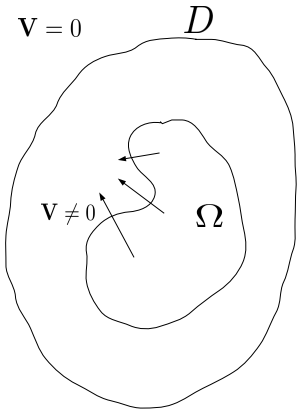

Figure 4.1: Example of velocity field within a hold-all domain.

of class C^k. The notion of admissible velocity field is discussed in [24], Sec.2.9-2.10. For our purpose, it is sufficient to assume all admissible velocity fields preserve the smoothness of the original domain Ω for $\forall t \in [0, \epsilon)$. Note that if $\mathbf{V}$ is tangent to $\partial\Omega$, Ω is not changed, i.e. $T_t(\Omega) = \Omega$. Following the convention in [24], we use $V^k(D)$ to denote the space of admissible velocity field.

4.4 Shape Derivative of a Function

In this section, we introduce the notion of *material derivative* and *shape derivative* of a function (cf. [24], Sec2.25, 2.30).

Let $\mathcal{W}(\Omega)$ be a Banach space of functions defined on the domain Ω and $y(\Omega) \in \mathcal{W}(\Omega)$. The dependence of y on Ω is indicated by the bracket on Ω; such dependence can be either explicitly defined by the spatial variable x or implicitly defined by such

as the solution operator of a boundary value problem. Similarly, we let $\mathcal{W}(\Gamma)$ be a Banach space on the boundary Γ and $z(\Gamma) \in \mathcal{W}(\Gamma)$.

In what follows, we assume a family of domain Ω_t is generated by an admissible velocity field $\mathbf{V}$. Correspondingly, a family of $y_t(\Omega_t)$ and $z_t(\Gamma_t)$ are generated by such transformations.

Definition 4.4.1 (Material derivative of a function, [24] Def 2.71)**.** The element $\dot{y} \in \mathcal{W}$ is the material derivative of $y(\Omega) \in \mathcal{W}(\Omega)$ in the direction of an admissible vector field $\mathbf{V}$ if the limit exists:

$$\dot{y}(\Omega; \mathbf{V}) = \lim_{t \to 0} \frac{y(\Omega_t) \circ T_t(\mathbf{V}) - y(\Omega)}{t} \tag{4.4.1}$$

Note the limit can be taken in either the strong sense or the weak sense in $\mathcal{W}(\Omega)$. A similar definition exists for $z(\Gamma)$.

Definition 4.4.2 (Shape derivative of a function of the domain Ω, [24] Def 2.85)**.** Assume the material derivative $\dot{y}(\Omega; \mathbf{V}) \in \mathcal{W}(\Omega)$ and $\nabla y \cdot \mathbf{V} \in \mathcal{W}(\Omega)$. Then the shape derivative of $y(\Omega)$ in the direction $\mathbf{V}$ is the element $y'(\Omega; \mathbf{V}) \in \mathcal{W}(\Omega)$ defined by

$$y'(\Omega; \mathbf{V}) = \dot{y}(\Omega; \mathbf{V}) - \nabla y(\Omega) \cdot \mathbf{V} \tag{4.4.2}$$

Definition 4.4.3 (Shape derivative of a function of the boundary Γ, [24] Def. 2.88)**.** Assume the material derivative $\dot{z}(\Gamma; \mathbf{V}) \in \mathcal{W}(\Gamma)$ and $\nabla_\Gamma z \cdot \mathbf{V} \in \mathcal{W}(\Gamma)$. Then the

shape derivative of $z(\Gamma)$ in the direction $\mathbf{V}$ is the element $z'(\Gamma;\mathbf{V}) \in \mathcal{W}(\Gamma)$ defined by

$$z'(\Gamma;\mathbf{V}) = \dot{z}(\Gamma;\mathbf{V}) - \nabla_\Gamma z(\Gamma)\cdot\mathbf{V} \tag{4.4.3}$$

Remark 4.4.4 (Chain rule for shape derivative). From the definition of shape derivative, it is not hard to see that the chain rule for ordinary derivatives also holds for the shape derivative. Specifically, if $y(\Omega)$ has shape derivative $y'(\Omega;\mathbf{V})$ and $f(y)$ is a smooth function in y, then the shape derivative of $f[y(\Omega)]$ is simply

$$f'(\Omega;\mathbf{V}) = \frac{\partial f}{\partial y} y'(\Omega;\mathbf{V})$$

Remark 4.4.5. Note the difference in the definition of $y'(\Omega)$ and $z'(\Gamma)$. It is quite often that $z(\Gamma)$ is the restriction of a domain function $y(\Omega)$ on Γ. In fact, if $z(\Gamma) = y(\Omega)|_\Gamma$, we have the simple but useful identity (cf. [24], Sec. 2.33)

$$z'(\Gamma;\mathbf{V}) = y'(\Omega;\mathbf{V}) + \frac{\partial y}{\partial \nu}\left\langle \mathbf{V}, \nu\right\rangle_{\mathbb{R}^d} \tag{4.4.4}$$

where ν is the unit normal vector on Γ.

Remark 4.4.6 (Understand *material derivative* and *shape derivative*). First of all, the material derivative $\dot{y}(\Omega;\mathbf{V})$ and the shape derivative $y'(\Omega;\mathbf{V})$ should be understood in the sense of directional derivative as defined in Chapter 2. Secondly, $\dot{y}(\Omega;\mathbf{V})$ and $y'(\Omega;\mathbf{V})$ are the analogs of "Lagrangian derivative" and "Eulerian derivative" in continuum mechanics, respectively. In some sense, $\dot{y}(\Omega;\mathbf{V})$ is the overal differential of y with respect to $\mathbf{V}$, whereas $y'(\Omega;\mathbf{V})$ keeps only the influence of "shape".

The following example can help understand the difference between *material derivative* and *shape derivative*.

Example 4.4.7. Let $y : \Omega \to \mathbb{R}$ be a smooth function on Ω and $\mathbf{V}$ be some admissible velocity field which generates a family of shapes $\Omega_t = T_t(\Omega; \mathbf{V})$. Apparently we have

$$x_t = T_t(x; \mathbf{V}) \quad \forall x \in \Omega$$

We define the Ω-dependent function y_t to be $y_t(x_t) = y(T_t(x))$. Then by the chain rule, its material derivative in the direction of $\mathbf{V}$ is simply

$$\dot{y}(\Omega; \mathbf{V}) = \nabla y \cdot \mathbf{V} \tag{4.4.5}$$

Let's consider its shape derivative as a domain function $y(\Omega)$ as well as its restriction on the boundary $y|_\Gamma$.

- The shape derivative of $y(\Omega)$ is

$$y'(\Omega; \mathbf{V}) \stackrel{d}{=} \dot{y} - \nabla y \cdot \mathbf{V} = 0 \tag{4.4.6}$$

  From this example, it is easy to see that $\dot{y}$ reflects the overall rate of change in y under the velocity field $\mathbf{V}$, whereas $y'(\Omega)$ removes the influence of convection and keeps solely the impact from the change in "shape".

- The shape derivative of $y(\Gamma)$ is

$$y'(\Gamma; \mathbf{V}) = \dot{y} - \nabla_\Gamma y \cdot \mathbf{V} = \frac{\partial y}{\partial \nu} \mathbf{V} \cdot \nu \tag{4.4.7}$$

  Thus we see that when y is viewed as only a function on Γ, its shape derivative is *not the same* as that of y.

In general, $y'(\Omega; \mathbf{V})$ is non-trivial. The map $y(\Omega)$ is usually defined by the solution operator of a boundary value problem on Ω, as we see in the example in Section 4.7.

Finally, we introduce a lemma from [9] for the computation of the shape derivative of unit normal vector and mean curvature on a boundary Γ.

Lemma 4.4.8 (Lemma 3.1 in [9])**.** *The shape derivatives of the normal ν and the mean curvature H of a surface Γ of class C^2 with respect to velocity $\mathbf{V} \in C^2$ are given by*

$$\nu' = \nu'(\Gamma; V) = -\nabla_\Gamma V \tag{4.4.8}$$

$$H' = H'(\Gamma; V) = -\Delta_\Gamma V \tag{4.4.9}$$

where $V = \mathbf{V} \cdot \nu$ is the normal component of the velocity field.

4.5 Shape Derivative of a Functional

Let $y(\Omega)$, $y'(\Omega; \mathbf{V})$, $z(\Gamma)$ and $z'(\Gamma; \mathbf{V})$ be as defined in Section 4.4. In addition, we let $y_\Gamma \overset{d}{=} y(\Omega)|_\Gamma$ to be the boundary value of $y(\Omega)$.

Below we present the shape derivative of two special types of functionals: *domain integrals* and *boundary integrals*. They are applied repeatedly in the shape sensitivity analysis of our drift-diffusion model in Section 5.3.

First, let us introduce a convenient notation of integral. In this work, we assume

the type of integration is indicated by the domain of integration, i.e.

$$\int_\Omega dV \longleftrightarrow \int_\Omega \tag{4.5.1}$$

$$\int_\Gamma dS \longleftrightarrow \int_\Gamma \tag{4.5.2}$$

Such a convention is kept for the remaining of this paper.

- Shape derivative of a domain integral (cf. [24], Sec 2.31)

$$\begin{aligned} J_1(\Omega) &= \int_\Omega y(\Omega) \\ \Rightarrow dJ_1(\Omega;\mathbf{V}) &= \int_\Omega y'(\Omega;\mathbf{V}) + \int_\Gamma y\mathbf{V}\cdot\nu \end{aligned} \tag{4.5.3}$$

- Shape derivative of a boundary integral (cf. [24], Sec 2.33)

$$\begin{aligned} J_2(\Gamma) &= \int_\Gamma z(\Gamma) \\ \Rightarrow dJ_2(\Gamma;\mathbf{V}) &= \int_\Gamma z'(\Gamma;\mathbf{V}) + z\,H\,\mathbf{V}\cdot\nu \end{aligned} \tag{4.5.4}$$

$$\begin{aligned} J_3(\Gamma) &= \int_\Gamma y_\Gamma = \int_\Gamma y(\Omega)|_\Gamma \\ \Rightarrow dJ_3(\Gamma;\mathbf{V}) &= \int_\Gamma \left(y'(\Omega;\mathbf{V}) + \frac{\partial y}{\partial \nu}\mathbf{V}\cdot\nu \right) + y\,H\,\mathbf{V}\cdot\nu \end{aligned} \tag{4.5.5}$$

Note in equation (4.5.5), we have applied the result of equation (4.4.4).

4.6 The Structure Theorem and Shape Gradient

One of the most important results of shape optimization is the *Hadamard-Zolésio Structure Theorem*. For accurate definition, we refer the readers to [24, 7, 30]. Here we state a short version of Theorem 3.1 in [30]:

Theorem 4.6.1 (Hadamard-Zolésio structure theorem)**.** *If the shape functional J is shape differentiable at Ω with respect to $V^k(\Omega)$, and Γ is sufficiently smooth, then there exists a scalar Γ-distribution $G(\Gamma)$ such that*

$$J'(\Omega; \mathbf{V}) = \langle G(\Gamma), \gamma(\mathbf{V}) \cdot \nu \rangle_\Gamma \tag{4.6.1}$$

with $\gamma(\cdot)$ the trace operator on Γ.

What this theorem states is that the sensitivity of a shape differentiable functional only dependes on the normal component of the velocity field. It is certainly an intuitive result: a velocity field that is tangential to $\partial\Omega$ does not change the shape of Ω, and we do not expect $J(\Omega)$ to change if Ω stays the same. In Chapter 5, we see that the shape sensitivity of photocurrent is supported only on the interface.

Before diving into the shape sensitivity of the photocurrent functional, let's compute the shape gradient of some simple examples of geometric quantities.

Example 4.6.2 (Volume of Ω).

$$J_1(\Omega) = \int_\Omega 1 \tag{4.6.2}$$

After taking shape derivative, we have

$$J_1'(\Omega; \mathbf{V}) = \int_{\partial\Omega} 1(\mathbf{V} \cdot \nu) \tag{4.6.3}$$

Therefore we have obtained the shape gradient of volume: $G_1 = 1$

Example 4.6.3 (Area of $\partial\Omega$).

$$J_2(\Omega) = \int_{\partial\Omega} 1 \tag{4.6.4}$$

After taking shape derivative, we have

$$J_2'(\Omega; \mathbf{V}) = \int_{\partial\Omega} 1 \cdot H(\mathbf{V} \cdot \nu) \tag{4.6.5}$$

Therefore the shape gradient of surface functional is $G_2 = H$.

As shown above, the computed shape gradients of these simple functionals are consistent with the structure theorem.

4.7 Example of Shape Optimization

When the functional is associated with some PDE's, we don't expect the shape gradient to take a form as simple as in the last section. To demonstrate the computation for *shape gradient*, we end this chapter with a simple shape optimization problem with PDE constraint.

Suppose $\Omega \subset D$ is a smooth domain in $\mathbb{R}^d$. We only consider the admissible domains Ω that are contained in some hold-all subset $D \subset \mathbb{R}^d$. As we apply the speed method to find shape sensitivity of a function or a functional, we assume transformation between admissible domains is generated by some smooth velocity field $\mathbf{V}$. In what follows, we use V denotes the normal component of $\mathbf{V}$ on the boundary $\partial\Omega$, i.e. $V = \mathbf{V} \cdot \nu$.

We define the following shape optimization problem with a PDE constraint:

$$\min_{\Omega} J = \int_{\Omega} \frac{1}{2}(y - y_d)^2 \tag{4.7.1}$$

$$\text{where} \qquad -\nabla^2 y = h \qquad \Omega \tag{4.7.2}$$

$$y = 0 \qquad \partial\Omega$$

Here we assume $y_d \in H^1(D)$ and $h \in L^2(\Omega)$ and they are not shape-dependent, i.e. $y_d' = h' = 0$. Note this problem is almost the same example that we presented in Chapter 2. The only difference is the "control": here the control is the domain Ω, or rather the shape of the boundary $\partial\Omega$.

There are two ways to proceed for computing the shape gradient functional.

- One way is to form the *nonlinear* Lagrangian functional $\mathcal{L}$ first, and then apply shape sensitivity analysis.
- The other way is to compute the shape derivatives of both y and J, i.e. y' and J'. In particular, we obtain a boundary value problem for y' which is linear even if the original PDE is not. The functional J' is also linear in y'. Then we form a different Lagrangian functional L based on y' and compute the shape gradient.

We show that both methods lead to the same adjoint equations and the same optimality conditions.

- Method 1:

  Let $\xi \in H^1(\Omega)$ be the adjoint variable, and thus we have the weak form of the state equation

$$\int_\Omega \nabla y \cdot \nabla \xi - \int_{\partial\Omega} \frac{\partial y}{\partial \nu} \xi = \int_\Omega h\xi \tag{4.7.3}$$

  Then we form the Lagrangian functional

$$\mathcal{L} = \int_\Omega \frac{1}{2}(y - y_d)^2 + \int_\Omega \nabla y \cdot \nabla \xi - \int_{\partial\Omega} \frac{\partial y}{\partial \nu} \xi - \int_\Omega h\xi \tag{4.7.4}$$

  Assume the shape derivative y' exists. Then we can take shape derivative of $\mathcal{L}$

$$\begin{aligned}
\mathcal{L}' = & \int_\Omega (y - y_d) y' + \int_{\partial\Omega} \frac{1}{2}(y - y_d)^2 V \\
& + \int_\Omega \nabla y' \cdot \nabla \xi + \int_{\partial\Omega} (\nabla y \cdot \nabla \xi) V \\
& - \int_{\partial\Omega} \langle \nabla y', \nu \rangle \xi - \int_{\partial\Omega} \langle \nabla y, \nu' \rangle \xi - \int_{\partial\Omega} \frac{\partial}{\partial \nu} \left(\frac{\partial y}{\partial \nu} \xi \right) V - \int_{\partial\Omega} \frac{\partial y}{\partial \nu} \xi H V \\
& - \int_{\partial\Omega} h\xi V
\end{aligned} \tag{4.7.5}$$

  where we have applied the formula for computing shape derivative of domain integral and boundary integral introduced in Section 4.5. We can simplify this formula further by applying the tangential Green's formula in Section 4.1 and the shape derivative of outward unit normal vector ν'

$$\begin{aligned}
\mathcal{L}' = & \int_\Omega (y - y_d) y' + \int_\Omega \nabla y' \cdot \nabla \xi - \int_{\partial\Omega} \langle \nabla y', \nu \rangle \xi \\
& + \int_{\partial\Omega} \left[\frac{1}{2}(y - y_d)^2 - \Delta_\Gamma y \, \xi - \frac{\partial}{\partial \nu} \left(\frac{\partial y}{\partial \nu} \right) \xi - \frac{\partial y}{\partial \nu} \xi H - h\xi \right] V
\end{aligned} \tag{4.7.6}$$

If we define the following adjoint equation

$$-\nabla^2\xi = -(y - y_d) \qquad \Omega \tag{4.7.7}$$

$$\text{where} \qquad \xi = 0 \qquad \partial\Omega \tag{4.7.8}$$

we have the following integral identities

$$\int_\Omega (y - y_d)y' + \int_\Omega \nabla\xi \cdot \nabla y' = \int_{\partial\Omega} y' \frac{\partial\xi}{\partial\nu} \tag{4.7.9}$$

$$\tag{4.7.10}$$

Therefore, we can update $\mathcal{L}'$ as

$$\mathcal{L}' = \int_{\partial\Omega} y' \frac{\partial\xi}{\partial\nu} + \int_{\partial\Omega} \frac{1}{2}(y - y_d)^2 V \tag{4.7.11}$$

We have written $\mathcal{L}'$ as a boundary integral. To finally recover the form in the Structure Theorem, we only need to compute y' on $\partial\Omega$. In fact, let ϕ be an arbitrary smooth function on D

$$\begin{aligned} & \left(\int_{\partial\Omega} y\phi\right)' = 0 \\ \Rightarrow \quad & \int_{\partial\Omega} y'\phi + \frac{\partial y}{\partial\nu}\phi V = 0 \\ \Rightarrow \quad & y' = -\frac{\partial y}{\partial\nu} V \end{aligned} \tag{4.7.12}$$

Hence we have obtained the shape sensitivity of J

$$J'(\Omega; \mathbf{V}) = \int_{\partial\Omega} \left[\frac{1}{2}(y - y_d)^2 - \frac{\partial y}{\partial\nu}\frac{\partial\xi}{\partial\nu}\right] V \tag{4.7.13}$$

$$\tag{4.7.14}$$

where ξ is the solution of the adjoint equation defined above.

- Method 2:

  First, we compute the shape derivative y' and the boundary value problem associated. Let $\phi \in C_c^\infty(\Omega)$ be an arbitrary smooth function that is 0 on the boundary. Then we have

$$\int_\Omega \nabla y \cdot \nabla \phi = \int_\Omega h\phi \tag{4.7.15}$$

  If y' exist, we can take shape derivative on both size. Making use of the fact that $\phi = 0$ on $\partial\Omega$ and $h' = 0$ we have

$$\int_\Omega \nabla y' \cdot \nabla \phi = 0 \tag{4.7.16}$$

$$\Rightarrow \quad -\nabla^2 y' = 0 \quad \text{in } \Omega \tag{4.7.17}$$

  On the bounary $\partial\Omega$, we proceed exactly as in "Method 1" and obtain

$$y' = -\frac{\partial y}{\partial \nu} V \tag{4.7.18}$$

  Therefore, the boundary value problem for y' is

$$-\nabla^2 y' = 0 \qquad \Omega \tag{4.7.19}$$

$$y' = -\frac{\partial y}{\partial \nu} V \qquad \partial\Omega \tag{4.7.20}$$

  The shape sensitivity of J is

$$J' = \int_\Omega (y - y_d) y' + \int_{\partial\Omega} \frac{1}{2}(y - y_d)^2 V \tag{4.7.21}$$

Again let the adjoint variable $\xi \in H^1(\Omega)$, so we can form the Lagrangian functional

$$\begin{aligned} L = &\int_\Omega (y - y_d)y' + \int_{\partial\Omega} \frac{1}{2}(y - y_d)^2 V \\ &+ \int_\Omega \nabla y' \cdot \nabla \xi - \int_{\partial\Omega} \frac{\partial y'}{\partial \nu}\xi \end{aligned} \tag{4.7.22}$$

Note $L = J'$ since $\int_\Omega \nabla y' \cdot \nabla \xi - \int_{\partial\Omega} \frac{\partial y'}{\partial \nu}\xi = 0$ by the PDE for y'.

From here we proceed in exactly the same way as in "Method 1". We define the adjoint equation

$$-\nabla^2 \xi = -(y - y_d) \qquad \Omega \tag{4.7.23}$$

$$\text{where} \qquad \xi = 0 \qquad \partial\Omega \tag{4.7.24}$$

Again, by the following identities

$$\int_\Omega (y - y_d)y' + \int_\Omega \nabla \xi \cdot \nabla y' = \int_{\partial\Omega} y' \frac{\partial \xi}{\partial \nu} \tag{4.7.25}$$

$$y' = -\frac{\partial y}{\partial \nu} V \tag{4.7.26}$$

we have the shape sensitivity J'

$$\begin{aligned} J'(\Omega; \mathbf{V}) &= L \\ &= \int_{\partial\Omega} y' \frac{\partial \xi}{\partial \nu} \frac{1}{2}(y - y_d)^2 V \\ &= \int_{\partial\Omega} \left[\frac{1}{2}(y - y_d)^2 - \frac{\partial y}{\partial \nu}\frac{\partial \xi}{\partial \nu} \right] V \end{aligned} \tag{4.7.27}$$

Remark 4.7.1 (Which method?). In both methods, we have exactly the same adjoint equations (4.7.7) and (4.7.23), and the same shape sensitivity (4.7.13) v.s. (4.7.27). But the Lagrangian functional (4.7.22) in "Method 2" is much simpler in form compared to the shape derivative of the Lagrangian functional (4.7.5) in "Method 1". This is because we do not introduce unnecessary boundary integrals **before** taking the shape derivative; such a difference is peculiar to shape optimization problem.

In Chapter 5, we take the second approach only for the sake of relatively simple computation when we compute the shape sensitivity of photocurrent. It shouldn not affect the sensitivity result just like in the example of this section.

Chapter 5

Shape Optimization with Drift-Diffusion Model

In this chapter, we apply the results of shape differential calculus to our drift-diffusion model presented in Chapter 3 to identify the shape gradient functional G. Specifically, we have the following optimization problem:

$$\min_{\Gamma_{\text{ad}}} \; J[\psi, n, p, u; \Gamma] = -\int_{\Gamma_{D1}} (\mathbf{F}_{p1} - \mathbf{F}_{n1}) \cdot \nu_1 \tag{5.0.1}$$

$$\tag{5.0.2}$$

where ψ, n, p, u are the solution of drift-diffusion equations and $\mathbf{F}_p - \mathbf{F}_n$ is the flux of charge carriers. Our purpose is to maximize the photocurrent, which is equivalent to minimizing its negative and therefore the "$-$" sign before the integral. We make this choice of formulation only to be consistent with the convention of optimization in general.

The method of computing shape gradient G is exactly the same as in the simple shape optimization problem presented in Section 4.7 (Method 2):

- In Section 5.1, we define the admissible velocity field $\mathbf{V}$ for our purpose.
- In Section 5.2, we specify some notations that simplify our later computations.
- In Section 5.3, we derive the boundary value problems for the shape derivative ψ', n', p', u'.
- In Section 5.4, we first compute the shape sensitivity of photocurrent, J'. We then form the Lagrangian functional based on J' (like in "Method 2" in Section 4.7) and derive the corresponding adjoint equation. Given the solution of drift-diffusion equation and adjoint equation, we finally obtain an explicit formula for the shape gradient functional of photocurrent. We show in the end that the shape gradient functional G is only supported on the interface Γ, which is what we should expect by the Structure Theorem.

Finally, we note that we always assume sufficient smoothness on the velocity field $\mathbf{V}$, the interface Γ and any parameters in the drift-diffusion equations to justify the formal computations in this chapter.

5.1 Admissible Velocity Field

Given that our interest is only in the donor-acceptor interface for a fixed domain Ω, we let $\mathbf{V}$ satisfy the following criterions:

- **Velocity field that only changes the interior of Ω**

  Our interest in this work is in the optimality condition of the donor-acceptor interface Γ. Therefore, we only consider the tranformations $T_t(\mathbb{R}^d; \mathbf{V})$ that change Γ but keep the whole domain $\overline{\Omega}$ fixed. A velocity field $\mathbf{V} : \mathbb{R}^d \to \mathbb{R}^d$ is admissible only if

$$\mathbf{V}(x) = \mathbf{0} \qquad \forall x \in \overline{\mathbb{R}^d \setminus \Omega} \tag{5.1.1}$$

  In particular, it guarantees that $\mathbf{V} = 0$ on $\partial\Gamma \subset \partial\Omega$. This requirment appears to be too restrictive, since in principle we can move $\partial\Gamma$ along $\partial\Omega$ without changing Ω. However, such restrictive requirement is convenient when we apply the tangential Green's formula (4.1.7) without adding boundary terms.

- **Smoothness of V**

  We also need to assume that both the interface Γ and the velocity field $\mathbf{V}$ are *smooth enough* so that the solutions $\{\psi, n, p, u\}$ to the drift-diffusion equations and their shape derivatives $\{\psi', n', p', u'\}$ exist in a proper Banach space $\mathcal{W}$.

Note that all shape derivatives in this chapter are defined in the sense of a chosen velocity field and hence the dependence of a shape derivative y' on $\mathbf{V}$ is kept **implicit**.

An example of a domain perturbed by an admissble velocity field is shown in Fig. 5.1.

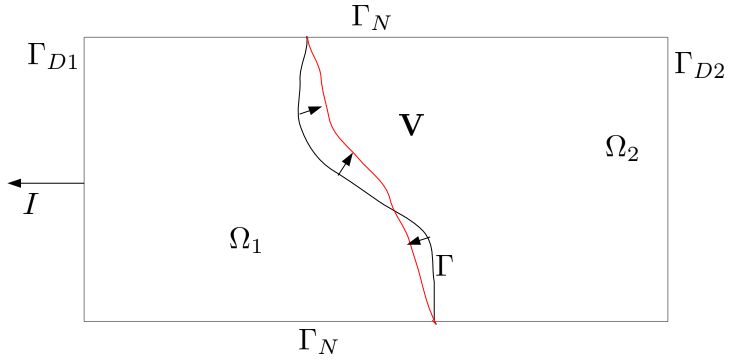

Figure 5.1: Example: shape transformation by admissible velocity field. Note that in this two-dimensional graph, the rectangle Ω is not changed under $\mathbf{V}$ but only the interface Γ is perturbed. Also note that the end nodes of Γ (i.e. $\partial\Gamma$) is fixed.

5.2 Preparation on Notations

- **Subscripts for quantities on interface Γ (cf. 3.1)**

  We use subscript "1" for quantities defined on $\overline{\Omega}_1$ and "2" for $\overline{\Omega}_2$. This convention is only necessary when interface quantities are considered.

- **Projection operators on interface Γ**

  Let $\mathbf{F} \in \mathbb{R}^d (d = 2, 3)$ be a vector field defined on Γ. Let $\nu_{1,2}$ be the unit outward normal vector on Γ for $\Omega_{1,2}$, respectively; apparently $\nu_1 = -\nu_2$ on Γ.

We define its normal projection

$$P_{\nu_1}(\mathbf{F}) = (\mathbf{F} \cdot \nu_1)\, \nu_1 \tag{5.2.1}$$

and its tangential projection

$$\begin{aligned} P_\Gamma(\mathbf{F}) &= \mathbf{F} - (\mathbf{F} \cdot \nu_1)\, \nu_1 \\ &= \left(\mathrm{I} - \nu_1 \otimes \nu_1^T\right) \cdot \mathbf{F} \end{aligned} \tag{5.2.2}$$

- **Normal component of velocity field on Γ**

  For convenience, we further define $V_1 = \langle \mathbf{V}, \nu_1 \rangle |_\Gamma$ and $V_2 = \langle \mathbf{V}, \nu_2 \rangle |_\Gamma$. Apparently $V_1 = -V_2$ on Γ.

- **Mean curvature of Γ**

  Similarly, we define the mean curvature of Γ to be $\bar{H}_1$ when Ω_1 is viewed as the *interior* side and $\bar{H}_2$ when Ω_2 is viewed as the *interior* side. By the definition of H in (4.1.1), we have $H_1 = -H_2$ on Γ.

5.3 Shape Sensitivity Analysis of Drift-Diffusion Model

The plan in this section is as follows:

- Shape sensitivity of physical parameters.

  We compute the shape derivatives of the physical parameters specified in

Section 3.2.3. In particular, care must be taken when the shape derivative of reaction rate f is computed, since f is a function only defined on the interface Γ.

- Shape sensitivity of Dirichlet boundary conditions on $\Gamma_{D1,2}$.

  The Dirichlet boundaries are fixed in space for the admissible velocity field defined in Section 5.1. The shape sensitivity of Dirichlet boundary conditions are shown to be trivial.

- Shape sensitivity of function values on the interface Γ.

  Specifically, we consider continuity conditions for the shape derivatives $\{\psi_1', n_1', p_1', u_1'\}$ and $\{\psi_2', n_2', p_2', u_2'\}$ across Γ.

- Shape sensitivity of PDE's in $\Omega_1 \cup \Omega_2$ and shape sensitivity of flux boundary conditions on Γ_N and Γ.

Note that in Section 5.3.2 and 5.3.3, we use y to denote any of $\{\psi, n, p, u\}$, since the derivations are essentially the same for all unknowns.

5.3.1 Shape sensitivity of physical parameters

Below we list the shape derivatives of all the physical parameters defined in Section 3.2.3. The chain rule for shape derivative is applied repeatedly. The only peculiar shape derivative is that of f, since f is a function **only** defined on the interface.

- **Relative electric permittivity ϵ in Ω**

  Since ϵ only depends on the spatial variable, we have

$$\epsilon' = 0 \tag{5.3.1}$$

- **Mobilities of particles in Ω**

  The mobilities of electrons and holes depend on both the spatial variable x and electric field $\nabla\psi$. Hence their shape derivatives are given by the chain rule

$$\mu'_{n,p} = \frac{\partial \mu_{n,p}}{\partial \nabla \psi} \cdot \nabla \psi' \tag{5.3.2}$$

  The mobility of excitons, on the other hand, has no dependence on the unknowns, and therefore has a trivial shape derivative

$$\mu'_u = 0 \tag{5.3.3}$$

- **Photo generation rate G and exciton decay rate d_u in Ω**

  G and d_u only dependes on the spatial variable x, and therefore we have

$$G' = 0 \tag{5.3.4}$$

$$d'_u = 0 \tag{5.3.5}$$

- **Reaction rate f on interface Γ**

  By the assumption in Section 3.2.3,functional form of f is

$$f = f(x, n|_\Gamma, p|_\Gamma, u|_\Gamma, \nabla\psi|_\Gamma, \mathbf{y} = \nu_1, H_1) \tag{5.3.6}$$

where $y|_\Gamma$ denotes the restriction of any function y on the interface Γ and ν_1 and H_1 are the unit normal vector and mean curvature of Γ with respect to Ω_1.

Let's recall that $\{\psi, \nabla\psi, n, p, u\}$ are all continuous across Γ as defined in 3.2.2. Therefore it is innocuous to write formula 5.3.6 in either way, i.e.

$$f = f(x, n = n_1|_\Gamma, p = p_1|_\Gamma, u = u_1|_\Gamma, \nabla\psi = \nabla\psi_1|_\Gamma, \mathbf{y} = \nu_1, H_1) \tag{5.3.7}$$

$$\stackrel{\text{or}}{=} f(x, n = n_2|_\Gamma, p = p_2|_\Gamma, u = u_2|_\Gamma, \nabla\psi = \nabla\psi_2|_\Gamma, \mathbf{y} = \nu_1, H_1) \tag{5.3.8}$$

However, it seems to lead to a confusion when computing f', since the chain rule of computing shape derivative leads to different expressions for f'

$$\begin{aligned} f' = &\frac{\partial f}{\partial n}(n_1|_\Gamma)' + \frac{\partial f}{\partial p}(p_1|_\Gamma)' + \frac{\partial f}{\partial u}(u_1|_\Gamma)' + \frac{\partial f}{\partial(\nabla\psi)} \cdot (\nabla\psi_1|_\Gamma)' \\ &+ \frac{\partial f}{\partial \mathbf{y}} \cdot \nu_1' + \frac{\partial f}{\partial H_1} H_1' \end{aligned} \tag{5.3.9}$$

$$\begin{aligned} \stackrel{\text{or}}{=} &\frac{\partial f}{\partial n}(n_2|_\Gamma)' + \frac{\partial f}{\partial p}(p_2|_\Gamma)' + \frac{\partial f}{\partial u}(u_2|_\Gamma)' + \frac{\partial f}{\partial(\nabla\psi)} \cdot (\nabla\psi_2|_\Gamma)' \\ &+ \frac{\partial f}{\partial \mathbf{y}} \cdot \nu_1' + \frac{\partial f}{\partial H_1} H_1' \end{aligned} \tag{5.3.10}$$

To resolve this confusion, one only needs to realize that $n_1|_\Gamma$, $p_1|_\Gamma$, $u_1|_\Gamma$ and $\nabla\psi_1|_\Gamma$ should be viewed as functions defined on Γ, rather than on the whole domain Ω. Such a subtlety makes a difference when computing their shape derivative (cf. Section 4.4).

In fact, if we let y be any of $\{n, p, u, \nabla\psi\}$, we can apply the formula 4.4.4 and

obtain the following identities

$$(y_1|_\Gamma)' = y_1'|_\Gamma + \frac{\partial y_1}{\partial \nu_1}\mathbf{V}\cdot\nu_1 \tag{5.3.11}$$

$$(y_2|_\Gamma)' = y_2'|_\Gamma + \frac{\partial y_2}{\partial \nu_2}\mathbf{V}\cdot\nu_2 \tag{5.3.12}$$

As shown in Section 5.3.3, for a function y such that $y_1|_\Gamma = y_2|_\Gamma$, we always have

$$(y_1|_\Gamma)' = (y_2|_\Gamma)' \tag{5.3.13}$$

although $y_1'|_\Gamma \neq y_2'|_\Gamma$ in general.

Therefore, we conclude that the shape derivative f' is well defined and either formula 5.3.9 or formula 5.3.10 is valid. For convenience, we assume f and f' are defined by the following forms:

$$f = f(x, n = n_1|_\Gamma, p = p_1|_\Gamma, u = u_1|_\Gamma, \nabla\psi = \nabla\psi_1|_\Gamma, \mathbf{y} = \nu_1, H_1) \tag{5.3.14}$$

$$\begin{aligned} f' = {} & \frac{\partial f}{\partial n}(n_1|_\Gamma)' + \frac{\partial f}{\partial p}(p_1|_\Gamma)' + \frac{\partial f}{\partial u}(u_1|_\Gamma)' + \frac{\partial f}{\partial(\nabla\psi)}\cdot(\nabla\psi_1|_\Gamma)' \\ & + \frac{\partial f}{\partial \mathbf{y}}\cdot\nu_1' + \frac{\partial f}{\partial H_1}H_1' \end{aligned} \tag{5.3.15}$$

5.3.2 Shape sensitivity of Dirichlet boundary conditions on Γ_D

Let y be any of $\{\psi, n, p, u\}$. Since the Dirichlet boundaries are fixed under the velocity field $\mathbf{V}$, the sensitivity of y on Γ_D is quite simple.

Let $y = y_D$ be the Dirichlet boundary condition which is the same for all admissible shapes. Let ϕ be any test function on Γ. If we consider the shape derivative of boundary integral of $\int_{\Gamma_D} y\phi$, we have the following idensity

$$\left(\int_{\Gamma_D} y\phi\right)' = 0 \tag{5.3.16}$$

On the other hand, we can apply the formula 4.4.4 and obtain

$$\begin{aligned}\left(\int_{\Gamma_D} y\phi\right)' &= \int_{\Gamma_D} (y|_{\Gamma_D}\phi)' + \int_{\Gamma_D} y\phi H\mathbf{V}\cdot\nu \\ &= \int_{\Gamma_D}\left(y'|_{\Gamma_D}\phi + \frac{\partial y}{\partial \nu}\mathbf{V}\cdot\nu\phi\right) + \int_{\Gamma_D} y\phi H\mathbf{V}\cdot\nu \end{aligned} \tag{5.3.17}$$

Since $\mathbf{V} = 0$ on Γ_D and ϕ is arbitrary, we conclude

$$y'|_{\Gamma_D} = 0 \qquad\qquad \forall x \in \Gamma_D \tag{5.3.18}$$

5.3.3 Shape sensitivity of function values on Γ

We again let y be any of $\{\psi, n, p, u\}$. We let y_1 be its restriction on $\overline{\Omega}_1$ and y_2 be its restriction on $\overline{\Omega}_2$. Recall that all 4 unknowns are continuous across the interface Γ as defined in Chapter 3, we conclude that $y_1(x) = y_2(x), \forall x \in \Gamma$.

Let ϕ be an arbitrary test function on Ω and we have the identity

$$\int_\Gamma y_1\phi = \int_\Gamma y_2\phi \tag{5.3.19}$$

We then take shape derivative on both sides and apply formula 4.4.4

$$\begin{aligned}&\int_\Gamma\left(y_1'\phi + \frac{\partial(y_1\phi)}{\partial\nu_1}\mathbf{V}\cdot\nu_1\right) + \int_\Gamma y_1\phi H_1\mathbf{V}\cdot\nu_1 \\ =&\int_\Gamma\left(y_2'\phi + \frac{\partial(y_2\phi)}{\partial\nu_2}\mathbf{V}\cdot\nu_2\right) + \int_\Gamma y_2\phi H_2\mathbf{V}\cdot\nu_2\end{aligned} \tag{5.3.20}$$

Note $\phi' = 0$ since it is an arbitrary test function that is not determined by the shape.

Now making use of the fact that $y_1 = y_2, V_1 = -V_2, \nu_1 = -\nu_2, H_1 = -H_2$ on Γ, and ϕ is an arbitrary smooth function on Ω, we have

$$\begin{aligned} y_1' + \frac{\partial y_1}{\partial \nu_1}(\mathbf{V} \cdot \nu_1) &= y_2' + \frac{\partial y_2}{\partial \nu_1}(\mathbf{V} \cdot \nu_1) \\ y_1' + \frac{\partial y_1}{\partial \nu_1} V_1 &= y_2' + \frac{\partial y_2}{\partial \nu_1} V_1 \end{aligned} \tag{5.3.21}$$

In view of Section 4.4, this is equivalent to

$$(y_1|_\Gamma)' = (y_2|_\Gamma)' \tag{5.3.22}$$

a result that is already used when f' was computed in Section 5.3.1.

5.3.4 Shape sensitivity of PDE's in $\Omega_1 \cup \Omega_2$ and shape sensitivity of flux boundary conditions on $\Gamma_N \cup \Gamma$

The spirit of the calculation in this section is similar to that of "Method 2" in Section 4.7, namely applying shape sensitivity analysis to the weak form of the original drift-diffusion equations. The detailed calculation in this section is rather lengthy and therefore saved for Appendix A.

5.3.5 Summary of boundary value problems for $\{\psi', n', p', u'\}$

We combine the results in Section 5.3.2, 5.3.3, and 5.3.4 and summarize them as 4 (*linear*) boundary value problems:

- Shape sensitivity of ψ-equation.

$$-\lambda^2\nabla\cdot(\epsilon\nabla\psi') = p' - n' \qquad \Omega_1\cup\Omega_2 \qquad (5.3.23)$$

$$\psi' = 0 \qquad \Gamma_{D1}\cup\Gamma_{D2} \qquad (5.3.24)$$

$$\frac{\partial\psi'}{\partial\nu} = 0 \qquad \Gamma_{N1}\cup\Gamma_{N2} \qquad (5.3.25)$$

$$\psi_1' = \psi_2' \qquad \Gamma \qquad (5.3.26)$$

$$\begin{aligned}&\epsilon_2\left(\frac{\partial\psi_1'}{\partial\nu_1} - \frac{\partial\psi_2'}{\partial\nu_1}\right)\\ &= \mathrm{div}_\Gamma\left[(\epsilon_1-\epsilon_2)\nabla_\Gamma\psi_1\right]V_1\\ &\quad + \frac{\partial}{\partial\nu_1}\left[(\epsilon_1-\epsilon_2)\frac{\partial\psi_1}{\partial\nu_1}\right]V_1\\ &\quad + (\epsilon_1-\epsilon_2)\frac{\partial\psi_1}{\partial\nu_1}H_1V_1 \qquad \Gamma\end{aligned} \qquad (5.3.27)$$

- Shape sensitivity of n-equation

$$\nabla\cdot\mathbf{F}_n' = 0 \qquad \Omega_1\cup\Omega_2 \qquad (5.3.28)$$

$$\begin{aligned}\mathbf{F}_n' &= -\mu_n\left(\nabla n' - n'\nabla\psi\right)\\ &\quad + \mu_n n\nabla\psi' - \left(\nabla n - n\nabla\psi\right)\frac{\partial\mu_n}{\partial(\nabla\psi)}\cdot\nabla\psi' \qquad \Omega_1\cup\Omega_2\end{aligned} \qquad (5.3.29)$$

$$n' = 0 \qquad \Gamma_D \qquad (5.3.30)$$

$$\mathbf{F}_n'\cdot\nu = 0 \qquad \Gamma_N \qquad (5.3.31)$$

$$n_1' + \frac{\partial n_1}{\partial\nu_1}V_1 = n_2' + \frac{\partial n_2}{\partial\nu_1}V_1 \qquad \Gamma \qquad (5.3.32)$$

$$\begin{aligned}-\mathbf{F}_{n1}'\cdot\nu_1 - \mathbf{F}_{n2}'\cdot\nu_2 &= -\mathrm{div}_\Gamma\left[V_1\ P_\Gamma\left(\mathbf{F}_{n1}-\mathbf{F}_{n2}\right)\right]\\ &\quad + \left(f' + fH_1V_1\right) \qquad \Gamma\end{aligned} \qquad (5.3.33)$$

- Shape sensitivity of p-equation

$$\nabla \cdot \mathbf{F}'_p = 0 \qquad \Omega_1 \cup \Omega_2 \qquad (5.3.34)$$

$$\mathbf{F}'_p = -\mu_p \left(\nabla p' + p' \nabla \psi\right)$$
$$- \mu_p p \nabla \psi' - \left(\nabla p + p \nabla \psi\right) \frac{\partial \mu_p}{\partial (\nabla \psi)} \cdot \nabla \psi' \qquad \Omega_1 \cup \Omega_2 \qquad (5.3.35)$$

$$p' = 0 \qquad \Gamma_D \qquad (5.3.36)$$

$$\mathbf{F}'_p \cdot \nu = 0 \qquad \Gamma_N \qquad (5.3.37)$$

$$p'_1 + \frac{\partial p_1}{\partial \nu_1} V_1 = p'_2 + \frac{\partial p_2}{\partial \nu_1} V_1 \qquad \Gamma \qquad (5.3.38)$$

$$- \mathbf{F}'_{p1} \cdot \nu_1 - \mathbf{F}'_{p2} \cdot \nu_2 = -\mathrm{div}_\Gamma \left[V_1 \; P_\Gamma \left(\mathbf{F}_{p1} - \mathbf{F}_{p2}\right)\right]$$
$$+ \left(f' + f H_1 V_1\right) \qquad \Gamma \qquad (5.3.39)$$

- Shape sensitivity of u-equations

$$\nabla \cdot \mathbf{F}'_u + d_u u' = 0 \qquad \Omega_1 \cup \Omega_2 \qquad (5.3.40)$$

$$\mathbf{F}'_u = -\mu_u \nabla u' \qquad \Omega_1 \cup \Omega_2 \qquad (5.3.41)$$

$$u' = 0 \qquad \Gamma_D \qquad (5.3.42)$$

$$\mathbf{F}'_u \cdot \nu = 0 \qquad \Gamma_N \qquad (5.3.43)$$

$$u'_1 + \frac{\partial u_1}{\partial \nu_1} V_1 = u'_2 + \frac{\partial u_2}{\partial \nu_1} V_1 \qquad \Gamma \qquad (5.3.44)$$

$$- \mathbf{F}'_{u1} \cdot \nu_1 - \mathbf{F}'_{u2} \cdot \nu_2 = -\mathrm{div}_\Gamma \left[V_1 \; P_\Gamma \left(\mathbf{F}_{u1} - \mathbf{F}_{u2}\right)\right]$$
$$- \left(f' + f H_1 V_1\right) \qquad \Gamma \qquad (5.3.45)$$

5.4 Shape Gradient of Photocurrent and the First Order Optimality Condition

5.4.1 Shape derivative of photocurrent J'

Given an admissible velocity field $\mathbf{V}$, the shape derivative of J is

$$J' = -\int_{\Gamma_{D1}} [(\mathbf{F}_{p1} - \mathbf{F}_{n1}) \cdot \nu_1]' - \int_{\Gamma_{D1}} (\mathbf{F}_{p1} - \mathbf{F}_{n1}) \cdot \nu_1 H_1 V_1 \tag{5.4.1}$$

where we have applied the formula 4.5.4. Note that $V_1 = 0$ on Γ_{D1}, and as a result $\nu_1'|_{\Gamma_{D1}} = 0$. Therefore, the shape derivative of J is simply

$$J' = -\int_{\Gamma_{D1}} \left(\mathbf{F}'_{p1} - \mathbf{F}'_{n1}\right) \cdot \nu_1 \tag{5.4.2}$$

5.4.2 Adjoint equations and the Lagrangian functional

We let $(\xi_\psi, \xi_n, \xi_p, \xi_u)$ to be the Lagrange multipliers for each of the shape sensitivity equations of the drift-diffusion model (cf. 5.3.5); for convenience, we use $\Xi = (\xi_\psi, \xi_n, \xi_p, \xi_u)$ to denote the collection of all the adjoint variables whenever necessary. Thus we can form the Lagrangian functional as below:

$$L \stackrel{d}{=} J' + L_\psi + L_n + L_p + L_u \tag{5.4.3}$$

where

$$L_\psi = \int_{\Omega_1 \cup \Omega_2} \left(-\lambda^2 \nabla \cdot (\epsilon \nabla \psi') - p' + n'\right) \xi_\psi \tag{5.4.4}$$

$$L_n = \int_{\Omega_1 \cup \Omega_2} \left(\nabla \cdot \mathbf{F}'_n\right) \xi_n \tag{5.4.5}$$

$$L_p = \int_{\Omega_1 \cup \Omega_2} \left(\nabla \cdot \mathbf{F}'_p\right) \xi_p \tag{5.4.6}$$

$$L_u = \int_{\Omega_1 \cup \Omega_2} \left(\nabla \cdot \mathbf{F}'_u + d_u u'\right) \xi_u \tag{5.4.7}$$

The derivation of adjoint equations is given in Appendix B; here we only state the results. For the adjoint variables $\xi_\psi, \xi_n, \xi_p, \xi_u$, we have the following boundary value problems:

- **In** $\Omega_1 \cup \Omega_2$

$$
\begin{aligned}
&- \lambda^2 \nabla \cdot (\epsilon \nabla \xi_\psi) \\
&+ \nabla \cdot (\mu_n n \nabla \xi_n) - \nabla \cdot \left(\nabla \xi_n \cdot (\nabla n - n \nabla \psi) \frac{\partial \mu_n}{\partial (\nabla \psi)} \right) \\
&- \nabla \cdot (\mu_p p \nabla \xi_p) - \nabla \cdot \left(\nabla \xi_p \cdot (\nabla p + p \nabla \psi) \frac{\partial \mu_p}{\partial (\nabla \psi)} \right) \qquad = 0
\end{aligned} \tag{5.4.8}
$$

$$
\xi_\psi - \nabla \cdot (\mu_n \nabla \xi_n) - \mu_n \nabla \psi \cdot \nabla \xi_n \qquad = 0 \tag{5.4.9}
$$

$$
- \xi_\psi - \nabla \cdot (\mu_p \nabla \xi_p) + \mu_p \nabla \psi \cdot \nabla \xi_p \qquad = 0 \tag{5.4.10}
$$

$$
- \nabla \cdot (\mu_u \nabla \xi_u) + d_u \xi_u \qquad = 0 \tag{5.4.11}
$$

- **On** Γ_{D1}

$$
\xi_{\psi 1} = 0 \tag{5.4.12}
$$

$$
\xi_{n1} = 1 \tag{5.4.13}
$$

$$
\xi_{p1} = -1 \tag{5.4.14}
$$

$$
\xi_{u1} = 0 \tag{5.4.15}
$$

- **On** Γ_{D2}

$$\xi_{\psi 2} = 0 \tag{5.4.16}$$

$$\xi_{n2} = 0 \tag{5.4.17}$$

$$\xi_{p2} = 0 \tag{5.4.18}$$

$$\xi_{u2} = 0 \tag{5.4.19}$$

- **On** Γ_N

$$\begin{aligned} &\lambda^2 \epsilon \frac{\partial \xi_\psi}{\partial \nu} \\ &+ \nabla \xi_n \cdot (\nabla n - n \nabla \psi) \frac{\partial \mu_n}{\partial (\nabla \psi)} \cdot \nu \\ &+ \nabla \xi_p \cdot (\nabla p + p \nabla \psi) \frac{\partial \mu_p}{\partial (\nabla \psi)} \cdot \nu = 0 \end{aligned} \tag{5.4.20}$$

$$\frac{\partial \xi_n}{\partial \nu} = 0 \tag{5.4.21}$$

$$\frac{\partial \xi_p}{\partial \nu} = 0 \tag{5.4.22}$$

$$\frac{\partial \xi_u}{\partial \nu} = 0 \tag{5.4.23}$$

- **On** Γ

We have 8 boundary conditions on Γ for the adjoint equations:

$$
\begin{aligned}
&- \lambda^2 \left(\epsilon_1 \frac{\partial \xi_{\psi 1}}{\partial \nu_1} + \epsilon_2 \frac{\partial \xi_{\psi 2}}{\partial \nu_2} \right) \\
&- \mu_{n1} n_1 \frac{\partial \xi_{n1}}{\partial \nu_1} - \mu_{n2} n_2 \frac{\partial \xi_{n2}}{\partial \nu_2} \\
&+ \nabla \xi_{n1} \cdot (\nabla n_1 - n_1 \nabla \psi_1) \frac{\partial \mu_{n1}}{\partial (\nabla \psi)} \cdot \nu_1 \\
&+ \nabla \xi_{n2} \cdot (\nabla n_2 - n_2 \nabla \psi_2) \frac{\partial \mu_{n2}}{\partial (\nabla \psi)} \cdot \nu_2 \\
&+ \mu_{p1} p_1 \frac{\partial \xi_{p1}}{\partial \nu_1} + \mu_{p2} p_2 \frac{\partial \xi_{p2}}{\partial \nu_2} \\
&+ \nabla \xi_{p1} \cdot (\nabla p_1 + p_1 \nabla \psi_1) \frac{\partial \mu_{p1}}{\partial (\nabla \psi)} \cdot \nu_1 \\
&+ \nabla \xi_{p2} \cdot (\nabla p_2 + p_2 \nabla \psi_2) \frac{\partial \mu_{p2}}{\partial (\nabla \psi)} \cdot \nu_2 \\
&- \operatorname{div}_\Gamma \left[(\xi_{u2} - \xi_{n2} - \xi_{p2}) P_\Gamma \left(\frac{\partial f}{\partial (\nabla \psi)} \right) \right] = 0
\end{aligned} \tag{5.4.24}
$$

$$
\mu_{n1} \frac{\partial \xi_{n1}}{\partial \nu_1} + \mu_{n2} \frac{\partial \xi_{n2}}{\partial \nu_2} + (\xi_{u2} - \xi_{n2} - \xi_{p2}) \frac{\partial f}{\partial n} = 0 \tag{5.4.25}
$$

$$
\mu_{p1} \frac{\partial \xi_{p1}}{\partial \nu_1} + \mu_{p2} \frac{\partial \xi_{p2}}{\partial \nu_2} + (\xi_{u2} - \xi_{n2} - \xi_{p2}) \frac{\partial f}{\partial p} = 0 \tag{5.4.26}
$$

$$
\mu_{u1} \frac{\partial \xi_{u1}}{\partial \nu_1} + \mu_{u2} \frac{\partial \xi_{u2}}{\partial \nu_2} + (\xi_{u2} - \xi_{n2} - \xi_{p2}) \frac{\partial f}{\partial u} = 0 \tag{5.4.27}
$$

$$
\lambda^2 \left(-\epsilon_1 \xi_{\psi 1} + \epsilon_2 \xi_{\psi 2} \right) + (\xi_{u2} - \xi_{n2} - \xi_{p2}) P_{\nu_1} \left(\frac{\partial f}{\partial (\nabla \psi)} \right) = 0 \tag{5.4.28}
$$

–

$$\xi_{n1} - \xi_{n2} = 0 \tag{5.4.29}$$

–

$$\xi_{p1} - \xi_{p2} = 0 \tag{5.4.30}$$

–

$$\xi_{u2} - \xi_{u1} = 0 \tag{5.4.31}$$

5.4.3 Shape gradient

Now we are ready to state the first order optimality condition for the photocurrent function J. Recall that the we form the Lagrangian functional L from J' and group the terms by their integral domain; cf. Appendix B.

$$\begin{aligned} L &= J' + L_\psi + L_n + L_p + L_u \\ &= L_{\Omega_1 \cup \Omega_2} + L_{\Gamma_{D1}} + L_{\Gamma_{D2}} + L_{\Gamma_N} + L_\Gamma \end{aligned} \tag{5.4.32}$$

Note J' has the same value as L, since L is formed by the method of Lagrange multipliers. By solving the adjoint equations, we effectively eliminate all the integrals of shape derivatives in L. What is left leads to an explicit formula for the shape gradient. Here we state the result:

$$J'(\mathbf{V}) = \int_\Gamma G\, V_1 \tag{5.4.33}$$

where G is the *shape gradient* of J at (ψ, n, p, u) in the direction of an admissible velocity field $\mathbf{V}$

$$
\begin{aligned}
G = (-\lambda^2)\xi_{\psi 2} & \left\{ \mathrm{div}_\Gamma \left[(\epsilon_1 - \epsilon_2) \nabla_\Gamma \psi_1 \right] + \frac{\partial}{\partial \nu_1} \left[(\epsilon_1 - \epsilon_2) \frac{\partial \psi_1}{\partial \nu_1} \right] + (\epsilon_1 - \epsilon_2) \frac{\partial \psi_1}{\partial \nu_1} H_1 \right\} \\
& - \mu_{n2} \frac{\partial \xi_{n2}}{\partial \nu_1} \left(\frac{\partial n_1}{\partial \nu_1} - \frac{\partial n_2}{\partial \nu_1} \right) \\
& - \nabla_\Gamma \xi_{n2} \cdot P_\Gamma \left(\mathbf{F}_{n1} - \mathbf{F}_{n2} \right) \\
& - \mu_{p2} \frac{\partial \xi_{p2}}{\partial \nu_1} \left(\frac{\partial p_1}{\partial \nu_1} - \frac{\partial p_2}{\partial \nu_1} \right) \\
& - \nabla_\Gamma \xi_{p2} \cdot P_\Gamma \left(\mathbf{F}_{p1} - \mathbf{F}_{p2} \right) \\
& - \mu_{u2} \frac{\partial \xi_{u2}}{\partial \nu_1} \left(\frac{\partial u_1}{\partial \nu_1} - \frac{\partial u_2}{\partial \nu_1} \right) \\
& - \nabla_\Gamma \xi_{u2} \cdot P_\Gamma \left(\mathbf{F}_{u1} - \mathbf{F}_{u2} \right) \\
& + \mathrm{div}_\Gamma \left[(\xi_{u2} - \xi_{n2} - \xi_{p2}) P_\Gamma \left(\frac{\partial f}{\partial \mathbf{y}} \right) \right] \\
& - \triangle_\Gamma \left[(\xi_{u2} - \xi_{n2} - \xi_{p2}) \frac{\partial f}{\partial H_1} \right] \\
& + (\xi_{u2} - \xi_{n2} - \xi_{p2}) \left[\frac{\partial f}{\partial n} \frac{\partial n_1}{\partial \nu_1} + \frac{\partial f}{\partial p} \frac{\partial p_1}{\partial \nu_1} + \frac{\partial f}{\partial u} \frac{\partial u_1}{\partial \nu_1} \right] \\
& + (\xi_{u2} - \xi_{n2} - \xi_{p2}) \left(\frac{\partial f}{\partial (\nabla \psi)} \cdot D^2 \psi \cdot \nu_1 + \frac{\partial f}{\partial H_1} \frac{\partial H_1}{\partial \nu_1} + f H_1 \right) \qquad (5.4.34)
\end{aligned}
$$

Chapter 6

Second Drift-Diffusion Model: the Phase-Field Method

The shape gradient G in Chapter 5 provides insights into the optimal shape of donor-acceptor interface Γ. On the other hand, it should raise concern when numerical implementation is considered. First of all, it is obviously a very complicated expression, and one must be careful when approximating the shape gradient G numerically. Furthermore, to handle the possibly complex geometry of Γ, one typically needs to put sample points on Γ and use the finite-element method to solve the drift-diffusion equations and the numerical optimization problem. However, solving such shape optimization problems involves updating the geometry and remeshing the domain for each step of optimization, which becomes complicated when the geometry is intricate.

In this chapter, we introduce the phase-field function ϕ as an alternative way to parametrize the geometry. Roughly speaking, ϕ can be viewed as a smooth approximation of a step function; instead of having an abrupt change in function values from one phase to the other, there is a narrow region near the boundary between two phases where this transition takes place, and the width of such region is controlled by a built-in small constant κ of the phase-field equation.

We start by introducing the phase-field method. In specific, we introduce the Allen-Cahn equation and see how this equation describes the evolution of shapes. In Section 6.2, we write down a new drift-diffusion model where all the physical parameters depend on the phase-field function ϕ. In particular, we see that the sharp interface Γ in Chapter 3 is not present in our new drift-diffusion model; instead, we have a volume term in the equations which is mostly supported within a narrow region near Γ. Now the optimal design problem nicely falls into the regime of ordinary optimal control theory of PDE's. In Section 6.3, we derive the sensitivity of our phase-field drift-diffusion model. In Section 6.4, we derive the functional gradient of the photocurrent where we again employ the method of adjoint equations. Having computed the phase-field gradient, we state a gradient-descent type of optimization algorithm in Section 6.5.

6.1 Introduction to Phase Field Method

Phase field method is a method of modeling phase transition. Its root in physics is apparent from its name. There are a variety of phase field models, but the key idea is the same for all of them: phase transition is a process of energy minimization. For a phase field model, let ϕ be the phase field function and $F[\phi]$ be the energy functional of ϕ. Then the evolution of ϕ is always such that $F[\phi]$ is minimized:

$$\frac{\partial \phi}{\partial t} = -\frac{\partial F}{\partial \phi} \tag{6.1.1}$$

The energy functional $F[\phi]$ fully characterizes the phase field model. $\frac{\partial F}{\partial \phi}$ is the *gradient* of F with respect to ϕ, therefore the evolution of phase field function is also referred as *gradient flow*.

A typical form of F is

$$F[\phi;\kappa] = \int_D \frac{\kappa}{2} |\nabla \phi|^2 + f(\phi;\kappa) \tag{6.1.2}$$

where κ is a small positive constant and $f(\phi;\kappa)$ is a double-well potential which attains local minimum at $\phi = 0$ and $\phi = 1$. A minimum value of F can only be obtained from the trade-off between the two terms of the integrand, both of which are controled by the small parameter κ. If ϕ is an element in $L^2(D)$, then the equation of L^2 gradient flow is the Allen-Cahn equation

$$\frac{\partial \phi}{\partial t} = \kappa \nabla^2 \phi - f'(\phi;\kappa) \tag{6.1.3}$$

In what follows, we present two simple examples using an energy functional of the form above to illustrate the phase field method.

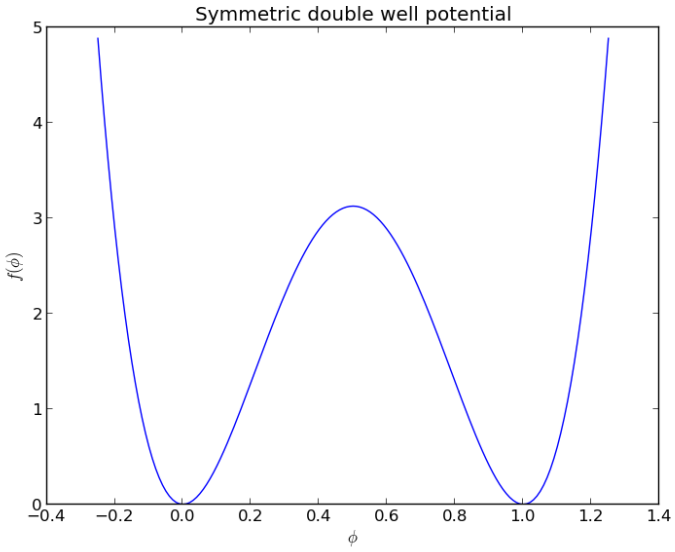

Figure 6.1: Double-well potential for phase field function

6.1.1 Example: mean curvature flow

Let the double well potential take the following form (cf. Figure 6.1)

$$f(\phi;\kappa) = \frac{1}{\kappa} f_s(\phi) \tag{6.1.4}$$

$$\text{where} \quad f_s(\phi;\kappa) = \phi^2(\phi-1)^2 \tag{6.1.5}$$

Therefore the energy functional is

$$F_1[\phi;\kappa] = \int_D \frac{\kappa}{2} |\nabla\phi|^2 + \frac{1}{\kappa}\phi^2(\phi-1)^2 \tag{6.1.6}$$

And the Allen-Cahn equation for (6.1.6) is

$$\frac{\partial\phi}{\partial t} = \kappa\nabla^2\phi - \frac{1}{\kappa} f_s'(\phi) \tag{6.1.7}$$

$$= \kappa\nabla^2\phi - \frac{2}{\kappa}\phi(\phi-1)(2\phi-1) \tag{6.1.8}$$

It is reasonable to assume that the initial phase field function $\phi(t = 0)$ only takes values from $[0, 1]$. The only stationary states of the reaction term are

$$\phi = \{0,\ 0.5,\ 1\}$$

If we ignore the diffusion part of this equation and take a close look at the reaction term, it's easy to see that, for any $\phi \in (0, 0.5)$, $\phi(t \to \infty)$ decays to 0 and for any $\phi \in (0.5, 1)$, $\phi(t \to \infty)$ grows to 1.

It is a well-known fact that in the limit of $\kappa \to 0$, $F_1[\phi; \kappa]$ converges to the interface area in the sense of Γ-convergence; cf. [10, 2] and the references therein. On the other hand, the shape gradient of the surface area $\int_{\Gamma_{01}} 1$ is simply the mean curvature H (Section 4.6). [1] When $\kappa \to 0$, (6.1.8) is indeed the mean curvature flow where the interface is driven by the local curvature on the interface.

We show a 2D example of mean curvature flow in Figure 6.2. The plots show the evolution of the interface $\{\phi = 0.5\}$ in time by solving the Allen-Cahn equation (6.1.8). It is evident that the interface tends to move outward when the curvature is negative and inward when the curvature is positive. The shape of the interface is evolving towards a circle. As time goes by, the phase in the middle eventually vanishes due to the positive curvature of a circle.

[1] Here Γ_{01} is to denote the interface between phase 0 and phase 1. It has nothing to do with Γ-convergence.

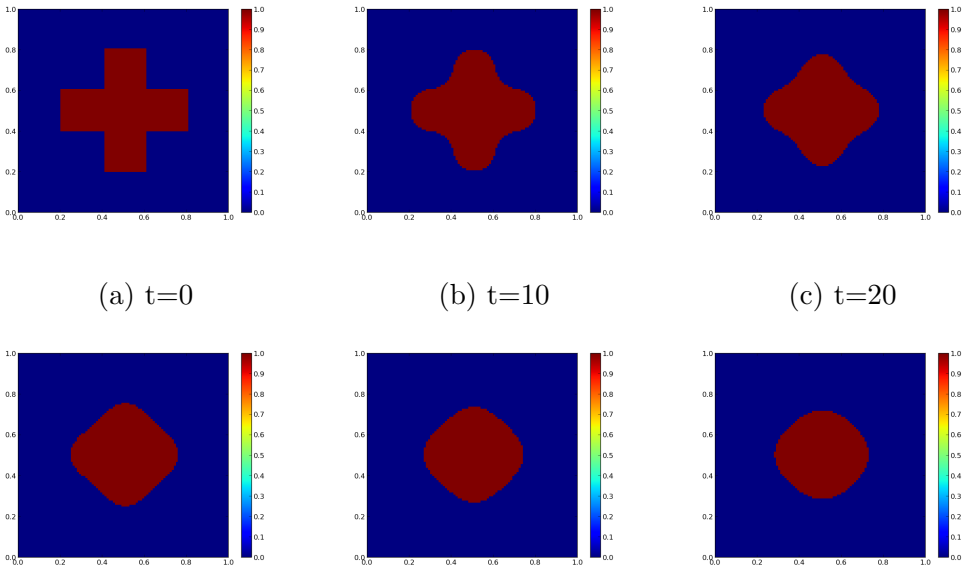

(a) t=0 (b) t=10 (c) t=20

(d) t=30 (e) t=40 (f) t=50

Figure 6.2: Mean curvature flow simulated by phase field method. The interface is the level set of $\{\phi = 0.5\}$. "t" is in numerical unit.

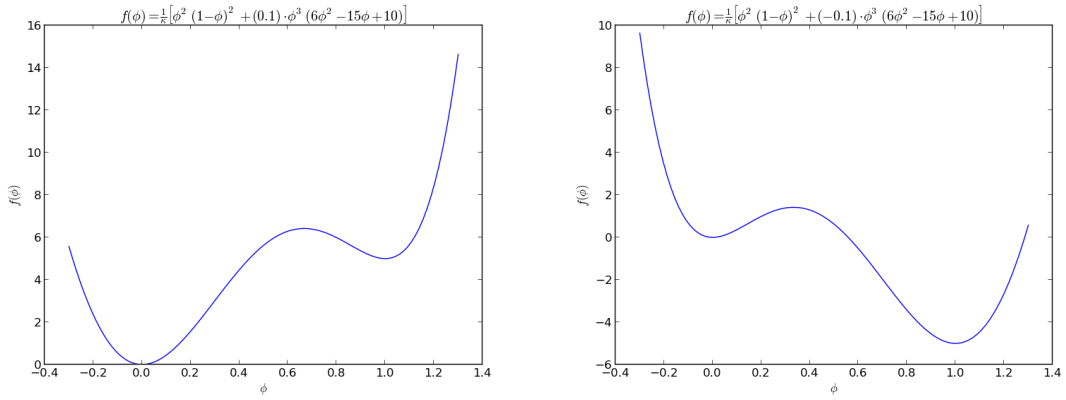

(a) $G = 0.1$ (b) $G = -0.1$

Figure 6.3: Asymmetric double well potentials with differnet values of G

6.1.2 Example: prescribed geometry

In this example, we show that, by choosing a particular form of the double-well potential f, in principle, we are able to realize arbitrary interface by the phase field method. This method is applied when the phase field method is used to solve a shape optimization problem in [25].

Following the idea in [25], we let the double well potential to be

$$f(\phi;\kappa) = \frac{1}{\kappa}\left(f_s(\phi) + G f_a(\phi)\right) \tag{6.1.9}$$

$$\text{where} \quad f_s(\phi) = \phi^2(\phi-1)^2 \tag{6.1.10}$$

$$f_a(\phi) = \phi^3(6\phi^2 - 15\phi + 10) \tag{6.1.11}$$

The corresponding energy functional is

$$F_2[\phi;\kappa] = \int_D \frac{\kappa}{2}\left|\nabla\phi\right|^2 + \frac{1}{\kappa}\left[\phi^2(\phi-1)^2 + G\phi^3(6\phi^2-15\phi+10)\right] \tag{6.1.12}$$

And the Allen-Cahn equation is

$$\begin{aligned}\frac{\partial\phi}{\partial t} &= \kappa\nabla^2\phi - \frac{1}{\kappa}\left[f_s'(\phi) + Gf_a'(\phi)\right] \\ &= \kappa\nabla^2\phi - \frac{1}{\kappa}\left[2\phi(\phi-1)(2\phi-1) + G\cdot 30\phi^2(\phi-1)^2\right]\end{aligned} \tag{6.1.13}$$

If $G \neq 0$, only one of the phases is global minimum and the other is local minimum as is shown in Figure 6.3. A non-zero G drives the local-minimum phase towards the global minimum phase.

To understand why this is so, let consider the case when $G > 0$ (the plot on the left in Figure 6.3). In this case 0 is the global minimum whereas 1 is only a local minimum. The second term of the reaction part of (6.1.13),

$$-\frac{1}{\kappa}G\cdot 30\phi^2(\phi-1)^2$$

is always negative. Therefore, if it dominates the diffusion part as well as the other reaction term, it drives the phase field function towards 0 as long as $\phi < 1$.

In the following 2D example, we would like to construct a phase field function whose $\Gamma_{01} = \{x \in D : \phi(x) = 0.5\}$ level set is a given sinusoidal curve: on the left to Γ_{01}, we have $\phi > 0.5$ and on the right to Γ_{01}, we have $\phi < 0.5$. Therefore, we choose G to be the following function

$$G(\phi) = \begin{cases} -1 & \text{left to } \Gamma_{01} \\ 1 & \text{right to } \Gamma_{01} \end{cases} \tag{6.1.14}$$

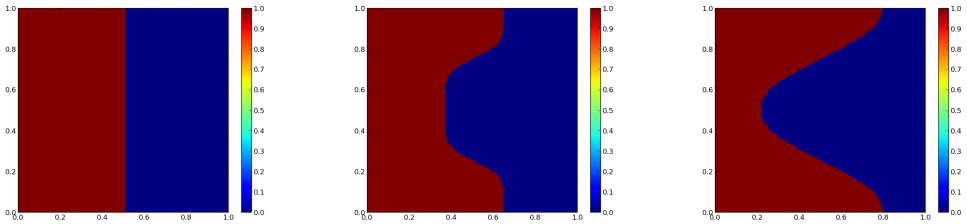

(a) t=0 (b) t=10 (c) t=20

Figure 6.4: Example: evolution towards some given prescribed geometry. t is in numerical unit.

The evolution of ϕ under the Allen-Cahn equation with G in (6.1.14) is given in Figure 6.4.

6.1.3 Optimal design with phase field method

The examples in Section 6.1.1 and 6.1.2 show that, when $G = 0$, the evolution of phase field function is merely an approximation of mean curvature flow, whereas when $G \neq 0$, phase field function may evolve towards a preferred configuration, given that G is sufficiently large to dominate other terms in the Allen-Cahn equation.

- Alternative double-well potentials.

  From a mathematical point of view, the double-well potential $f(\phi; \kappa)$ in (6.1.3) is needed to penalize any value of ϕ between 0 and 1. The particular choices we made in Section 6.1.1 and 6.1.2 are by no means the only viable options. For example, we can consider a family of phase field functions parametrized

by both κ and w in the following way:

$$f(\phi;\kappa,w)=\frac{1}{\kappa}\left(wf_s(\phi)+Gf_a(\phi)\right) \tag{6.1.15}$$

$$\text{where}\quad f_s(\phi)=\phi^2(\phi-1)^2 \tag{6.1.16}$$

$$f_a(\phi)=\phi^3(6\phi^2-15\phi+10) \tag{6.1.17}$$

Note w has to be a positive constant, and if $w=1$, we recover the exact double-well potential in (6.1.9).

The L^2 gradient flow of $\phi(t)$ defined by (6.1.15) incorporates two factors: $wf_s(\phi)$ drives the phase field function to have smaller interface area (i.e. the mean curvature flow), whereas $Gf_a(\phi)$ drives the phase field function according to some given gradient functional. Therefore, $\phi(t)$ is the result of two competing processes. For the purpose of optimization, we have the convenience of choosing w.

- Shape optimization with phase field method

  To adapt a phase field method to shape (i.e. phase) optimization problem, we need to find a proper G which breaks the symmetry between the two phases. In the problem of optimizing photocurrent J with drift-diffusion model, we replace this G with the gradient functional of photocurrent J with respect to the phase field function, i.e.

$$G=\frac{\delta J}{\delta\phi} \tag{6.1.18}$$

  G is again obtained by the optimal control theory introduced in Chapter 2.

In the next section, we specify a drift-diffusion model which depends on a phase field function ϕ. From the point of view of optimal control, ϕ is our control variable. By computing the sensitivity of J with respect to ϕ, we are able to identify the phase-field gradient $\frac{\delta J}{\delta \phi}$.

6.2 Phase-Field Drift-Diffusion Model

In this section, we introduce a drift-diffusion model which is parametrized by a phase field function. Adding to that, we use the Allen-Cahn equation introduced in 6.1.2 as our equation for the phase field function. We show in later sections how we use this equation to find an optimal design.

6.2.1 Drift-diffusion model

For a given design of donor-acceptor complex of an organic solar cell, we can parametrize it by a step function which takes value "1" in the donor phase and "0" in the acceptor phase, and we let ϕ be its phase-field approximation. Like before, the level set $\{\phi = 0.5\}$ has the meaning of donor-acceptor interface.

In the drift-diffusion model we are about to write down, the physical parameters are modeled similar to those in [6] without explaining their physics origin. Their phase dependence is enforced by their dependence on the phase-field function ϕ. Also note that all the equations and physical parameters are nondimensionalized.

- ψ-equation

$$-\lambda^2\nabla\cdot(\epsilon(\phi)\nabla\psi) = p - n \qquad \Omega \qquad (6.2.1)$$

$$\psi = \psi_D \qquad \Gamma_D \qquad (6.2.2)$$

$$\frac{\partial\psi}{\partial\nu} = 0 \qquad \Gamma_N \qquad (6.2.3)$$

- n-equation

$$\begin{cases} \nabla\cdot\mathbf{F}_n = k(\nabla\psi,\phi)u - \gamma(\nabla\psi,\phi)np \\ \mathbf{F}_n = -\mu_n(\nabla\psi,\phi)\left(\nabla n - n\nabla\psi\right) \end{cases} \qquad \Omega \qquad (6.2.4)$$

$$n = n_D \qquad \Gamma_D \qquad (6.2.5)$$

$$\mathbf{F}_n\cdot\nu = 0 \qquad \Gamma_N \qquad (6.2.6)$$

- p-equation

$$\begin{cases} \nabla\cdot\mathbf{F}_p = k(\nabla\psi,\phi)u - \gamma(\nabla\psi,\phi)np \\ \mathbf{F}_p = -\mu_p(\nabla\psi,\phi)\left(\nabla p + p\nabla\psi\right) \end{cases} \qquad \Omega \qquad (6.2.7)$$

$$p = p_D \qquad \Gamma_D \qquad (6.2.8)$$

$$\mathbf{F}_p\cdot\nu = 0 \qquad \Gamma_N \qquad (6.2.9)$$

- u-equation

$$\begin{cases} \nabla\cdot\mathbf{F}_u + d_u(\phi)u = Q - [k(\nabla\psi,\phi)u - \gamma(\nabla\psi,\phi)np] \\ \mathbf{F}_u = -\mu_u(\phi)\nabla u \end{cases} \qquad \Omega \qquad (6.2.10)$$

$$u = u_D \qquad \Gamma_D \qquad (6.2.11)$$

$$\mathbf{F}_u\cdot\nu = 0 \qquad \Gamma_N \qquad (6.2.12)$$

And the physical parameters are modeled as

- Permittivity

$$\begin{aligned}\epsilon(\phi) &= \epsilon_D\ \phi + \epsilon_A(1-\phi) \\ &= \epsilon_A + (\epsilon_D - \epsilon_A)\,\phi \end{aligned} \tag{6.2.13}$$

  where ϵ_D and ϵ_A are constant permittivities for donor and acceptor, respectively.

- Mobilities

$$\mu_p(\nabla\psi,\phi) = \mu_{p,A}(|\nabla\psi|) + [\mu_{p,D}(|\nabla\psi|) - \mu_{p,A}(|\nabla\psi|)]\,\phi \tag{6.2.14}$$

$$\mu_n(\nabla\psi,\phi) = \mu_{n,A}(|\nabla\psi|) + [\mu_{n,D}(|\nabla\psi|) - \mu_{n,A}(|\nabla\psi|)]\,\phi \tag{6.2.15}$$

$$\mu_u(\nabla\psi,\phi) = \mu_{u,A} + [\mu_{u,D} - \mu_{u,A}]\,\phi \tag{6.2.16}$$

  Here we assume that exciton mobility μ_u takes constant values $\mu_{u,D}$ in donor and $\mu_{u,A}$ in acceptor. The mobilities of charge carriers are assumed to take the Poole-Frenkel form (i.e. exponential dependence on the amplitude of electric field). Taking the mobilities in donor for example, we have

$$\mu_{p,D}(\nabla\psi) = \mu_{p,D}(|\nabla\psi| = 0)\exp(\gamma_{p,D}|\nabla\psi|) \tag{6.2.17}$$

$$\mu_{n,D}(\nabla\psi) = \mu_{n,D}(|\nabla\psi| = 0)\exp(\gamma_{n,D}|\nabla\psi|) \tag{6.2.18}$$

  The carrier mobilities in the acceptor have similar form.

- Decay rate of excitons

$$d_u(\phi) = d_{u,A} + (d_{u,D} - d_{u,A})\phi \tag{6.2.19}$$

Here $d_{u,D}$ and $d_{u,A}$ are both assumed to be constant.

- Recombintation coefficient is

$$\gamma(\nabla\psi, \phi) = \frac{1}{\epsilon(\phi)} \left[\mu_n(\nabla\psi, \phi) + \mu_p(\nabla\psi, \phi)\right] \tag{6.2.20}$$

- Dissociation rate of excitons

$$k(\nabla\psi, \phi, \nabla\phi) = k_0 \; g\left(\frac{|\nabla\psi|}{\epsilon(\phi)}\right) f(\phi, |\nabla\phi|) \tag{6.2.21}$$

Here k_0 is understood as a constant. The dependence of k on the electric field $-\nabla\psi$ is enforced by $g\left(\frac{|\nabla\psi|}{\epsilon(\phi)}\right)$. In the series formula (6) of [6], g is a infinite series in the amplitude of electric field. For computational purposes, one must truncate this series into finitely many terms. Here we only keep up to the 1st order term in the electric field for simplcity, assuming $g = 1 + b$ and

$$b = b_0 \frac{|\nabla\psi|}{\epsilon(\phi)} \tag{6.2.22}$$

where b_0 is a numeric constant after nondimensionalization.

In addition, $f(\phi, |\nabla\phi|)$ is a positive smooth function of ϕ and $\nabla\phi$ such that it is significant only when ϕ is not flat, i.e. near the donor-acceptor interface. We also expect f to be bounded when $\kappa \to 0$ and $|\nabla\phi| \to \infty$, Therefore we assume

$$f(\phi, |\nabla\phi|) = \frac{\kappa|\nabla\phi|^2}{1 + \kappa|\nabla\phi|^2} \tag{6.2.23}$$

Note that although all the parameter models are *ad hoc*, they are selected to contain all the desired physics of organic solar cells.

Remark 6.2.1 (Neumann boundary conditions). The boundary conditions on Γ_N are equivalent to homogeneous Neumann boundary conditions, i.e.

$$\frac{\partial \psi}{\partial \nu} = \frac{\partial n}{\partial \nu} = \frac{\partial p}{\partial \nu} = \frac{\partial u}{\partial \nu} = 0 \quad \Gamma_N \tag{6.2.24}$$

Remark 6.2.2 (Comparison with the first drift-diffusion model in Chapter 3). Note that in Chapter 3, we effectively have boundary value problems associated with two distinct regions and we need to define a coupling boundary condition on the interface Γ, whereas in this new drift-diffusion model based on phase field function, we no longer handle Γ explicitly.

Remark 6.2.3 (Dependence on $|\nabla\psi|$). We have assumed that all the parameters only depend on the amplitude of electric field $|\nabla\psi|$, not its direction. This simplifies the boundary conditions on Γ_N for the *adjoint equations* derived in Section 6.4. Note that this is also consistent with all the aforementioned existing drift-diffusion models for organic solar cells [1, 6, 12].

6.2.2 Boundary value problem for the phase field function of an organic solar cell

We use the Allen-Cahn equation in Section 6.1.3 as our equation for the phase field function ϕ. In particular, we choose $w = \frac{1}{4}$ for the double-well potential (6.1.15), which is the same as equation (41) in [25].

Since the phase field function is confined within the region of donor-acceptor complex Ω, we need to impose proper boundary conditions on $\partial\Omega = \Gamma_D \cup \Gamma_N$. On

the Dirichlet boundaries, we require $\phi = 1$ on the anode contact and $\phi = 0$ on the cathode contact to make sure anode is always connected to the donor and cathode is always connected to the acceptor. For the Neumann boundaries Γ_N, we simply let ϕ have homogenous Neumann boundary condition, i.e. $\frac{\partial \phi}{\partial \nu} = 0$.

Hence, we end up with the following boundary value problem for the phase field function:

$$\frac{\partial \phi}{\partial t} = \kappa \nabla^2 \phi - \frac{1}{\kappa}\left[\phi(\phi-1)(\phi-\frac{1}{2}) + G \cdot 30\phi^2(\phi-1)^2\right] \qquad \Omega \qquad (6.2.25)$$

$$\phi = 1 \qquad \Gamma_{D1} \qquad (6.2.26)$$

$$\phi = 0 \qquad \Gamma_{D2} \qquad (6.2.27)$$

$$\frac{\partial \phi}{\partial \nu} = 0 \qquad \Gamma_N \qquad (6.2.28)$$

where G reflects our "preference" on phase distribution.

6.3 Sensitivity Analysis of Phase Field Model

We compute the sensitivity of the drift-diffusion model in Section 6.2.1. with respect to a change in the phase field function. To be specific, if $\phi \in H^1(\Omega)$ is our current phase field function and $\{\psi(\phi), n(\phi), p(\phi), u(\phi)\}$ are the solution to the drift-diffusion equation, we want to determine the equation for their directional derivatives

$$\{\psi'(\phi;\phi_1), n'(\phi;\phi_1), p'(\phi;\phi_1), u'(\phi;\phi_1)\}$$

in the direction of some $\phi_1 \in H^1(\Omega)$. In fact, given that the boundary conditions of ϕ are not supposed to change after any valid perturbation, ϕ_1 must satisfy the constraints

$$\phi_1 = 0 \qquad \Gamma_D \tag{6.3.1}$$

$$\frac{\partial \phi_1}{\partial \nu} = 0 \qquad \Gamma_N \tag{6.3.2}$$

6.3.1 Sensitivity of parameters

For all the parameters, their dependence on ϕ is either explicitly on ϕ and $\nabla\phi$ or through their dependence on the state variables $\{\psi, n, p, u\}$. Let X be any of $\{\psi, n, p, u\}$ or their gradient and consider a general function $y(X, \phi, \nabla\phi)$ To be consistent with the notation of directional derivative introduced in Chapter 2, we let y' be the **complete** sensitivity of y with respect to ϕ in the direction ϕ_1. Then the directional derivative of $y(\phi, \nabla\phi)$ is simply given by the chain rule.

$$\begin{aligned} y'(X, \phi, \nabla\phi; \phi_1) &= \frac{\partial y}{\partial X} X' + \frac{\partial y}{\partial \phi}\phi_1 + \frac{\partial y}{\partial(\nabla\phi)} \cdot \nabla\phi_1 \\ &= \frac{\partial y}{\partial X} X' + \delta y(X, \phi, \nabla\phi; \phi_1) \end{aligned} \tag{6.3.3}$$

Therefore we have defined the **partial** sensitivity of y through its explicit dependence on ϕ and $\nabla\phi$ as [2]

[2]The notation is not standard outside this thesis: in most literature, δy typically refers to the first variation of a function. The author hope this unconventional notation does not cause much confusion.

$$\delta y(\phi;\phi_1) \stackrel{d}{=} \frac{\partial y}{\partial \phi}\phi_1 + \frac{\partial y}{\partial(\nabla\phi)} \cdot \nabla\phi_1 \tag{6.3.4}$$

In what follows, we use the abbreviation $y'(\phi;\phi_1) = y'$ and $\delta y(\phi;\phi_1) = \delta y$; the directional dependence is always implied.

- Partial sensitivity of the permittivity

$$\delta\epsilon = (\epsilon_D - \epsilon_A)\,\phi_1 \tag{6.3.5}$$

- Partial sensitivity of mobilities

$$\delta\mu_p = (\mu_{p,D} - \mu_{p,A})\,\phi_1 \tag{6.3.6}$$

$$\delta\mu_n = (\mu_{n,D} - \mu_{n,A})\,\phi_1 \tag{6.3.7}$$

$$\delta\mu_u = (\mu_{u,D} - \mu_{u,A})\,\phi_1 \tag{6.3.8}$$

- Partial sensitivity of decay rate of excitons

$$\delta d_u = (d_{u,D} - d_{u,A})\phi_1 \tag{6.3.9}$$

- Partial sensitivity of recombintation rate of electrons and holes

$$\delta\gamma = \left(-\frac{\delta\epsilon}{\epsilon^2}\right)(\mu_n + \mu_p) + \frac{1}{\epsilon}\,(\delta\mu_n + \delta\mu_p) \tag{6.3.10}$$

- Partial sensitivity of exciton dissociation rate

$$\delta k = k_0\frac{\partial g}{\partial \phi} f\phi_1 + k_0 g\left(\frac{\partial f}{\partial \phi}\phi_1 + \frac{\partial f}{\partial(\nabla\phi)} \cdot \nabla\phi_1\right) \tag{6.3.11}$$

Given the explicit definition of g and f, it is straightforward to compute their partial derivatives with respect to ϕ and $\nabla\phi$.

6.3.2 Sensitivity of drift-diffusion equations

Details of the computation are saved in Appendix C. Here we only state the result. In particular, $\{\psi', n', p', u'\}$ satisfy the following boundary value problems:

- Sensitivity of ψ-equation

$$-\lambda^2\nabla\cdot(\epsilon\nabla\psi') - p' + n' = \lambda^2\nabla\cdot(\delta\epsilon\,\nabla\psi) \qquad \Omega \qquad (6.3.12)$$

$$\psi' = 0 \qquad \Gamma_D \qquad (6.3.13)$$

$$\frac{\partial\psi'}{\partial\nu} = 0 \qquad \Gamma_N \qquad (6.3.14)$$

- Sensitivity of n-equation

$$\begin{aligned}
&-\nabla\cdot\left[\frac{\partial\mu_n}{\partial(\nabla\psi)}\cdot\nabla\psi'\,(\nabla n - n\nabla\psi) - \mu_n n\nabla\psi'\right]\\
&-\left(u\frac{\partial k}{\partial(\nabla\psi)} - np\frac{\partial\gamma}{\partial(\nabla\psi)}\right)\cdot\nabla\psi'\\
&-\nabla\cdot\left[\mu_n\,(\nabla n' - n'\nabla\psi)\right] + \gamma n' p\\
&+\gamma n p'\\
&-ku'\\
&=\nabla\cdot\left[(\delta\mu_n)\,(\nabla n - n\nabla\psi)\right] + \left[(\delta k)u - (\delta\gamma)np\right] \qquad \Omega \qquad (6.3.15)
\end{aligned}$$

$$n' = 0 \qquad \Gamma_D \qquad (6.3.16)$$

$$\frac{\partial n'}{\partial\nu} = 0 \qquad \Gamma_N \qquad (6.3.17)$$

- Sensitivity of p-equation

$$
\begin{aligned}
&- \nabla \cdot \left[\frac{\partial \mu_p}{\partial(\nabla\psi)} \cdot \nabla\psi' \left(\nabla p + p\nabla\psi\right) + \mu_p p \nabla\psi' \right] \\
&- \left(u \frac{\partial k}{\partial(\nabla\psi)} - np \frac{\partial \gamma}{\partial(\nabla\psi)} \right) \cdot \nabla\psi' \\
&+ \gamma n' p \\
&- \nabla \cdot \left[\mu_p \left(\nabla p' + p'\nabla\psi\right) \right] + \gamma n p' \\
&- k u' \\
&= \nabla \cdot \left[(\mu_p) \left(\nabla p + p\nabla\psi\right) \right] + \left[(\delta k) u - (\delta\gamma) np \right] \qquad \Omega \qquad (6.3.18)
\end{aligned}
$$

$$
p' = 0 \qquad \Gamma_D \qquad (6.3.19)
$$

$$
\frac{\partial p'}{\partial \nu} = 0 \qquad \Gamma_N \qquad (6.3.20)
$$

- Sensitivity of u-equation

$$\begin{aligned}
&\left(u\frac{\partial k}{\partial(\nabla\psi)} - np\frac{\partial \gamma}{\partial(\nabla\psi)}\right)\cdot\nabla\psi' \\
&-\gamma n'p \\
&-\gamma np' \\
&-\nabla\cdot(\mu_u\nabla u') + (d_u + k)u' \\
&= \nabla\cdot[(\delta\mu_u)\nabla u] - (\delta d_u)u - [(\delta k)u - (\delta\gamma)np] \qquad \Omega \qquad (6.3.21)
\end{aligned}$$

$$u' = 0 \qquad \Gamma_D \qquad (6.3.22)$$

$$\frac{\partial u'}{\partial \nu} = 0 \qquad \Gamma_N \qquad (6.3.23)$$

6.4 Phase-Field Gradient and First-Order Optimality Condition

In this section, we derive the first-order sensitivity of photocurrent with respect to the phase field function ϕ. To that end, we again form the Lagrangian functional and then the adjoint equations. By the end of this section, we obtain an explicit formula for the L^2 phase-field gradient functional G.

We introduce the Lagrange multiplier $\{\xi_\psi, \xi_n, \xi_p, \xi_u\}$, and form the Lagrangian functional as below

$$\mathcal{L} = J - \mathcal{L}_\psi - \mathcal{L}_n - \mathcal{L}_p - \mathcal{L}_u \qquad (6.4.1)$$

where

$$J = -\int_{\Gamma_{D1}} (\mathbf{F}_p - \mathbf{F}_n) \cdot \nu \tag{6.4.2}$$

$$\mathcal{L}_\psi = \int_\Omega \lambda^2 \epsilon \nabla\psi \cdot \nabla\xi_\psi + (n-p)\xi_\psi - \int_{\Gamma_D} \lambda^2 \epsilon \frac{\partial\psi}{\partial\nu}\xi_\psi \tag{6.4.3}$$

$$\mathcal{L}_n = \int_\Omega \mu_n(\nabla n - n\nabla\psi) \cdot \nabla\xi_n - (ku - \gamma np)\xi_n + \int_{\Gamma_D} \mathbf{F}_n \cdot \nu\, \xi_n \tag{6.4.4}$$

$$\mathcal{L}_p = \int_\Omega \mu_p(\nabla p + p\nabla\psi) \cdot \nabla\xi_p - (ku - \gamma np)\xi_n + \int_{\Gamma_D} \mathbf{F}_p \cdot \nu\, \xi_p \tag{6.4.5}$$

$$\mathcal{L}_u = \int_\Omega \mu_u \nabla u \cdot \nabla\xi_u + [d_u u - Q + (ku - \gamma np)]\, \xi_u + \int_{\Gamma_D} \mathbf{F}_u \cdot \nu\, \xi_u \tag{6.4.6}$$

Each of $\{\mathcal{L}_\psi, \mathcal{L}_n, \mathcal{L}_p, \mathcal{L}_u\}$ is the weak form of one of the drift-diffusion equations. Note that we have applied the flux boundary conditions of $\{\psi, n, p, u\}$ on Γ_N to obtain the expressions above.

Now we take the directional derivative of $\mathcal{L}$ in some valid direction ϕ_1. In order to simplify the derivation, we repeatedly make use of the boundary conditions of $\{\psi, n, p, u\}$ and $\{\psi', n', p', u'\}$ and the fact that $\{\mu_n, \mu_p, k, \gamma\}$ only depend on the amplitude of electric field $|\nabla\psi|$.

- J'

$$J' = -\int_{\Gamma_{D1}} \left(\mathbf{F}'_p - \mathbf{F}'_n\right) \cdot \nu \tag{6.4.7}$$

- $\mathcal{L}'_\psi$

$$
\begin{aligned}
&\mathcal{L}'_{\psi} \\
&= \int_{\Omega} \lambda^2(\delta\epsilon)\nabla\psi\cdot\nabla\xi_{\psi} + \lambda^2\epsilon\nabla\psi'\cdot\nabla\xi_{\psi} + (n'-p')\xi_{\psi} - \int_{\Gamma_D}\lambda^2\epsilon\frac{\partial\psi'}{\partial\nu}\xi_{\psi} \\
&= \int_{\Omega} \lambda^2(\delta\epsilon)\nabla\psi\cdot\nabla\xi_{\psi} + \int_{\Omega}\left[-\lambda^2\nabla\cdot(\epsilon\nabla\xi_{\psi})\right]\psi' + \xi_{\psi}n' - \xi_{\psi}p' \\
&\quad + \int_{\Gamma_N}\lambda^2\epsilon\frac{\partial\xi_{\psi}}{\partial\nu}\psi' - \int_{\Gamma_D}\lambda^2\epsilon\frac{\partial\psi'}{\partial\nu}\xi_{\psi}
\end{aligned} \tag{6.4.8}
$$

- $\mathcal{L}'_n$

$$
\begin{aligned}
&\mathcal{L}'_n \\
&= \int_{\Omega}(\delta\mu_n)(\nabla n - n\nabla\psi)\cdot\nabla\xi_n - \left[(\delta k)u - (\delta\gamma)np\right]\xi_n \\
&\quad + \int_{\Omega}\left[(\nabla n - n\nabla\psi)\cdot\nabla\xi_n\frac{\partial\mu_n}{\partial(\nabla\psi)} - \xi_n\left(u\frac{\partial k}{\partial(\nabla\psi)} - np\frac{\partial\gamma}{\partial(\nabla\psi)}\right)\right]\cdot\nabla\psi' \\
&\quad + \int_{\Omega}\mu_n(\nabla n' - n'\nabla\psi - n\nabla\psi')\cdot\nabla\xi_n - (ku' - \gamma n'p - \gamma np')\xi_n \\
&\quad + \int_{\Gamma_D}\mathbf{F}'_n\cdot\nu\,\xi_n \\
&= \int_{\Omega}(\delta\mu_n)(\nabla n - n\nabla\psi)\cdot\nabla\xi_n - \left[(\delta k)u - (\delta\gamma)np\right]\xi_n \\
&\quad + \int_{\Omega}\left[-\nabla\cdot(\mu_n\nabla\xi_n) - \mu_n\nabla\psi\cdot\nabla\xi_n + \gamma p\xi_n\right]n' - k\xi_n u' + \gamma n\xi_n p' \\
&\quad + \int_{\Omega}\Bigg[\quad\nabla\cdot(\mu_n n\nabla\xi_n) \\
&\qquad\quad - \nabla\cdot\left((\nabla n - n\nabla\psi)\cdot\nabla\xi_n\frac{\partial\mu_n}{\partial(\nabla\psi)}\right) \\
&\qquad\quad + \nabla\cdot\left(\xi_n\left(u\frac{\partial k}{\partial(\nabla\psi)} - np\frac{\partial\gamma}{\partial(\nabla\psi)}\right)\right)\Bigg]\psi' \\
&\quad + \int_{\Gamma_N}\mu_n\left(n' - n\psi'\right)\frac{\partial\xi_n}{\partial\nu} + \int_{\Gamma_D}\mathbf{F}'_n\cdot\nu\,\xi_n
\end{aligned} \tag{6.4.9}
$$

- $\mathcal{L}'_p$

$$
\begin{aligned}
&\mathcal{L}'_p \\
=&\int_\Omega (\delta\mu_p)(\nabla p + p\nabla\psi)\cdot\nabla\xi_p - [(\delta k)u - (\delta\gamma)np]\,\xi_p \\
&+\int_\Omega \left[(\nabla p + p\nabla\psi)\cdot\nabla\xi_p \frac{\partial\mu_p}{\partial(\nabla\psi)} - \xi_p\left(u\frac{\partial k}{\partial(\nabla\psi)} - np\frac{\partial\gamma}{\partial(\nabla\psi)}\right)\right]\cdot\nabla\psi' \\
&+\int_\Omega \mu_p(\nabla p' + p'\nabla\psi + p\nabla\psi')\cdot\nabla\xi_p - (ku' - \gamma n'p - \gamma np')\xi_p \\
&+\int_{\Gamma_D} \mathbf{F}'_p\cdot\nu\,\xi_p \\
=&\int_\Omega (\delta\mu_p)(\nabla p + p\nabla\psi)\cdot\nabla\xi_p - [(\delta k)u - (\delta\gamma)np]\,\xi_p \\
&+\int_\Omega [-\nabla\cdot(\mu_p\nabla\xi_p) + \mu_p\nabla\psi\cdot\nabla\xi_p + \gamma n\xi_p]\,p' - k\xi_p u' + \gamma p\xi_p n' \\
&+\int_\Omega [-\nabla\cdot(\mu_p p\nabla\xi_p) \\
&\qquad -\nabla\cdot\left((\nabla p + p\nabla\psi)\cdot\nabla\xi_p\frac{\partial\mu_p}{\partial(\nabla\psi)}\right) \\
&\qquad +\nabla\cdot\left(\xi_p\left(u\frac{\partial k}{\partial(\nabla\psi)} - np\frac{\partial\gamma}{\partial(\nabla\psi)}\right)\right)]\,\psi' \\
&+\int_{\Gamma_N}\mu_p\,(p' + p\psi')\,\frac{\partial\xi_p}{\partial\nu} + \int_{\Gamma_D}\mathbf{F}'_p\cdot\nu\,\xi_p
\end{aligned}
\tag{6.4.10}
$$

- $\mathcal{L}'_u$

$$
\begin{aligned}
&\mathcal{L}'_u \\
&= \int_\Omega (\delta\mu_u)\nabla u \cdot \nabla\xi_u + \left[(\delta d_u)u + (\delta k)u - (\delta\gamma)np)\right]\xi_u \\
&\quad + \int_\Omega \mu_u \nabla u' \cdot \nabla\xi_u + d_u u'\xi_u + (ku' - \gamma n'p - \gamma np')\xi_u \\
&\quad + \int_{\Gamma_D} \mathbf{F}'_u \cdot \nu\xi_u \\
&= \int_\Omega (\delta\mu_u)\nabla u \cdot \nabla\xi_u + \left[(\delta d_u)u + (\delta k)u - (\delta\gamma)np)\right]\xi_u \\
&\quad + \int_\Omega \left[-\nabla\cdot(\mu_u\nabla\xi_u) + d_u\xi_u + k\xi_u\right]u' - \gamma p\xi_u n' - \gamma n\xi_u p' \\
&\quad + \int_{\Gamma_N} \mu_u u' \frac{\partial\xi_u}{\partial\nu} + \int_{\Gamma_D} \mathbf{F}'_u \cdot \nu\xi_u
\end{aligned}
\tag{6.4.11}
$$

By re-arranging the integrals in $\mathcal{L}$ by their domain of integration and their integrands, we obtain the boundary value problems for the adjoint variables $\xi_\psi, \xi_n, \xi_p, \xi_u$.

- In Ω, we have a system of linear partial differential equations

$$
\begin{aligned}
&-\lambda^2\nabla\cdot(\epsilon\nabla\xi_\psi)\\
&+[\nabla\cdot(\mu_n n\nabla\xi_n)\\
&\quad-\nabla\cdot\left((\nabla n-n\nabla\psi)\cdot\nabla\xi_n\frac{\partial\mu_n}{\partial(\nabla\psi)}\right)\\
&\quad+\nabla\cdot\left(\xi_n\left(u\frac{\partial k}{\partial(\nabla\psi)}-np\frac{\partial\gamma}{\partial(\nabla\psi)}\right)\right)]\\
&+[-\nabla\cdot(\mu_p p\nabla\xi_p)\\
&\quad-\nabla\cdot\left((\nabla p+p\nabla\psi)\cdot\nabla\xi_p\frac{\partial\mu_p}{\partial(\nabla\psi)}\right)\\
&\quad+\nabla\cdot\left(\xi_p\left(u\frac{\partial k}{\partial(\nabla\psi)}-np\frac{\partial\gamma}{\partial(\nabla\psi)}\right)\right)]=0
\end{aligned}
\tag{6.4.12}
$$

$$
\xi_\psi+[-\nabla\cdot(\mu_n\nabla\xi_n)-\mu_n\nabla\psi\cdot\nabla\xi_n+\gamma p\xi_n]+\gamma p\xi_p-\gamma p\xi_u=0 \tag{6.4.13}
$$

$$
-\xi_\psi+\gamma n\xi_n+[-\nabla\cdot(\mu_p\nabla\xi_p)+\mu_p\nabla\psi\cdot\nabla\xi_p+\gamma n\xi_p]-\gamma n\xi_u=0 \tag{6.4.14}
$$

$$
-k\xi_n-k\xi_p+[-\nabla\cdot(\mu_u\nabla\xi_u)+(d_u+k)\xi_u]=0 \tag{6.4.15}
$$

- Boundary conditions

$$
\xi_\psi=\xi_u=0,\ \xi_n=1,\ \xi_p=-1 \qquad \Gamma_{D1} \tag{6.4.16}
$$

$$
\xi_\psi=\xi_n=\xi_p=\xi_u=0 \qquad \Gamma_D\setminus\Gamma_{D1} \tag{6.4.17}
$$

$$
\frac{\partial\xi_\psi}{\partial\nu}=\frac{\partial\xi_n}{\partial\nu}=\frac{\partial\xi_p}{\partial\nu}=\frac{\partial\xi_u}{\partial\nu}=0 \qquad \Gamma_N \tag{6.4.18}
$$

Note that, compared to the adjoint quations obtained in Chapter 5, the adjoint equations for the phase-field drift-diffusion model is much more "friendly". In particular, we don't need to handle the complicated boundary condition on the interface Γ.

Finally, given the solution to the state equations ψ, n, p, u and the solutions to the adjoint equations $\xi_\psi, \xi_n, \xi_p, \xi_u$, we obtain the sensitivity of current J with respect to the phase field function ϕ

$$\begin{aligned} J' = \int_\Omega & \left(-\lambda^2 \nabla\psi \cdot \nabla\xi_\psi\right)(\delta\epsilon) \\ & + \left[-(\delta\mu_n)\left(\nabla n - n\nabla\psi\right) \cdot \nabla\xi_n\right] \\ & + \left[-(\delta\mu_p)\left(\nabla p + p\nabla\psi\right) \cdot \nabla\xi_p\right] \\ & + \left[-(\delta\mu_u)\nabla u \cdot \nabla\xi_u - (\delta d_u)u\xi_u\right] \\ & + \left[(\delta k)u - (\delta\gamma)np\right](\xi_n + \xi_p - \xi_u) \end{aligned} \tag{6.4.19}$$

Next we substitute the sensitivities of parameters into the formula above.

$$
\begin{aligned}
J'(\phi;\phi_1) = \int_\Omega & \left(-\lambda^2 \nabla\psi\cdot\nabla\xi_\psi\right)(\epsilon_D-\epsilon_A)\phi_1 \\
& + \left[-(\mu_{n,D}-\mu_{n,A})\left(\nabla n - n\nabla\psi\right)\cdot\nabla\xi_n\right]\phi_1 \\
& + \left[-(\mu_{p,D}-\mu_{p,A})\left(\nabla p + p\nabla\psi\right)\cdot\nabla\xi_p\right]\phi_1 \\
& + \left[-(\mu_{u,D}-\mu_{u,A})\nabla u\cdot\nabla\xi_u - (d_{u,D}-d_{u,A})u\xi_u\right]\phi_1 \\
& + u(\xi_n+\xi_p-\xi_u)\left[k_0\frac{\partial g}{\partial\phi}f\phi_1 + k_0 g\left(\frac{\partial f}{\partial\phi}\phi_1 + \frac{\partial f}{\partial(\nabla\phi)}\cdot\nabla\phi_1\right)\right] \\
& - np(\xi_n+\xi_p-\xi_u)\left\{-\frac{\epsilon_D-\epsilon_A}{\epsilon^2}(\mu_n+\mu_p)\right. \\
& \qquad \left. + \frac{1}{\epsilon}\left[(\mu_{n,D}-\mu_{n,A})+(\mu_{p,D}-\mu_{p,A})\right]\right\}\phi_1
\end{aligned}
\tag{6.4.20}
$$

Note the presence of $\nabla\phi_1$ in the formula above. To obtain the L^2 **gradient functional** G with respect to ϕ, we apply one last integration by parts and make use of the boundary condition of ϕ. Finally we have an explicit formula

$$
J'(\phi;\phi_1) = \int_\Omega G\ \phi_1 \tag{6.4.21}
$$

where

$$
\begin{aligned}
G = & \left(-\lambda^2 \nabla\psi \cdot \nabla\xi_\psi\right)(\epsilon_D - \epsilon_A) \\
& + \left[-(\mu_{n,D} - \mu_{n,A})(\nabla n - n\nabla\psi) \cdot \nabla\xi_n\right] \\
& + \left[-(\mu_{p,D} - \mu_{p,A})(\nabla p + p\nabla\psi) \cdot \nabla\xi_p\right] \\
& + \left[-(\mu_{u,D} - \mu_{u,A})\nabla u \cdot \nabla\xi_u - (d_{u,D} - d_{u,A})u\xi_u\right] \\
& + u(\xi_n + \xi_p - \xi_u)k_0 \frac{\partial g}{\partial \phi} f \\
& + u(\xi_n + \xi_p - \xi_u)k_0 g \frac{\partial f}{\partial \phi} \\
& - \nabla \cdot \left[u(\xi_n + \xi_p - \xi_u)k_0 g \frac{\partial f}{\partial(\nabla\phi)}\right] \\
& - np(\xi_n + \xi_p - \xi_u)\left\{-\frac{\epsilon_D - \epsilon_A}{\epsilon^2}(\mu_n + \mu_p)\right. \\
& \qquad \left. + \frac{1}{\epsilon}\left[(\mu_{n,D} - \mu_{n,A}) + (\mu_{p,D} - \mu_{p,A})\right]\right\} \qquad (6.4.22)
\end{aligned}
$$

6.5 Optimization Algorithm

The optimization algorithm we use was introduced in [25]: the Allen-Cahn equation (6.2.25) is used to update the phase field function from some given ϕ towards the optimal phase field function $\phi_{optimal}$, where the asymmetry term G in (6.2.25) is replaced by the L^2-gradient functional obtained in (6.4.22) up to a normalization constant. It has a gradient-descent flavor because a positive G drives ϕ towards 0 and a negative G drives ϕ towards 1. On the other hand, one should keep in mind that (6.2.25) tends to reduce interface area when G is not large enough; cf. Section

6.1.2 and 6.1.3.

Given the nonlinear nature of the optimization problem, we must use an iterative method to search for the optimal phase field function. Let $\{\phi^{(i)}\}$ $i = 0, 1, ...$ be the optimization sequence of the phase field function. We start with some $\phi^{(0)}$, solve the state equations to obtain $\{\psi^{(0)}, n^{(0)}, p^{(0)}, u^{(0)}\}$, and compute the anode photocurrent $J^{(0)} = -\int_{\Gamma_{D1}} (\mathbf{F}_p^{(0)} - \mathbf{F}_n^{(0)}) \cdot \nu$. We also predefine a positive tolerance parameter $\epsilon_{tol} << 1$ to determine when the iteration should be terminated.

Then for each $i = 1, 2, ...,$

1. Solve the adjoint equations (6.4.12-6.4.15) and obtain $\{\xi_\psi^{(i)}, \xi_n^{(i)}, \xi_p^{(i)}, \xi_u^{(i)}\}$
2. Compute the L^2 gradient functional $G^{(i)}$ in (6.4.22)
3. Substitute $\widetilde{G}^{(i)} = \frac{G^{(i)}}{C}$ into the Allen-Cahn equation (6.2.25) [3]. and solve it with initial time $t^{(i)}$ and some chosen terminal time $t^{(i+1)}$.
4. Solve the state equations to update the state variables to $\{\psi^{(i+1)}, n^{(i+1)}, p^{(i+1)}, u^{(i+1)}\}$.
5. Compute the photocurrent $J^{(t+1)} = -\int_{\Gamma_{D1}} (\mathbf{F}_p - \mathbf{F}_n) \cdot \nu$ using the newly obtained state variables.
    - If $J^{(t+1)} - J^{(t)} < -\epsilon_{tol}$, we go back to Step "1" to start another iteration step;

[3] Here C is a normalization constant and can be chosen to be $\|G^{(i)}\|_{L^\infty(\Omega)}$

- If $J^{(t+1)} - J^{(t)} > -\epsilon_{tol}$, we decrease the step size of $\Delta t^{(i+1)} = t^{(i+1)} - t^{(i)}$ to avoid overshooting and go to Step "4". We do this line search for a finite number of times. If a descent step $\Delta t^{(i+1)}$ satisfying the criterion $J^{(t+1)} - J^{(t)} < -\epsilon_{tol}$ is found, we continue the iteration by going to Step "1"; otherwise, we terminate the iteration and return the current phase field function $\phi^{(i)}$.

In next chapter, we move into the nitty-gritty of the numerical implementation of this optimization algorithm and present some examples of optimal design.

Chapter 7

Numerical Optimization with the Phase-Field Drift-Diffusion Model

This chapter is a continuation of Chapter 6. We look at the numerical implementation of the optimization algorithm in Section 6.5. The numerical methods are illustrated with two-dimensional examples, but its generalization to three dimensions is straightforward.

7.1 Numerical Methods for Solving Partial Differential Equations

According to the optimization algorithm in Section 6.5, each iteration step involves three successive steps:

- solving the adjoint equations for adjoint variables $\{\xi_\psi, \xi_n, \xi_p, \xi_u\}$
- solving the Allen-Cahn equation for updating the phase field function ϕ
- solving the state equations (i.e. the drift-diffusion equations) for $\{\psi, n, p, u\}$.

These steps are discussed in details seperately, but the method we use to solve all the equations is based on a *finite difference method*.

7.1.1 Mesh for numerical solutions

We let Ω be the unit square in the xy-plane and generate a uniform rectangular mesh on it. The x-spacing is $h_x = \frac{1}{N_x}$ and the y-spacing is $h_y = \frac{1}{N_y}$. Therefore, for each row and each column, there are $N_x + 1$ and $N_y + 1$ grid points, respectively. The coordinates of any grid point are $P_{ij} = (x_i, y_j) = (\frac{i}{N_x}, \frac{j}{N_y})$, where $0 \leq i \leq N_x$ and $0 \leq j \leq N_y$. In particular, P_{ij} is on the Dirichlet boundaries if $i \in \{0, N_x\}, 0 \leq j \leq N_y$, and it is on the Neumann boundaries if $0 < i < N_x, j \in \{0, N_y\}$.

(*a graph of rectangular mesh should be included*)

7.1.2 Numerical method for solving state equations

1. Stationary solutions as the limit of time-dependent solutions

The state equations of our optimization problem are the *stationary* drift-

diffusion equations defined in Section 6.2. Note that, without the exciton equation, it becomes the standard drift-diffusion model for semiconductor devices. The numerical solutions to the drift-diffusion model have been a challenging task, mostly because of the convection terms in both equations for the electrons and the holes. Nonetheless, much has been known about its numerical solution. There are two perspectives on how to solve the stationary drift-diffusion equations.

- Iterative methods

  Most iterative methods are built upon two basic methods: the Gummel's map and the Newton's method. For both methods, one needs to have some initial guess of the solution and hope the solution converges to a faithful numerical approximation of an analytical solution.

  Gummel's map is known to be less sensitive to the initial guess but also has a relatively slow rate of convergence. By contrast, Newton's map has better convergence rate, but it's much more sensitive to the initial guess. Note that, before convergence, any intermediate step of the iterative process has no physical meaning. Details of the Gummel's map and the Newton's method can be found in [21, 22].

- Limiting solution of the transient drift-diffusion model.

  Recall that the stationary drift-diffusion model is in fact obtained from the time-dependent drift-diffusion model by setting the time derivative $\frac{\partial}{\partial t}$

to be zero [22]. Therefore, it is natural to obtain the stationary solution by solving the time-dependent drift-diffusion equations for a sufficiently large time period. This approach is arguably more "physical" in that it in fact simulates the evolution of electrical potentials and particle densities in time, and can be compared to experimental results.

In our work, we adopt the **second** perspective and solve the following time dependent drift-diffusion equations

$$-\lambda^2 \nabla \cdot (\epsilon \nabla \psi) = p - n \tag{7.1.1}$$

$$\frac{\partial n}{\partial t} = -\nabla \cdot \mathbf{F}_n + (ku - \gamma np) \tag{7.1.2}$$

$$\frac{\partial p}{\partial t} = -\nabla \cdot \mathbf{F}_p + (ku - \gamma np) \tag{7.1.3}$$

$$\frac{\partial u}{\partial t} = -\nabla \cdot \mathbf{F}_u + Q - d_u u - (ku - \gamma np) \tag{7.1.4}$$

$$\tag{7.1.5}$$

Letting $t \to \infty$, we obtain the stationary solutions.

2. Spatial discretization

To illustrate the spatial discretization of the divergence operator and gradient operator, we pick an arbitrary interior node $P_{i,j} = (x_i, y_j)$, We also let $P_{i+\frac{1}{2},j} = (x_{i+\frac{1}{2}}, y_j)$ be the mid-point between $P_{i,j}$ and $P_{i+1,j}$. Therefore $x_{i+\frac{1}{2}} = (i+\frac{1}{2})h_x$. Similar definitions hold for $P_{i,j+\frac{1}{2}}$, $P_{i-\frac{1}{2},j}$, and $P_{i,j-\frac{1}{2}}$.

- Approximation of divergence operator $(\nabla \cdot \mathbf{F})_{ij}$

  We let $\mathbf{F} = (F^x, F^y)$ be a two-dimensional flux vector. We then use the

standard central difference scheme to discretize divergence operator

$$(\nabla \cdot \mathbf{F})_{i,j} = \frac{F^x_{i+\frac{1}{2},j} - F^x_{i-\frac{1}{2},j}}{h_x} + \frac{F^y_{i,j+\frac{1}{2}} - F^y_{i,j+\frac{1}{2}}}{h_y} \tag{7.1.6}$$

Note that $F^x_{i,j+\frac{1}{2}}$ and $F^y_{i+\frac{1}{2},j}$ are not needed for our purpose, since all we care about is the divergence of a flux at a grid point.

- Approximation of diffusion flux $\mathbf{F} = -\mu\nabla y$

  If the flux is a simple diffusive flux, we again apply central difference scheme to discretize the gradient operator

$$F^x_{i+\frac{1}{2},j} = -\mu_{i+\frac{1}{2},j}\frac{u_{i+1,j} - u_{i,j}}{h_x} \tag{7.1.7}$$

$$F^y_{i,j+\frac{1}{2}} = -\mu_{i,j+\frac{1}{2}}\frac{u_{i,j+1} - u_{i,j}}{h_y} \tag{7.1.8}$$

- Approximation of convection-diffusion flux $\mathbf{F} = -\mu(\nabla y + y\nabla\psi)$

  It is well-known that, for the convection-diffusion flux, an ordinary central difference scheme causes numerical instability. The **Scharfetter-Gummel** discretization scheme was invented to ensure the stability of convection-diffusion fluxes in drift-diffusion models, and it can be implemented on either a structured mesh (such as the one we use) or an unstructured finite element mesh. We refer the readers to [21] and [29] for details of the formulation. Below we simply state the formula for the Scharfetter-Gummel flux approximation for the electron flux $\mathbf{F}_n = -\mu_n(\nabla n - n\nabla\psi)$; the expression for $\mathbf{F}_p$ is easily obtained by chang-

ing the ψ in $\mathbf{F}_n$ to $-\psi$.

$$F^x_{n\,(i+\frac{1}{2},j)} = -\mu_{n\,(i+\frac{1}{2},j)}\,\frac{n_{i+1,j}B(\psi_{i+1,j}-\psi_{i,j}) - n_{i,j}B(\psi_{i,j}-\psi_{i+1,j})}{h_x} \tag{7.1.9}$$

$$F^y_{n\,(i,j+\frac{1}{2})} = -\mu_{n\,(i,j+\frac{1}{2})}\,\frac{n_{i,j+1}B(\psi_{i,j+1}-\psi_{i,j}) - n_{i,j}B(\psi_{i,j}-\psi_{i,j+1})}{h_y} \tag{7.1.10}$$

where $B(z)$ is the Bernoulli function

$$B(z) = \begin{cases} \frac{z}{e^z-1} & z \neq 0 \\ 1 & z = 0 \end{cases} \tag{7.1.11}$$

Note that when there is no convection, i.e. $\nabla\psi = 0$, we effectively have a pure diffusion, and this Scharfetter-Gummel flux recovers exactly the central-difference scheme for diffusive fluxes.

3. Time discretization

To numerically solve the time-dependent equations, we need to discretize "time" and transform differentiation into a difference. We pick a sufficiently small $\Delta t > 0$ as our time step for solving (7.1.2-7.1.4). Specifically, let

$$t_l = l\Delta t,\ l = 0, 1, ...$$

be the discretized times, and we use the following formulae for updating so-

lutions in time

$$-\lambda^2 \nabla \cdot (\epsilon \nabla \psi^{(l+1)}) = p^{(l)} - n^{(l)} \tag{7.1.12}$$

$$\frac{n^{(l+1)} - n^{(l)}}{\Delta t} = -\nabla \cdot \mathbf{F}_n^{(l+1)} + (ku - \gamma np)^{(l)} \tag{7.1.13}$$

$$\frac{p^{(l+1)} - p^{(l)}}{\Delta t} = -\nabla \cdot \mathbf{F}_p^{(l+1)} + (ku - \gamma np)^{(l)} \tag{7.1.14}$$

$$\frac{u^{(l+1)} - u^{(l)}}{\Delta t} = -\nabla \cdot \mathbf{F}_u^{(l+1)} + (ku - \gamma np)^{(l)} \tag{7.1.15}$$

where the superscript of $y^{(l)}$ is the numerical approximation of $y(t)$ at time $t_l = l\Delta t$.

Note that the equations (7.1.13-7.1.15) are all reaction-diffusion equations. To ensure numerical stability, we use a **backward Euler scheme** for the divergence of fluxes; **forward Euler scheme** is applied for the reaction terms for simplicity.

We also add a note on the numerical implementation of the fluxes. In fact, the fluxes $\mathbf{F}_n$, $\mathbf{F}_p$, and $\mathbf{F}_u$ are not fully evaluated at time t_{l+1}. We take $\mathbf{F}_n^{(l+1)}$ as an example; $\mathbf{F}_p^{(l+1)}$ and $\mathbf{F}_u^{(l+1)}$ have similar expression. To have a numerical approximation that is linear in the particle densities, we re-write (7.1.9-7.1.10)

as below

$$F^{x,\,(l+1)}_{n\;(i+\frac{1}{2},j)} = -\mu^{(l)}_{n\;(i+\frac{1}{2},j)}\;\frac{n^{(l+1)}_{i+1,j}B(\psi^{(l)}_{i+1,j}-\psi^{(l)}_{i,j}) - n^{(l+1)}_{i,j}B(\psi^{(l)}_{i,j}-\psi^{(l)}_{i+1,j})}{h_x} \tag{7.1.16}$$

$$F^{y,\,(l+1)}_{n\;(i,j+\frac{1}{2})} = -\mu^{(l)}_{n\;(i,j+\frac{1}{2})}\;\frac{n^{(l+1)}_{i,j+1}B(\psi^{(l)}_{i,j+1}-\psi^{(l)}_{i,j}) - n^{(l+1)}_{i,j}B(\psi^{(l)}_{i,j}-\psi^{(l)}_{i,j+1})}{h_y} \tag{7.1.17}$$

In other words, in the expression of $\mathbf{F}_n^{(l+1)}$, only the unknown n is evaluated at time t_{l+1}, and all the other terms are evaluated at time t_l.

For each time step, we solve the equations (7.1.12-7.1.15) successively. The time marching process is terminated when the rate of change for all of $\{\psi^{(l)}$, $n^{(l)}$, $p^{(l)}$, $u^{(l)}\}$ is smaller than some chosen tolerance $\epsilon > 0$.

7.1.3 Numerical method for solving adjoint equations

The adjoint equations (6.4.12-6.4.15) are a system of linear elliptic equations. The spatial discretization of these equations are all standard central difference method (the same as in the discretization of *divergence operator* and *gradient operator* in Section 7.1.2). In what follows, we introduce an iterative solution map to solve the system of adjoint equations.

Among the four equations, (6.4.12) is different from the other 3 adjoint equations: (6.4.12) is second order in all three unknowns $\{\xi_\psi, \xi_n, \xi_p\}$, whereas (6.4.13), (6.4.14), and (6.4.15) are second order in only ξ_n, ξ_p and ξ_u, respectively.

Therefore, instead of solving the whole system all at once, we propose an iterative solution map.

We start with an initial guess solutions $\{\xi_\psi^{(0)},\ \xi_n^{(0)},\ \xi_p^{(0)},\ \xi_u^{(0)}\}$. Then given the adjoint variables $\{\xi_\psi^{(l)},\ \xi_n^{(l)},\ \xi_p^{(l)},\ \xi_u^{(l)}\}$ at $l \geq 0$, we solve for $\{\xi_\psi^{(l+1)},\ \xi_n^{(l+1)},\ \xi_p^{(l+1)},\ \xi_u^{(l+1)}\}$ by the following two steps

1. Given $\xi_\psi^{(l)}$, we solve for $\{\xi_n^{(l+1)},\ \xi_p^{(l+1)},\ \xi_u^{(l+1)}\}$

$$\left[-\nabla\cdot(\mu_n\nabla\xi_n^{(l+1)}) - \mu_n\nabla\psi\cdot\nabla\xi_n^{(l+1)} + \gamma p\xi_n^{(l+1)}\right] + \gamma p\xi_p^{(l+1)} - \gamma p\xi_u^{(l+1)} = -\xi_\psi^{(l)} \tag{7.1.18}$$

$$\gamma n\xi_n^{(l+1)} + \left[-\nabla\cdot(\mu_p\nabla\xi_p^{(l+1)}) + \mu_p\nabla\psi\cdot\nabla\xi_p^{(l+1)} + \gamma n\xi_p^{(l+1)}\right] - \gamma n\xi_u^{(l+1)} = \xi_\psi^{(l)} \tag{7.1.19}$$

$$-k\xi_n^{(l+1)} - k\xi_p^{(l+1)} + \left[-\nabla\cdot(\mu_u\nabla\xi_u^{(l+1)}) + (d_u+k)\xi_u^{(l+1)}\right] = 0 \tag{7.1.20}$$

2. Given $\{\xi_n^{(l)}, \xi_p^{(l)}, \xi_u^{(l)}\}$, we solve for $\xi_\psi^{(l+1)}$

$$
\begin{aligned}
&-\lambda^2\nabla\cdot(\epsilon\nabla\xi_\psi^{(l+1)}) \\
&= -\Big[\nabla\cdot(\mu_n n\nabla\xi_n^{(l)}) \\
&\qquad -\nabla\cdot\left((\nabla n - n\nabla\psi)\cdot\nabla\xi_n^{(l)}\frac{\partial\mu_n}{\partial(\nabla\psi)}\right) \\
&\qquad +\nabla\cdot\left(\xi_n^{(l)}\left(u\frac{\partial k}{\partial(\nabla\psi)} - np\frac{\partial\gamma}{\partial(\nabla\psi)}\right)\right)\Big] \\
&\quad -\big[-\nabla\cdot(\mu_p p\nabla\xi_p^{(l)}) \\
&\qquad -\nabla\cdot\left((\nabla p + p\nabla\psi)\cdot\nabla\xi_p^{(l)}\frac{\partial\mu_p}{\partial(\nabla\psi)}\right) \\
&\qquad +\nabla\cdot\left(\xi_p^{(l)}\left(u\frac{\partial k}{\partial(\nabla\psi)} - np\frac{\partial\gamma}{\partial(\nabla\psi)}\right)\right)\Big]
\end{aligned}
\tag{7.1.21}
$$

The solution map is analogous to the Jacobi Method in linear algebra. In fact, if we think of $\{\xi_\psi, \xi_n, \xi_p, \xi_u\}$ as a vector of functions, and the linear operators as a matrix, the adjoint system can be re-written in an symbolic way as

$$
\begin{pmatrix}
A_{11} & A_{12} & A_{13} & A_{14} \\
A_{21} & A_{22} & A_{23} & A_{24} \\
A_{31} & A_{32} & A_{33} & A_{34} \\
A_{41} & A_{42} & A_{43} & A_{44}
\end{pmatrix}
\begin{pmatrix}
\xi_\psi \\ \xi_n \\ \xi_p \\ \xi_u
\end{pmatrix}
=
\begin{pmatrix}
b_1 \\ b_2 \\ b_3 \\ b_4
\end{pmatrix}
\tag{7.1.22}
$$

Here the subscripts "1", "2", "3" and "4" corresponds to ξ_ψ, ξ_n, ξ_p, and ξ_u, respectively. A_{ij} denotes the differential operator which acts on the j-th adjoint variables in the i-th adjoint equation. And b_i is the right-hand side vector that has incorporated the boundary conditions of the i-th adjoint equation.

With the help of such symblic representation, we can re-write our iterative method. For each step, we effectively are solving the following linear system:

$$\begin{pmatrix} A_{11} & 0 & 0 & 0 \\ 0 & A_{22} & A_{23} & A_{24} \\ 0 & A_{32} & A_{33} & A_{34} \\ 0 & A_{42} & A_{43} & A_{44} \end{pmatrix} \begin{pmatrix} \xi_\psi^{(l+1)} \\ \xi_n^{(l+1)} \\ \xi_p^{(l+1)} \\ \xi_u^{(l+1)} \end{pmatrix} = \begin{pmatrix} & A_{12} & A_{13} & A_{14} \\ A_{21} & 0 & 0 & 0 \\ A_{31} & 0 & 0 & 0 \\ A_{41} & 0 & 0 & 0 \end{pmatrix} \begin{pmatrix} \xi_\psi^{(l)} \\ \xi_n^{(l)} \\ \xi_p^{(l)} \\ \xi_u^{(l)} \end{pmatrix} + \begin{pmatrix} b_1 \\ b_2 \\ b_3 \\ b_4 \end{pmatrix} \tag{7.1.23}$$

The validity of such iterative solution map needs to be justified, but in practice, we have observed convergence within 10 iterations for fairly small tolerance (e.g. 10^{-6}).

7.1.4 Numerical method for solving the Allen-Cahn equation

Finally, to update the phase field function, we need to solve the Allen-Cahn equation (6.2.25). We re-write the equation below

$$\frac{\partial \phi}{\partial t} = \kappa \nabla^2 \phi + \phi(1-\phi) r(\phi) \tag{7.1.24}$$

where

$$r(\phi) = \frac{1}{\kappa} \left[(\phi - \frac{1}{2}) + \widetilde{G}(\phi) \cdot 30\phi^2(\phi-1)^2 \right] \tag{7.1.25}$$

Here $\widetilde{G}(\phi)$ is the *normalized* phase field gradient functional and in general it depends on the current phase field function $\phi(t)$; cf. Section 6.5.

The numerical implementation of solving the Allen-Cahn equation is similar to that in [25]. In fact, the only difference is that we use a **backward Euler scheme** for the diffusion term $\kappa\nabla^2\phi$.

Let $\phi_{i,j}^{(l)}$ be the finite difference approximation of the phase field function evaluated at $P_{i,j} = (x_i, y_j)$ and time t_l. Then the difference equation of the Allen-Cahn equation is

$$\frac{\phi_{i,j}^{(l+1)} - \phi_{i,j}^{(l)}}{\Delta t} = \left(\kappa\nabla_h^2\phi_{i,j}\right)^{(l+1)} + \begin{cases} \phi_{i,j}^{(l+1)}\left(1 - \phi_{i,j}^{(l)}\right) r\left(\phi_{i,j}^{(l)}\right) & \text{for } r\left(\phi_{i,j}^{(l)}\right) \leq 0 \\ \phi_{i,j}^{(l)}\left(1 - \phi_{i,j}^{(l+1)}\right) r\left(\phi_{i,j}^{(l)}\right) & \text{for } r\left(\phi_{i,j}^{(l)}\right) \geq 0 \end{cases} \tag{7.1.26}$$

Note that the spatial discretization of $\left(\kappa\nabla_h^2\phi_{i,j}\right)^{(l+1)}$ is just the standard center difference scheme for Laplacian operator, and the backward Euler scheme is to ensure numerical stability, like in the case of solving state equations in Section 7.1.2.

The special treatment of the reaction term is to enforce that $\phi_{i,j}^{(l)}$ is a value between 0 and 1 for all grid points $P_{i,j}$ and all times t_l. The detailed analysis can be found in Appendix B of [25].

We also note that in our implementation of the optimization algorithm, (7.1.26) is solved for only one time step for each iteration of the optimization, since the gradient functional $G^{(l)}$ at any time step is in general dependent on the current phase field function $\phi^{(l)}$.

7.2 Numerical values for physical parameters

We specify typical values for the physical parameters in our phase-field drift-diffusion model in Section 6.2. In later sections, we make changes to the numerical values of some parameters when needed. We note that many of the values below are chosen from the examples in [6].

- Environmental parameters and universal constants

Temperature	$T = 300\text{K}$
Device length	$L = 100\text{nm}$
Built-in potential	$\psi_{bi} = -0.6V$
Vacuum permittivity	$\epsilon_0 = 8.854 \times 10^{-12}\ F \cdot m^{-1}$
Boltzmann constant	$k_B = 1.38 \times 10^{-23}\ m^2 \cdot kg \cdot s^{-2} \cdot K^{-1}$
Unit charge	$q = 1.602 \times 10^{-19}\ C$

In particular, we compute the thermal potential

$$U_T = \frac{k_B T}{q} \approx 0.0259\ V \tag{7.2.1}$$

- Relative permittivity

relative permittivity of donor	$\epsilon_D = 4$
relative permittivity of acceptor	$\epsilon_A = 4$

- Mobility and diffusivity

Zero-field electron mobility in donor	$\mu_{n,D} = 10^{-9}\ m^2 \cdot V^{-1} \cdot s^{-1}$
Zero-field electron mobility in acceptor	$\mu_{n,A} = 10^{-8}\ m^2 \cdot V^{-1} \cdot s^{-1}$
Field dependent coefficient of electron mobility	$\gamma_{n,D} = \gamma_{n,A} = 5 \times 10^{-4}\ m^{\frac{1}{2}} \cdot V^{-\frac{1}{2}}$

Zero-field hole mobility in donor	$\mu_{p,D} = 2 \times 10^{-8}\ m^2 \cdot V^{-1} \cdot s^{-1}$
Zero-field hole mobility in acceptor	$\mu_{p,A} = 2 \times 10^{-9}\ m^2 \cdot V^{-1} \cdot s^{-1}$
Field dependent coefficient of hole mobility	$\gamma_{p,D} = \gamma_{p,A} = 5 \times 10^{-4}\ m^{\frac{1}{2}} \cdot V^{-\frac{1}{2}}$

Exciton diffusivity in donor	$\mu_{u,D} = 10^{-10}\ m^2 \cdot s^{-1}$
Exciton diffusivity in acceptor	$\mu_{u,A} = 10^{-10}\ m^2 \cdot s^{-1}$

Note that $\mu_{n,D} << \mu_{n,A}$, whereas $\mu_{p,D} >> \mu_{p,A}$. This reflects the observation that hole transport is dominant in donor material, whereas electron transport is dominant in acceptor materials. This can be seen in later computations on electron flux and hole flux.

- Reactions

Photogeneration rate	$Q = 10^{27}\ m^{-3} \cdot s^{-1}$
Exciton dissociation rate at zero electrical field	$k_0 = 10^6\ s^{-1}$
Exciton decay rate	$d_D = d_A = 10^6\ s^{-1}$

Here the recombination coefficient γ is missing, because it is defined as a derived quantity which depends on permittivity ϵ and carrier mobilities μ_n and μ_p; cf. Section 6.2.1

- Dirichlet boundaries

Electrical potential at Γ_{D1}	$\psi_{\Gamma_{D1}} = \psi_{app} + \psi_{bi}\ V$
Electrical potential at Γ_{D2}	$\psi_{\Gamma_{D2}} = 0\ V$

Here ψ_{app} is the applied potential on anode Γ_{D1}; we fix the electrical potential on cathode Γ_{D2} to be 0. The reason to choose these Dirichlet boundary conditions for ψ are explained in [21, 22].

Electron density at Γ_{D1}	$n_{\Gamma_{D1}} = 0\ m^{-3}$
Electron density at Γ_{D2}	$n_{\Gamma_{D2}} = 10^{20}\ m^{-3}$

Hole density at Γ_{D1}	$p_{\Gamma_{D1}} = 10^{20}\ m^{-3}$
Hole density at Γ_{D2}	$p_{\Gamma_{D2}} = 0\ m^{-3}$

Exciton density at Γ_{D1}	$u_{\Gamma_{D1}} = 0\ m^{-3}$
Exciton density at Γ_{D2}	$u_{\Gamma_{D2}} = 0\ m^{-3}$

All these quantities need to be converted dimensionless values before substituted into the drift-diffusion equations. In particular, we want to compute the dimensionless constant λ^2 in (6.2.1) from Section 6.2. To this end, we only need to introduce a "typical particle density constant"

$$\widetilde{N} = 10^{20} m^{-3} \tag{7.2.2}$$

By scaling the particle densities with $\widetilde{N}$, we note that the Dirichlet boundary conditions for dimensionless $\widetilde{n}$ and $\widetilde{p}$ are

$$\widetilde{n}_{D1} = 0 \qquad \widetilde{n}_{D2} = 1 \tag{7.2.3}$$

$$\widetilde{p}_{D1} = 1 \qquad \widetilde{p}_{D2} = 0 \tag{7.2.4}$$

Finally, following the procedure in [21], we compute the scaling factor λ^2 as

$$\lambda^2 = \frac{\epsilon_0 U_T}{q\widetilde{N}L^2} \approx 1.4287 \tag{7.2.5}$$

.

7.3 Numerical Examples

7.3.1 An example of a phase field function

We first look at the numerical solutions of phase field function ϕ. Recall that ϕ is the solution to the Allen-Cahn equation

$$\frac{\partial \phi}{\partial t} = \kappa \nabla^2 \phi - \frac{1}{\kappa}\left[\phi(\phi-1)(\phi-\frac{1}{2}) + G \cdot 30\phi^2(\phi-1)^2\right] \qquad \Omega \tag{7.3.1}$$

This is the same equation as in (6.2.25) with the boundary conditions omitted. Obviously, the solution of $\phi(t)$ is determined by both κ and G; recall $\kappa > 0$ is the (small) phase field parameter and G is a function defining the asymmetric double-well potential.

In [5] and [11], the authors consider an interface morphology which consists of a few rectangular barriers. Apparently, by increasing the number of barriers, one

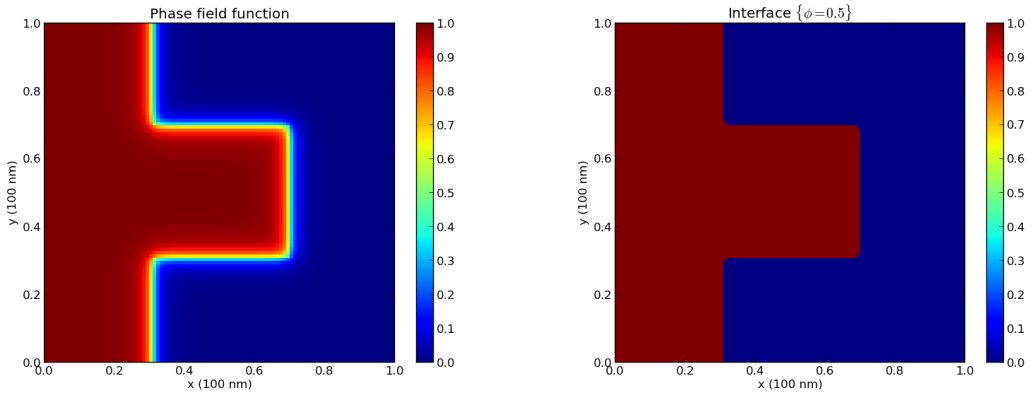

(a) Phase field function

(b) Indicator function

Figure 7.1: Phase field function and the corresponding indicator function for the interface of 1 rectangular barrier. Mesh: 101x101. Phase field parameter: $\kappa = 0.03$

effectively increases the interface length (area in 3D). As mentioned in Chapter 1, it is our goal to improve such intuition of an "optimal" interface. Hence, we first consider the morphology of only one rectangular barrier.

To obtain the corresponding phase field function, we set $\kappa = 0.03$ and define G to be

$$G_1 = \begin{cases} -1 & \text{phase 1} \\ 1 & \text{phase 0} \end{cases} \tag{7.3.2}$$

in the Allen-Cahn equation. The obtained phase field function is shown in Figure 7.1. The corresponding indicator function is included as well to show the level set $\{\phi = 0.5\}$.

For the underlying geometry, we are mainly concerned with two quantities: the area of each phase, and the interface length. Since the phase field function is the level-set function of the underlying geometry, we instead compute the following two quantities.

- Area of phase 1 is approximated by

$$A_1[\phi] = \int_\Omega \phi \tag{7.3.3}$$

- Interface length

  In Section 6.1.1, we have seen how phase field function can be used to represent interface and the flow associated with its curvature. We also have mentioned that one can recover the interface area/length by taking the limit of $\kappa \to 0$ in solving the Allen-Cahn equation. Hence, we consider the following integral functional as a measure of interface length (or "area of the interface neighborhood")

$$A_{int}[\phi] = \int_\Omega \frac{\kappa}{2} |\nabla\phi|^2 + \frac{1}{4\kappa}\phi^2(1-\phi)^2 \tag{7.3.4}$$

7.3.2 Solutions to the phase-field drift-diffusion model

We substitute the phase field function ϕ obtained in Section 7.3.1 into our phase-field drift-diffusion model.

We use the values of physical parameters in Section 7.2 for our drift-diffusion equations. We also need to specify the applied electrical potential ψ_{app} on anode

(i.e. Γ_{D1}) for the boundary condition of ψ; ψ_{app} is sometimes called "bias". Here we set $\psi_{app} = 0$, i.e. the organic solar cell is short-circuited, to show the solutions at a fixed bias.

As described in Section 7.1.2, we solve for the stationary solution by evolving the time-dependent drift-diffusion equations. We choose the discrete time step to be $t^{(l+1)} - t^{(l)} = 0.01$ for all $l \geq 0$ and exit the marching in time when

$$\left| \frac{f^{(l+1)} - f^{(l)}}{t^{(l+1)} - t^{(l)}} \right| < 10^{-2},$$

where f can be any of $\{\psi, n, p, u\}$.

Figure 7.2 is the stationary solution of electrical potential. In spite of the non-smooth structure of the interface, the electrical potential changes almost linearly from the anode Γ_{D1} to cathode Γ_{D2}. This is also seen by the plot of electrical field, which is almost a constant vector field. This may be the result of choosing the same value for relative permittivity $\epsilon_A = \epsilon_D = 4.0$.

Unlike ψ, the particle densities clearly "see" the existence of an interface. Figure 7.3, Figure 7.4, and Figure 7.5 show the stationary solution of density and flux for electrons, holes, and excitons, respectively.

In Figure 7.3 and Figure 7.4, electrons and holes are escaping the interface region towards the electrodes, whereas in Figure 7.5, excitons are moving towards

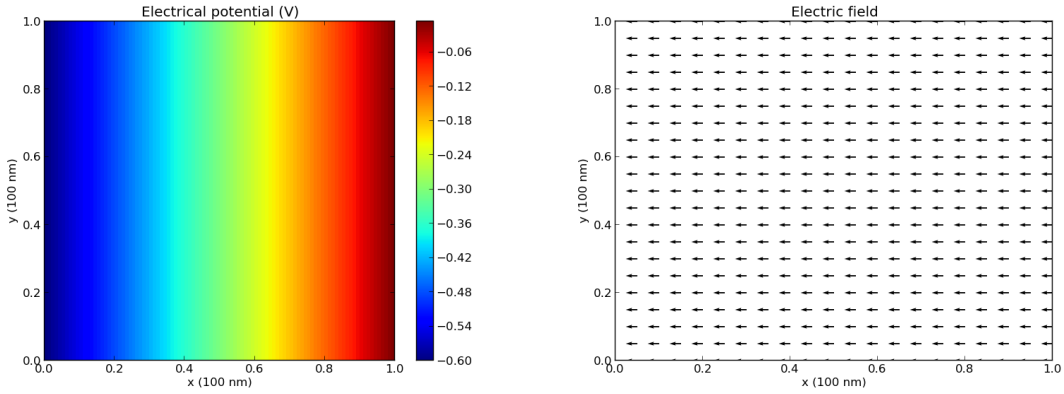

(a) Electrical potential (b) Electrical field

Figure 7.2: Electrical potential and electrical field when $\psi_{app} = 0$. Mesh: 101x101. Phase field parameter: $\kappa = 0.03$

the interface. This is consistent with the physics of organic solar cells: free carriers are generated from excitons near the interface.

It is also observed that electron transport is much more active in the donor region and hole transport is much more active in the acceptor region. This is also intuitive because the imbalance of mobilities for both carriers:

$$\mu_{n,D} << \mu_{n,A} \qquad \mu_{p,D} >> \mu_{p,A}$$

. .

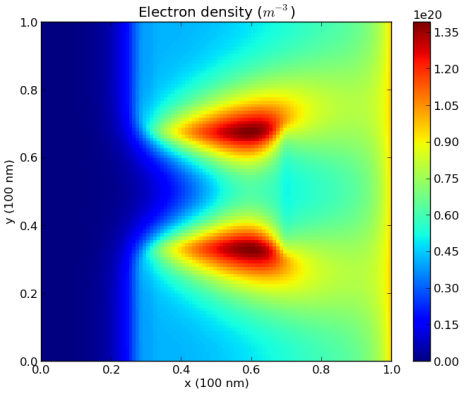

(a) Electron density

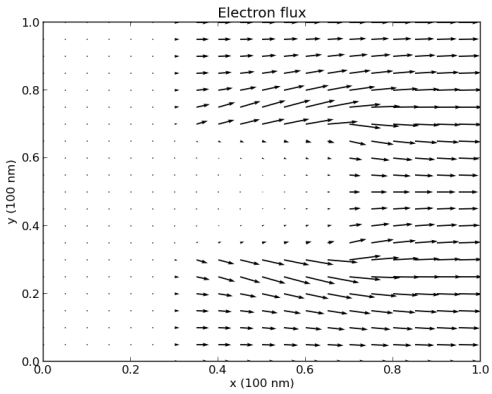

(b) Electron flux

Figure 7.3: Electron density and flux when $\psi_{app} = 0$. Mesh: 101x101. Phase field parameter: $\kappa = 0.03$

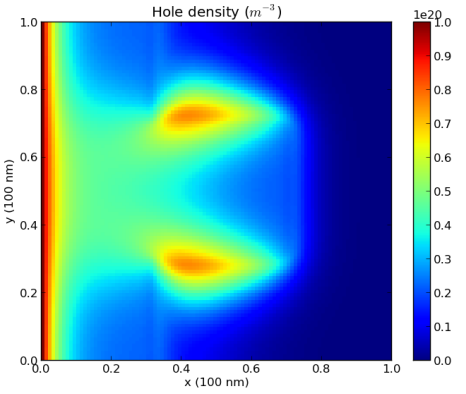

(a) Hole density

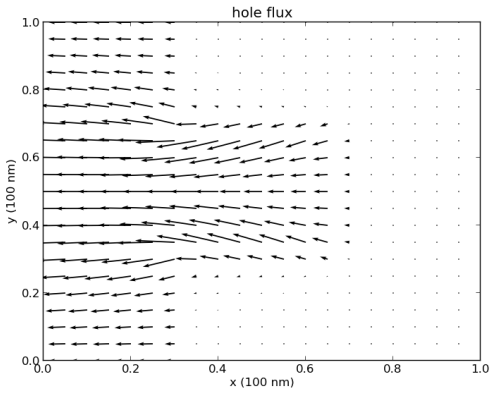

(b) Hole flux

Figure 7.4: Hole density and flux. Mesh: 101x101. Phase field parameter: $\kappa = 0.03$

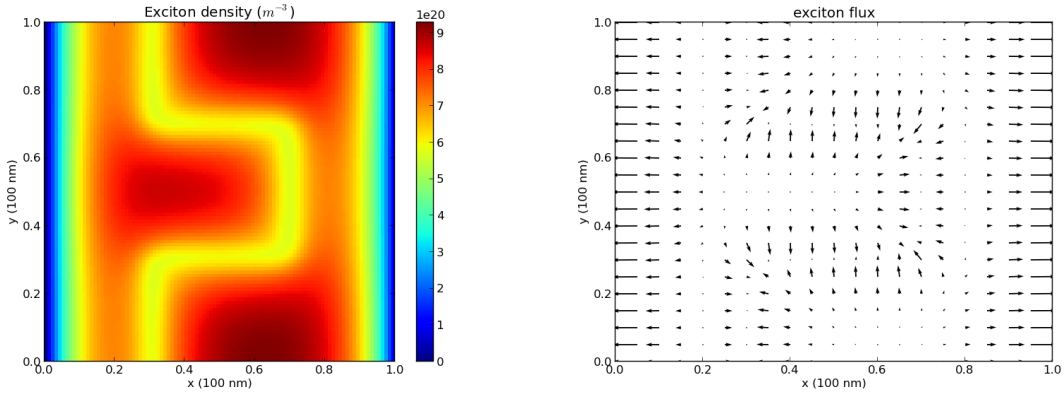

(a) Exciton density

(b) Exciton flux

Figure 7.5: Exciton density and flux when $\psi_{app} = 0$. Mesh: 101x101. Phase field parameter: $\kappa = 0.03$

Finally we add a plot of total current density $F_p - F_n$ in Figure 7.6. We see that, although the total current density varies near the interface both in its amplitude and direction, its amplitude is not significantly different from one side of the interface to the other side; this is in contrast to the fluxes of electrons and holes. We can also conclude that, in donor material, hole tranport is dominant, whereas electron transport is dominant in acceptor material.

7.3.3 Optimal phase field function

In this section, we present the results of implementing the optimization algorithm in Section 6.5 on the example in Section 7.3.1 and 7.3.2. In particular, the algorithm

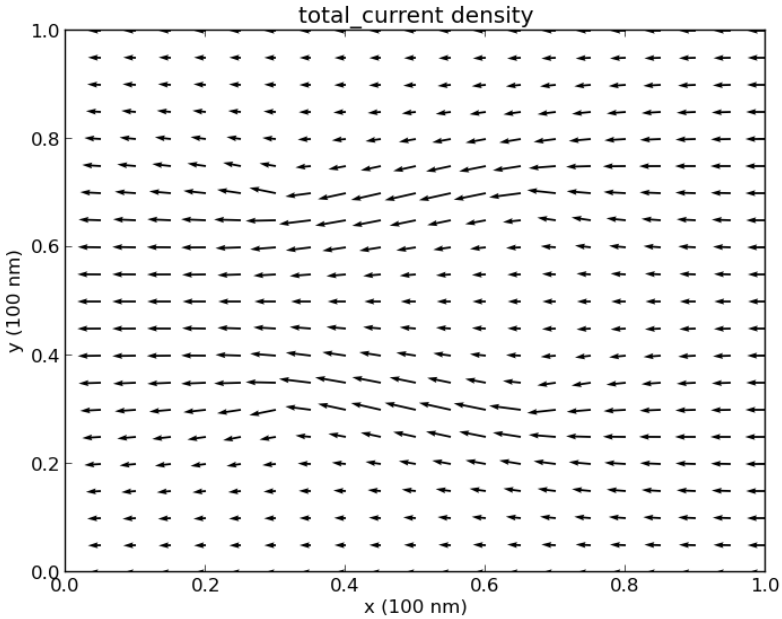

Figure 7.6: Total current density when $\psi_{app} = 0$. Mesh: 101x101. Phase field parameter: $\kappa = 0.03$

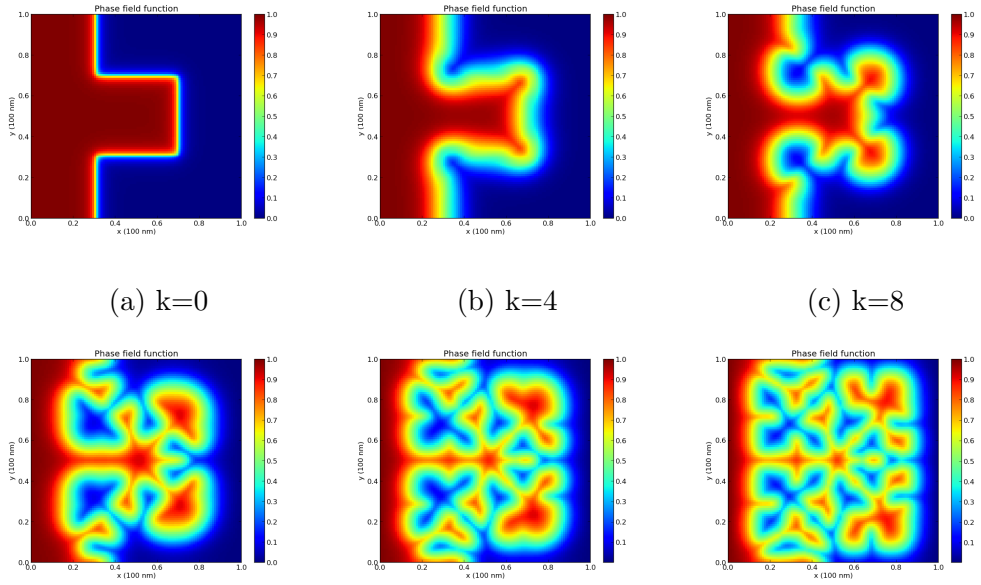

(a) k=0 (b) k=4 (c) k=8

(d) k=12 (e) k=16 (f) k=20

Figure 7.7: Optimization sequence of phase field functions Mesh: 101x101. Phase field parameter: $\kappa = 0.03$

generates a sequence of phase field functions $\phi^{(k)}$, and $\phi^{(0)}$ is the phase field function in Section 7.3.1.

Figure 7.7 shows the sequence of phase field functions obtained by running the optimization algorithm in Section 6.5. The corresponding sequence of indicator functions follows in Figure 7.8. An optimal phase field function is obtained at step $k = 20$.

As in Section 7.3.2, we also solve the drift-diffusion model of the optimal phase

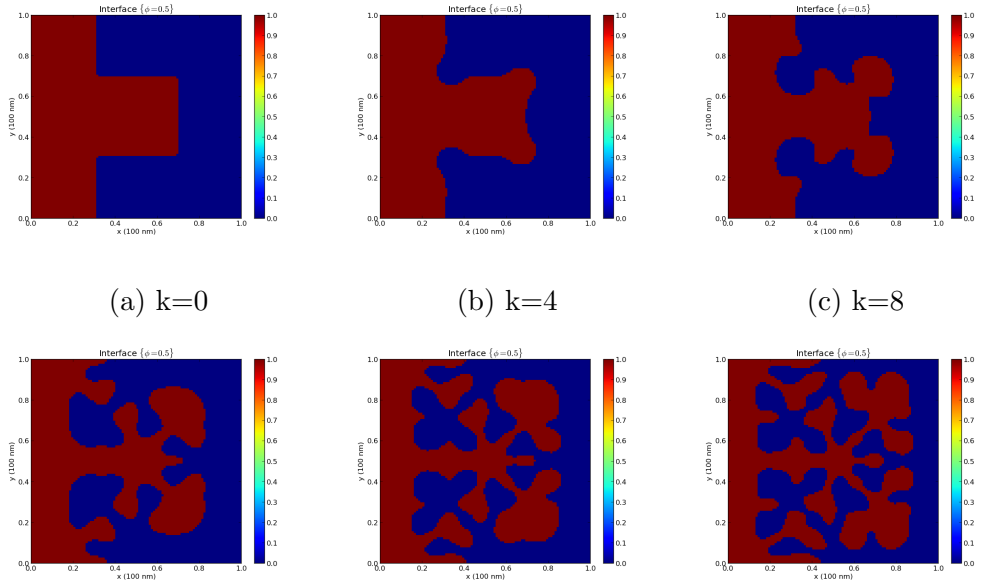

(a) k=0 (b) k=4 (c) k=8

(d) k=12 (e) k=16 (f) k=20

Figure 7.8: Optimization sequence of indicator functions. Mesh: 101x101. Phase field parameter: $\kappa = 0.03$

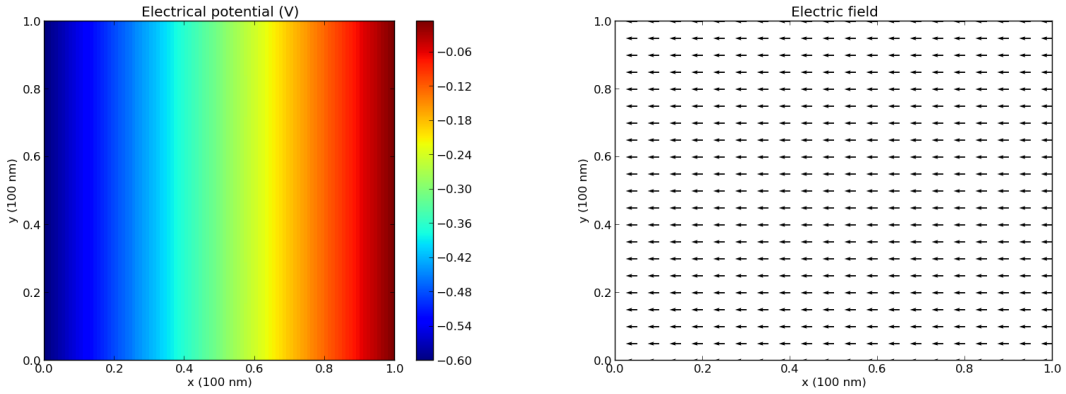

Figure 7.9: Electrical potential and electrical field for $\phi^{(20)}$. Mesh: 101x101. Phase field parameter: $\kappa = 0.03$.

field function$\phi^{(20)}$; the solutions are saved in Figure (7.9 -7.13).

Figure 7.14 shows the average current density at anode for each step of the optimization sequence. Clearly, it shows that our optimization algorithm leads to

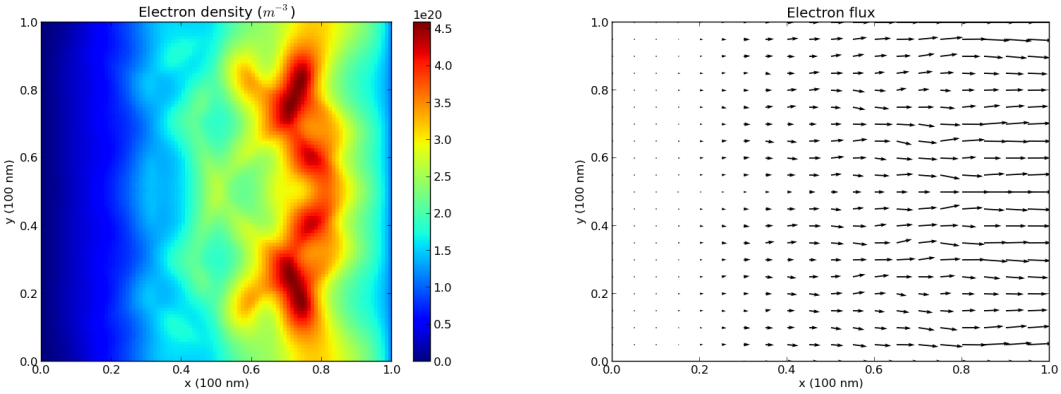

Figure 7.10: Electron density and flux for $\phi^{(20)}$. Mesh: 101x101. Phase field parameter: $\kappa = 0.03$.

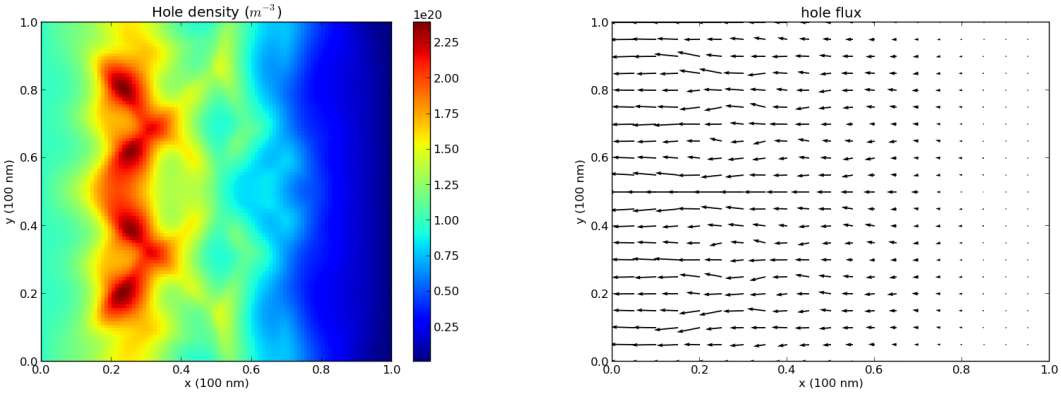

Figure 7.11: Hole density and flux for $\phi^{(20)}$. Mesh: 101x101. Phase field parameter: $\kappa = 0.03$.

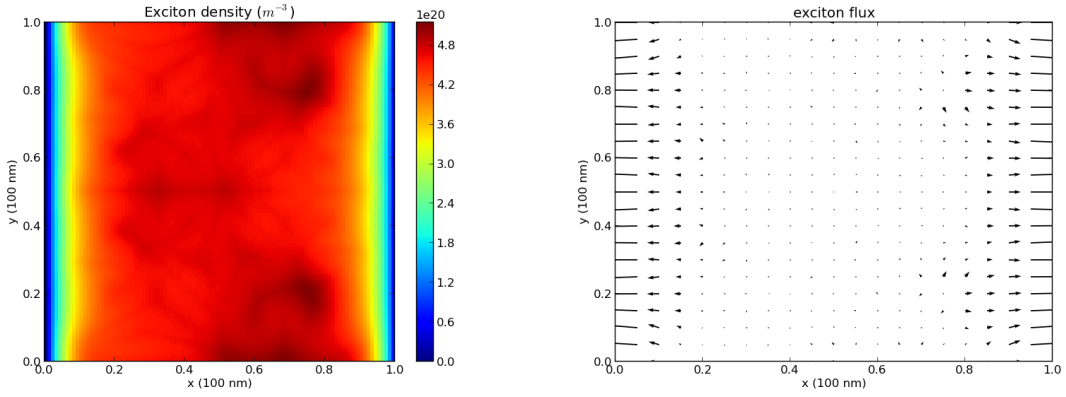

Figure 7.12: Exciton density and flux for $\phi^{(20)}$. Mesh: 101x101. Phase field parameter: $\kappa = 0.03$.

a phase field function that has larger short-curcuit photocurrent; recall we are still considering the particular example of zero bias, i.e. $\psi_{app} = 0$.

Figure 7.15 plots the integral functional $A_{int}[\phi]$ against the optimization steps. Recall that $A_{int}[\phi]$ is a measure of the interface length of the underlying geometry. Therefore Figure 7.15 shows that, under our optimization algorithm, the phase field function tends to evolve in such a way that generates more interface region. We also note the counter-intuitive and significant drop from $A_{int}[\phi^{(0)}]$ to $A_{int}[\phi^{(1)}]$. This is in fact not the effect of the optimization algorithm but rather a result of the gradient G that we used to generate the initial phase field function $\phi^{(0)}$; we address this issue in Section 7.4.1.

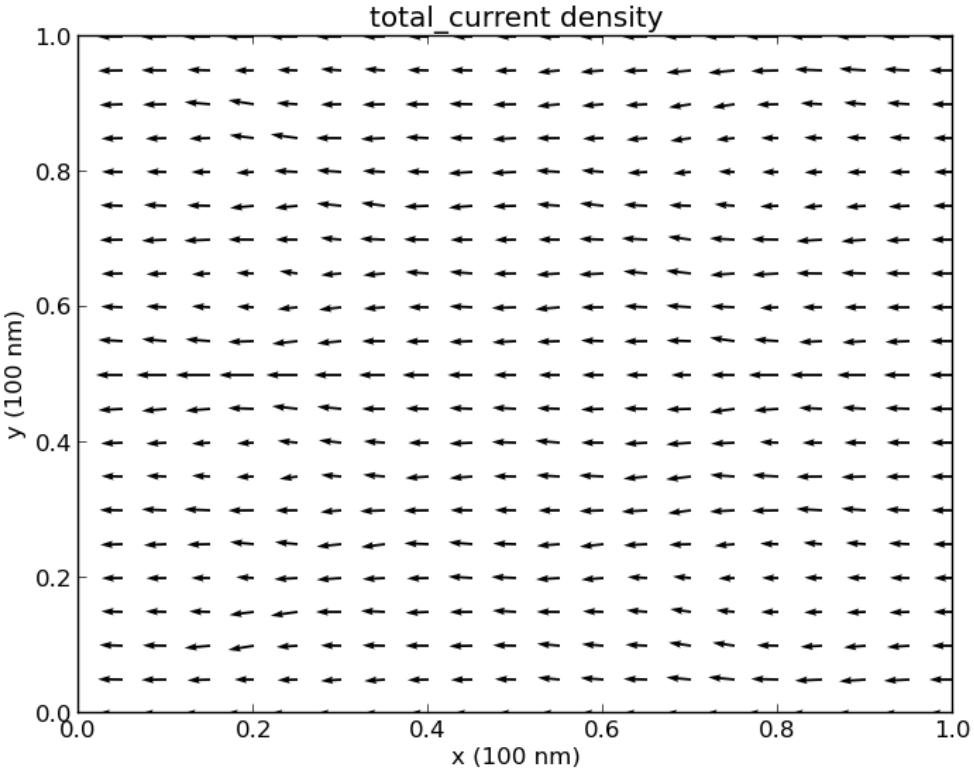

Figure 7.13: Current density for $\phi^{(20)}$. Mesh: 101x101. Phase field parameter: $\kappa = 0.03$.

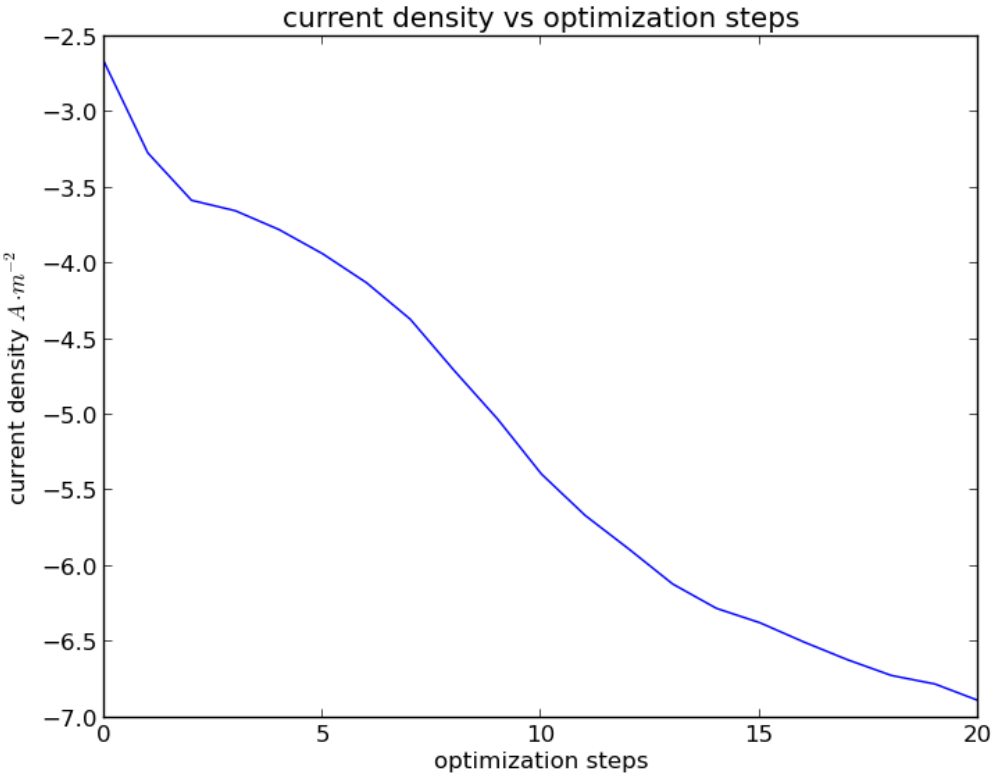

Figure 7.14: Average current density at anode vs optimization steps. Mesh: 101x101. Phase field parameter: $\kappa = 0.03$

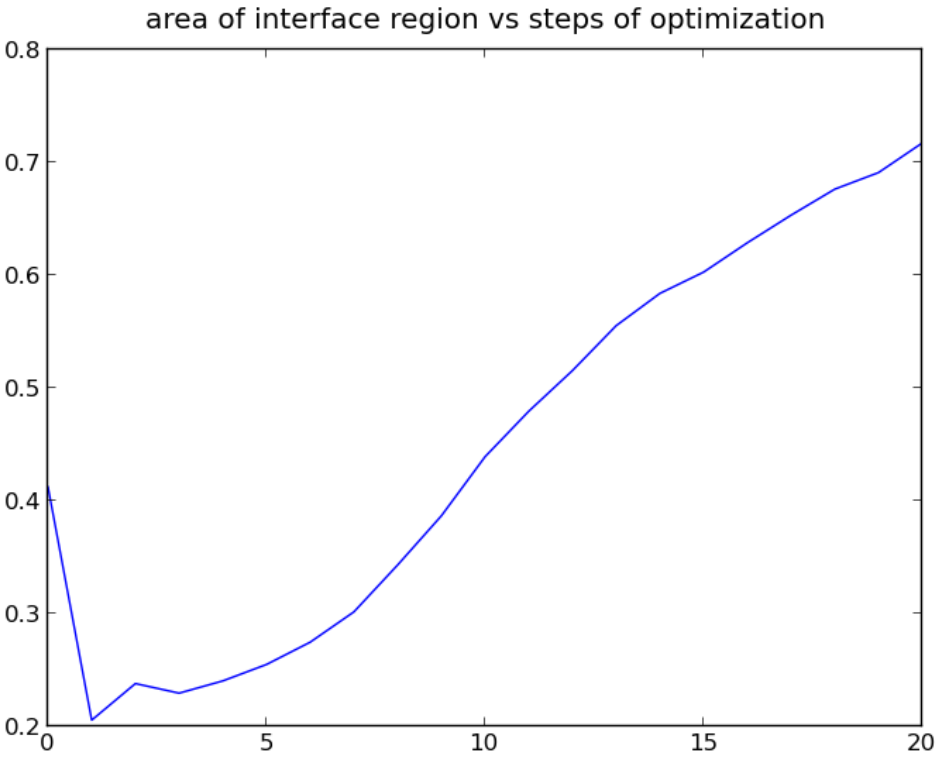

Figure 7.15: $A_{int}[\phi^{(k)}]$ vs optimization steps k. Mesh = 101x101. Phase field parameter: $\kappa = 0.03$

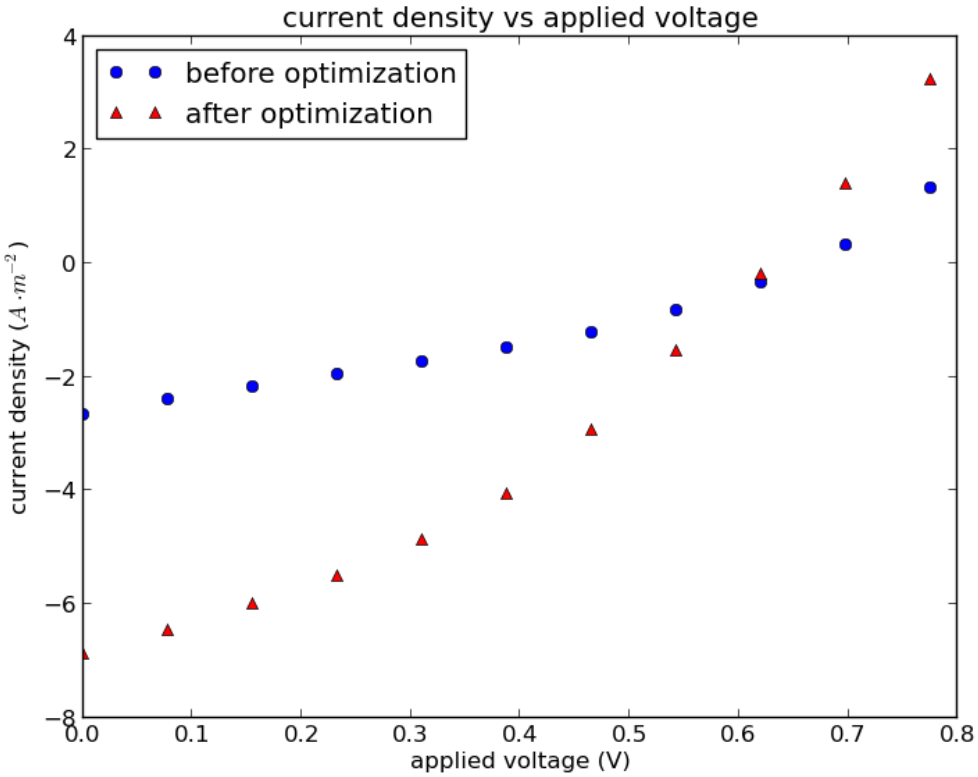

Figure 7.16: I-V characterstics of initial phase field $\phi^{(0)}$ and optimal phase field $\phi^{(20)}$. Mesh = 101x101. Phase field parameter: $\kappa = 0.03$

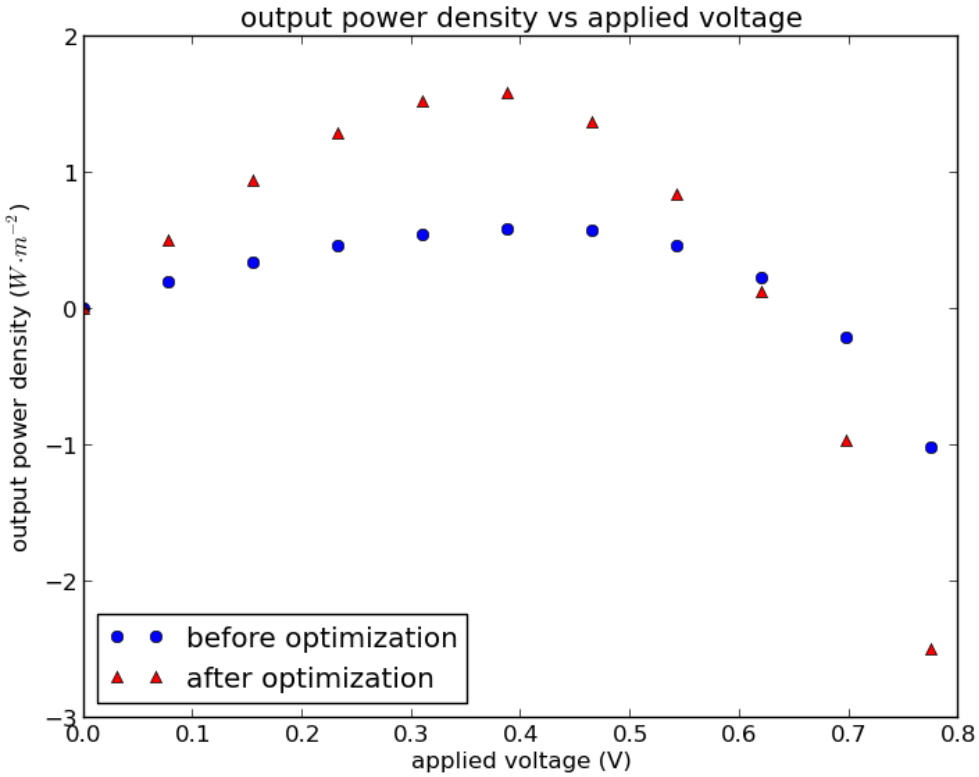

Figure 7.17: Output power P_{out} of initial phase field $\phi^{(0)}$ and optimal phase field $\phi^{(20)}$. Mesh = 101x101. Phase field parameter: $\kappa = 0.03$

A larger short-curcuit current density is not a sufficient proof of a better design for an organic solar cell, because solar cells do not operate with zero bias. It is the output power $P_{out} = -\psi_{app} \times I_{photo}$ that we should compare. The bias at which solar cells operates can be any value between 0 and ψ_{oc}, where ψ_{oc} is the open-curcuit voltage at which photocurrent is zero. Hence, we compare the I-V characteristic and the output power density between the initial phase field $\phi^{(0)}$ and the optimal phase field $\phi^{(20)}$.

Figure 7.16 shows, for most biases ψ_{app} that are below ψ_{oc}, the design of optimal phase field $\phi^{(20)}$ generates much more photocurrent than that of $\phi^{(0)}$. ψ_{oc}, on the other hand, is not significantly affected by our optimization algorithm. Figure 7.17 is the plot of P_{out} versus applied bias ψ_{app}. It is clear that the maximum output power of the solar cell $\phi^{(20)}$ is much larger than that of the solar cell $\phi^{(0)}$. This shows that the solar cell $\phi^{(20)}$ indeed has a better performance than $\phi^{(0)}$.

7.4 Discussion

7.4.1 Amplitude of G

In Figure 7.15, we observed a counter-intuitive drop of $A_{int}[\phi]$ at the beginning of the optimization from $\phi^{(0)}$ to $\phi^{(1)}$. And we mentioned that this should not be caused by our optimization algorithm but rather by the gradient $G^{(k)}$ we used to generate the new phase field function $\phi^{(k)}$:

- $k \geq 1$

  For $k \geq 1$, $G^{(k)}$ is chosen to be the normalized gradient functional $\widetilde{G}$. In numerical implementation, we choose the normalization constant to be the maximum of G which is computed by (6.4.22). Therefore we have $|G^{(k)}| \leq 1$ for $k \geq 1$.

- $k = 0$

  For $k = 0$, in order to obtain the desired initial phase field function $\phi^{(0)}$, we set $G^{(0)}$ to have constant value 1 in phase 0 and constant value -1 in phase 1, just like in Section 6.1.2. Therefore we have $|G^{(0)}| = 1$.

We postulate that it is the difference between the amplitude of $G^{(0)}$ and $G^{(k)}$ for $k \geq 1$ that causes the drop from $\phi^{(0)}$ to $\phi^{(1)}$ in Figure 7.15.

To show the impact of $|G|$, we consider the following simple example. Concretely, we consider two choices of G for generating the initial phase field function $\phi^{(0)}$.

$$G_1 = \begin{cases} -1 & \text{phase 1} \\ 1 & \text{phase 0} \end{cases} \tag{7.4.1}$$

and

$$G_{100} = \begin{cases} -100 & \text{phase 1} \\ 100 & \text{phase 0} \end{cases} \tag{7.4.2}$$

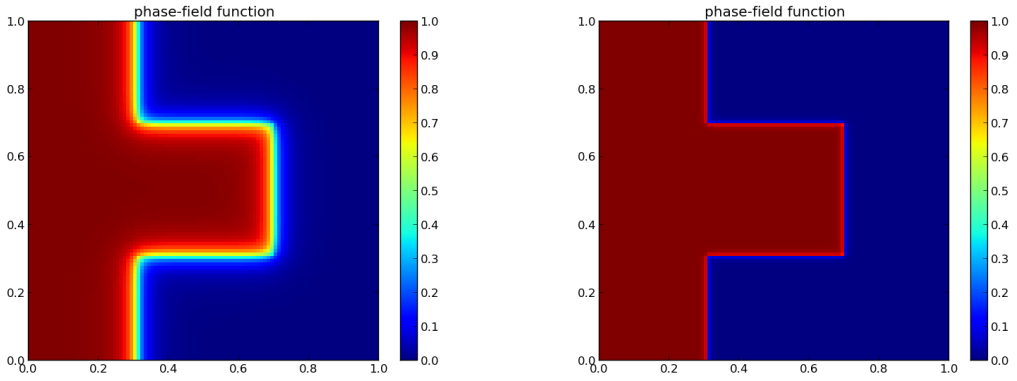

(a) G_1 (b) G_{100}

Figure 7.18: Phase field function for different gradient G. Mesh: 101x101. Phase field parameter: $\kappa = 0.03$

In other words, we intentionally let $|G_{100}| >> |G_1|$. We plot the obtained phase field functions for both G's in Figure 7.18. Apparently, the larger $|G|$ is, the "sharper" the interfacial region is. If we compute the integral functional $A_{int}[\phi^{(0)}]$ for both phase field functions, we have

$$A_{int}[\phi^{(0)}] = 0.4164 \qquad \text{if } G^{(0)} = G_1 \tag{7.4.3}$$

$$A_{int}[\phi^{(0)}] = 1.4890 \qquad \text{if } G^{(0)} = G_{100} \tag{7.4.4}$$

Therefore, it doesn't make much sense to compare $A_{int}[\phi^{(0)}]$ with $A_{int}[\phi^{(1)}]$ as they are generated by very different gradient functionals G.

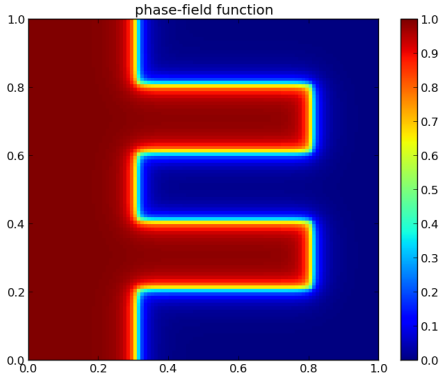

(a) ϕ_1

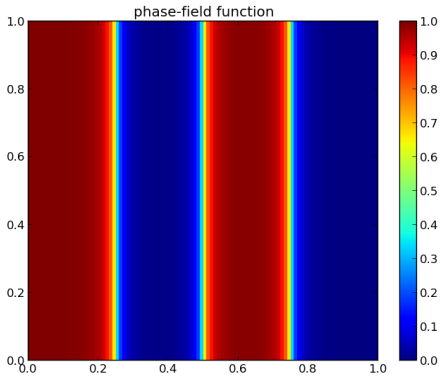

(b) ϕ_2

Figure 7.19: Two phase field functions: ϕ_1 and ϕ_2. Mesh: 101x101. Phase field parameter: $\kappa = 0.03$

7.4.2 Interface length v.s. domain connectivity

Now we address the following question: does connectivity of the domain have significant impact on the performance of organic solar cells?

To answer this question, we consider two phase field functions, ϕ_1 and ϕ_2, plotted in Figure 7.19. In particular, the interface corresponding to ϕ_1 is connected, whereas the interface corresponding to ϕ_2 is not connected. For ϕ_2, we set the positions of interfaces to be $x = 0.25, 0.5, 0.75$. Thus the interface length for ϕ_2 is 3, as the whole domain is a unit square. For ϕ_1, we set the coordinates of all the corner vertices along the interface to be $(0.3, 0.2)$, $(0.8, 0.2)$, $(0.8, 0.4)$, $(0.3, 0.4)$, $(0.3, 0.6)$, $(0.8, 0.6)$, $(0.8, 0.8)$, and $(0.3, 0.8)$. Note that we intentionally choose these coordinates such

that the total length of the interface for ϕ_1 is also 3.

We solve the phase-field drift-diffusion models of both phase field functions with zero bias. Physical parameters of the models are the same as in Section 7.2 except for the zero-field mobilities of minority carriers, i.e. electron mobility in donor material $\mu_{n,D}$ and hole mobility in acceptor material $\mu_{p,A}$.

We consider the particular case where $\mu_{n,D} = \mu_{p,A} = 0\ m^2 \cdot V^{-1} \cdot s^{-1}$. Recall the definition of phase-field-dependent mobilities of charge carriers from Section 6.2.1

$$\mu_p(\nabla\psi, \phi) = \mu_{p,A}(|\nabla\psi|) + [\mu_{p,D}(|\nabla\psi|) - \mu_{p,A}(|\nabla\psi|)]\,\phi \tag{7.4.5}$$

$$\mu_n(\nabla\psi, \phi) = \mu_{n,A}(|\nabla\psi|) + [\mu_{n,D}(|\nabla\psi|) - \mu_{n,A}(|\nabla\psi|)]\,\phi \tag{7.4.6}$$

When $\mu_{p,A} = 0$, $\mu_p = [\mu_{p,D}(|\nabla\psi|) - \mu_{p,A}(|\nabla\psi|)]\,\phi \approx 0$ in acceptor, because the value of ϕ in acceptor is close to 0. Similarly, when $\mu_{n,D} = 0$, $\mu_n = \mu_{n,A}(|\nabla\psi|)(1-\phi) \approx 0$ in donor, because the value of ϕ in donor is close to 1.

Figure 7.20 and Figure 7.21 include the charge carrier densities and fluxes for the model of ϕ_1 and the model of ϕ_2, respectively. In particular, for both models, we see a high concentration of electrons in the donor region near the interface, and, similarly, a high concentration of holes in the acceptor region near the interface.

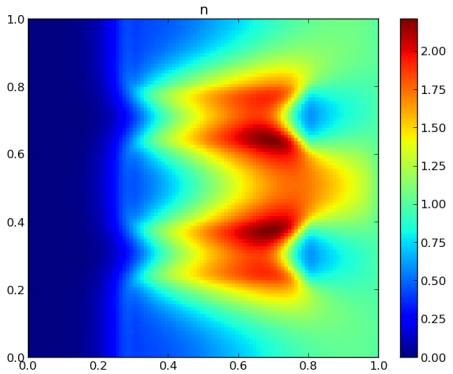

(a) n

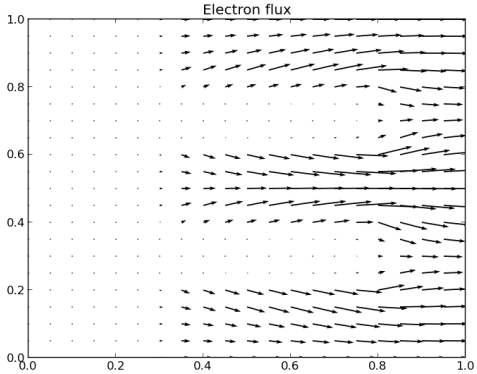

(b) F_n

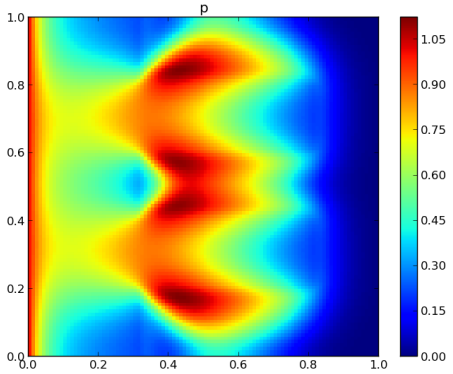

(c) p

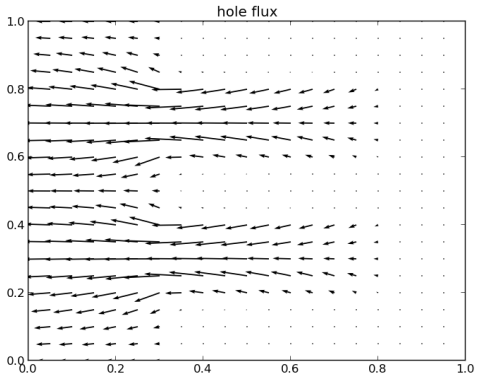

(d) F_p

Figure 7.20: Solutions for the drift-diffusion equations of ϕ_1 in Case 1. Mesh: 101x101. Phase field parameter: $\kappa = 0.03$

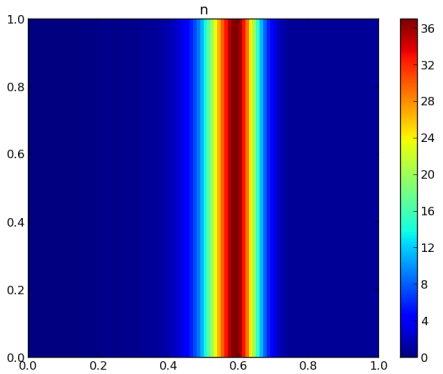

(a) n

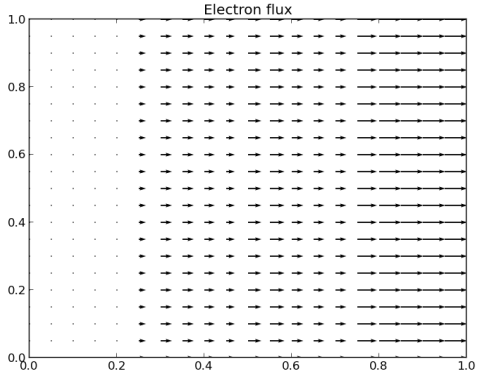

(b) F_n

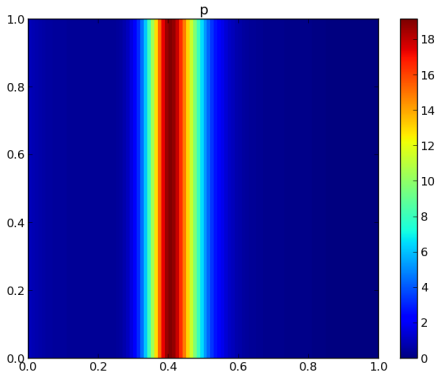

(c) p

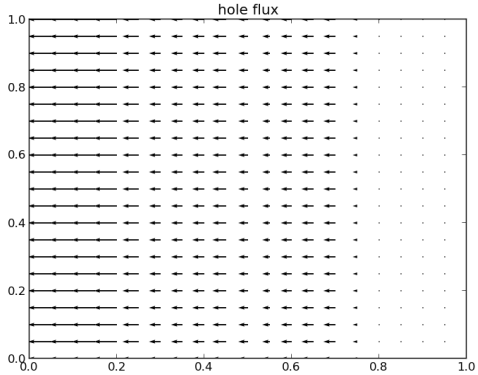

(d) F_p

Figure 7.21: Solutions for the drift-diffusion equations of ϕ_2 in Case 1. Mesh: 101x101. Phase field parameter: $\kappa = 0.03$

	ϕ_1	ϕ_2
$\mu_{n,D} = 0$, $\mu_{p,A} = 0$	-3.801	-2.888
$\mu_{n,D} = 10^{-9}$, $\mu_{p,A} = 2 \times 10^{-9}$	-3.807	-3.916

Table 7.1: Shortcurcuit photocurrent densities for both ϕ_1 and ϕ_2 with different choices for minority mobilities. Current density has unit $A \cdot m^{-2}$. Mobility has unit $m^2 \cdot V^{-1} \cdot s^{-1}$.

We have computed the short-curcuit photocurrent densities for the models of both ϕ_1 and ϕ_2. To make a comparison, we also compute the short-curcuit photocurrent densities with the non-zero values for $\mu_{n,D}$ and $\mu_{p,A}$ from Section 7.2. All the results are summarized in Table 7.1.

When $\mu_{n,D}$ and $\mu_{p,A}$ are set to zero, we see that the photocurrent for the model of ϕ_1 is much larger than that for the model of ϕ_2. In contrast, when $\mu_{n,D}$ and $\mu_{p,A}$ are positive and well above zero, we see little difference in the photocurrent between the models of ϕ_1 and ϕ_2. Hence, we conclude that *connectivity* of the domain is important especially when the carrier mobilites vary significantly from donor to acceptor. In fact, if the carrier mobilites are not very different for donor and acceptor, we should see little difference between donor and acceptor if only charge transport is concerned.

7.4.3 Phase parameters κ

We now consider the choice for the value of κ. κ is the small parameter that determines the width of interface neighborhood where $0 < \phi < 1$. Intuitively, one would expect that a smaller value for κ should allow one to discover finer structures than is possible for larger κ.

We consider 3 values for κ: 0.04, 0.03, and 0.02. The optimization algorithm is run for all these 3 cases. As we see here, this intuition is indeed correct: the optimal phase field function for $\kappa = 0.02$ has much more fine structure than that for $\kappa = 0.04$, and the optimal phase field function for $\kappa = 0.03$ is the intermediate case.

We also plot the photocurrents for all 3 optimization sequences in Figure 7.23 This plot, combined with Figure 7.22, shows that, if a larger photocurrent is desired, we should use a small enough value for κ to implement the numerical algorithm in this paper.

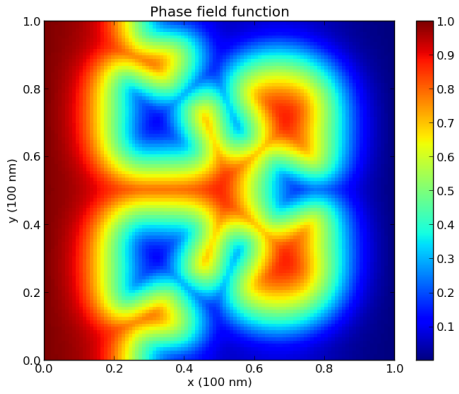

(a) Optimal ϕ for $\kappa = 0.04$

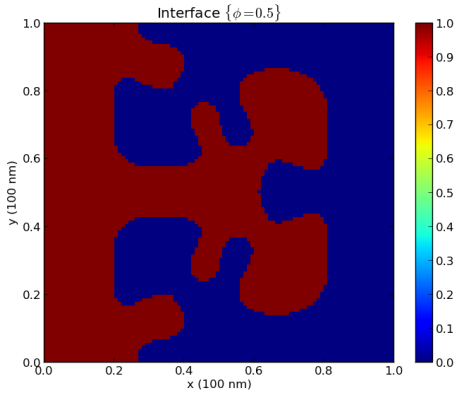

(b) Optimal indicator function for $\kappa = 0.04$

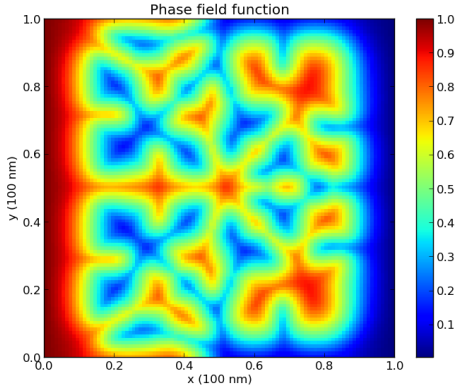

(c) Optimal ϕ for $\kappa = 0.03$

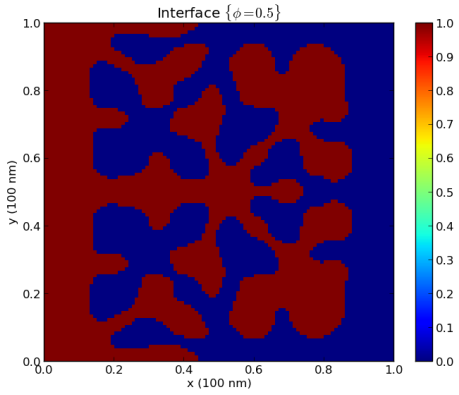

(d) Optimal indicator function for $\kappa = 0.03$

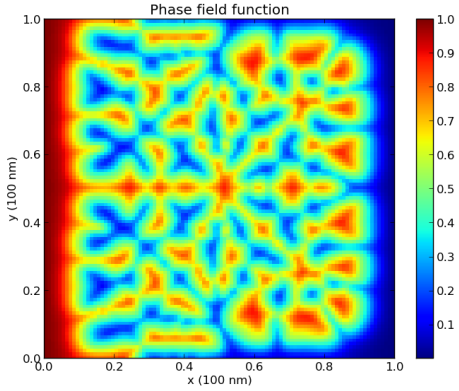

(e) Optimal ϕ for $\kappa = 0.02$

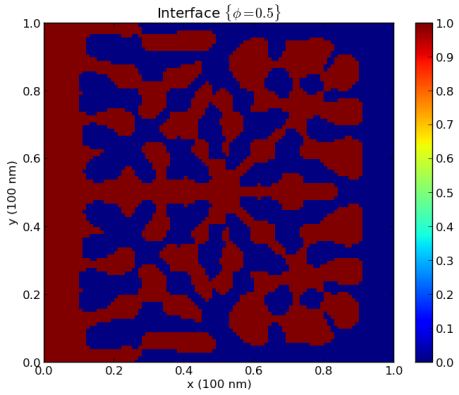

(f) Optimal indicator function for $\kappa = 0.02$

Figure 7.22: Optimal phase field functions and indicator functions for different κ's. Mesh: 101x101.

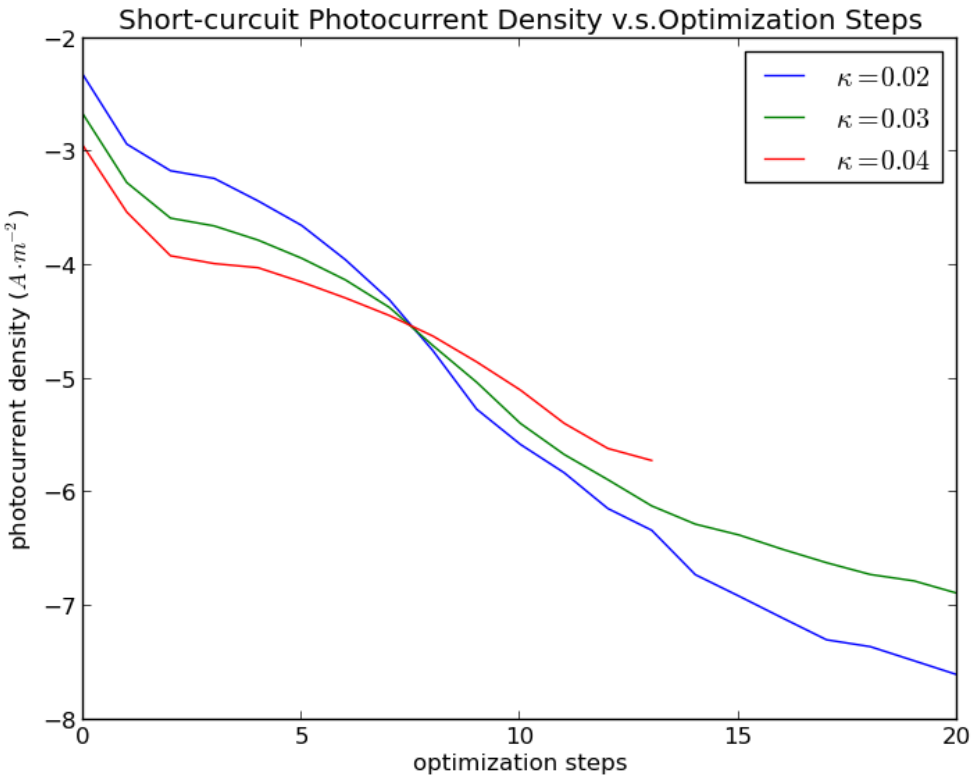

Figure 7.23: Photocurrent densities of optimization sequence for different κ's. Mesh = 101x101.

Chapter 8

Conclusion

In this paper, we present a rational quantitative approach for the optimal design of organic solar cells. We focus on the specific goal of maximizing the amplitude of photocurrent. In our approach, organic solar cells are modeled by the drift-diffusion equations and the design problem is formulated as an optimal control problem for the partial differential equations.

In the first drift-diffusion model, we explicitly define the position of the donor-acceptor interface Γ. The optimal design problem becomes the shape optimization problem of finding an optimal Γ. To this end, we apply the theory of shape differential calculus to this drift-diffusion model and obtain the formula for computing the shape gradient G of photocurrent as a linear functional along the interface Γ. However, it appears difficult to adapt this shape gradient functional to numerical optimization algorithm.

In the second drift-diffusion model, we parametrize the interface Γ by the level set $\{\phi = 0.5\}$ of a phase field function ϕ. The shape dependence of this drift diffusion model is defined through the explicit dependence of each physical parameter on the phase field function ϕ. Hence, the optimal design problem becomes a standard optimal control problem where the control ϕ is in the coefficients of the system of partial differential equations. Sensitivity analysis for this phase-field drift-diffusion model leads to a relatively simple formula for the gradient functional. Numerical examples of optimal design using this approach are also provided to show its applicability.

This current work can be continuted in a few directions.

- The existence of optimal solution in both drift-diffusion models are lacking. A proper functional analytical framework is in need to validate the sensitivity computations.

- The connection between the two drift-diffusion models can be explored. In particular, in the limit of $\kappa \to 0$, it is expected to recover the first drift-diffusion model from the second phase-field approach.

- For the implementation of the optimization algorithm in Chapter 6, it desirable to re-write the programs for parallel computing environment so that the computation can be implemented on a much finer grid and with a smaller phase field parameter (e.g. $\kappa < 0.01$). This may reveal possible finer structure

of the optimal shape.

- It is also interesting to use the same ideas from shape optimization to improve the performance of conventional semiconductor devices.

Appendices

Appendix A

Shape Sensitivity of the First Drift-Diffusion Model

In this appendix, we let ϕ be an arbitrary smooth function on $\overline{\Omega}$ that is 0 on Dirichlet boundaries $\Gamma_D = \Gamma_{D1} \cup \Gamma_{D2}$.

A.1 Shape sensitivity of ψ-equation

The boundary value problem of electric potential is

$$-\lambda^2 \nabla \cdot (\epsilon \nabla \psi) = p - n \qquad \Omega_1 \cup \Omega_2 \tag{A.1.1}$$

$$\psi = \psi_D \qquad \Gamma_{D1} \cup \Gamma_{D2} \tag{A.1.2}$$

$$\frac{\partial \psi}{\partial \nu} = 0 \qquad \Gamma_{N1} \cup \Gamma_{N2} \tag{A.1.3}$$

$$\begin{cases} \psi_1 = \psi_2 \\ \frac{\partial \psi_1}{\partial \nu_1} + \frac{\partial \psi_2}{\partial \nu_2} = 0 \end{cases} \qquad \Gamma \tag{A.1.4}$$

We note that

$$\nabla \psi_1 = \nabla \psi_2 \qquad \forall x \in \Gamma \tag{A.1.5}$$

by A.1.4.

We multiply ϕ on both sides of ψ-equation and apply integration by parts on both Ω_1 and Ω_2 to obtain the weak form

$$\int_{\Omega_1} \epsilon_1 \nabla \psi_1 \cdot \nabla \phi + \int_{\Omega_2} \epsilon_2 \nabla \psi_2 \cdot \nabla \phi - \int_{\partial \Omega_1} (\epsilon_1 - \epsilon_2) \frac{\partial \psi_1}{\partial \nu_1} \phi = \int_{\Omega_1 \cup \Omega_2} (p - n) \phi \tag{A.1.6}$$

where we have applied the boundary condition A.1.4.

We then compute shape derivative with respect to $\mathbf{V}$ and apply formulas 4.5.3

and 4.5.5 to obtain

$$\begin{aligned}
&\int_{\Omega_1} \lambda^2 \epsilon_1 \nabla \psi_1' \cdot \nabla \phi + \int_{\Gamma} \lambda^2 \epsilon_1 \nabla \psi_1 \cdot \nabla \phi \, V_1 \\
&+ \int_{\Omega_2} \lambda^2 \epsilon_2 \nabla \psi_2' \cdot \nabla \phi + \int_{\Gamma} \lambda^2 \epsilon_2 \nabla \psi_2 \cdot \nabla \phi \, V_2 \\
&- \int_{\Gamma} \lambda^2 \left(\epsilon_1 - \epsilon_2\right) \left(\nabla \psi_1' \cdot \nu_1 + \nabla \psi_1 \cdot \nu_1'\right) \phi \\
&- \int_{\Gamma} \left\{ \frac{\partial}{\partial \nu_1} \left[\lambda^2 (\epsilon_1 - \epsilon_2) \frac{\partial \psi_1}{\partial \nu_1} \phi \right] + \lambda^2 (\epsilon_1 - \epsilon_2) \frac{\partial \psi_1}{\partial \nu_1} H_1 \phi \right\} V_1 \\
&= \int_{\Omega} (p' - n') \phi
\end{aligned} \tag{A.1.7}$$

We then apply another integration by parts for the domain integral and make use of 4.4.8 and A.1.5 to obtain

$$\begin{aligned}
&\int_{\Omega_1} \left[-\lambda^2 \nabla \cdot (\epsilon_1 \nabla \psi_1') \right] \phi + \int_{\Omega_2} \left[-\lambda^2 \nabla \cdot (\epsilon_2 \nabla \psi_2') \right] \phi \\
&+ \int_{\partial \Omega_1} \lambda^2 \epsilon_1 \frac{\partial \psi_1'}{\partial \nu_1} \phi + \int_{\partial \Omega_2} \lambda^2 \epsilon_2 \frac{\partial \psi_2'}{\partial \nu_2} \phi - \int_{\Gamma} \lambda^2 (\epsilon_1 - \epsilon_2) \frac{\partial \psi_1'}{\partial \nu_1} \phi \\
&+ \int_{\Gamma} \lambda^2 (\epsilon_1 - \epsilon_2) \nabla_{\Gamma} \psi_1 \cdot \nabla_{\Gamma} \phi \, V_1 + \int_{\Gamma} \lambda^2 (\epsilon_1 - \epsilon_2) \nabla_{\Gamma} \psi_1 \cdot \nabla_{\Gamma} V_1 \, \phi \\
&- \int_{\Gamma} \left\{ \frac{\partial}{\partial \nu_1} \left[\lambda^2 (\epsilon_1 - \epsilon_2) \frac{\partial \psi_1}{\partial \nu_1} \phi \right] + \lambda^2 (\epsilon_1 - \epsilon_2) \frac{\partial \psi_1}{\partial \nu_1} H_1 \phi \right\} V_1 \\
&= \int_{\Omega} (p' - n') \phi
\end{aligned} \tag{A.1.8}$$

Then we apply the tangential Green's formula 4.1.7 and rearrange the integrals

to obtain

$$\int_{\Omega_1} \left[-\lambda^2 \nabla \cdot (\epsilon_1 \nabla \psi_1')\right] \phi + \int_{\Omega_2} \left[-\lambda^2 \nabla \cdot (\epsilon_2 \nabla \psi_2')\right] \phi$$
$$\int_{\partial\Omega} \lambda^2 \epsilon \frac{\partial \psi'}{\partial \nu} \phi + \int_{\Gamma} \lambda^2 \epsilon_2 \left(\frac{\partial \psi_1'}{\partial \nu_1} - \frac{\partial \psi_2'}{\partial \nu_1}\right) \phi$$
$$- \int_{\Gamma} \lambda^2 \left\{ \mathrm{div}_\Gamma \left[(\epsilon_1 - \epsilon_2) \nabla_\Gamma \psi_1\right] V_1 + \frac{\partial}{\partial \nu_1} \left[(\epsilon_1 - \epsilon_2) \frac{\partial \psi_1}{\partial \nu_1}\right] V_1 + (\epsilon_1 - \epsilon_2) \frac{\partial \psi_1}{\partial \nu_1} H_1 V_1 \right\} \phi$$
$$= \int_{\Omega} (p' - n') \phi \tag{A.1.9}$$

By observing that ϕ was arbitrarily chosen, we reached the final results, which are summarized below together with 5.3.18 and 5.3.21

$$-\lambda^2 \nabla \cdot (\epsilon \nabla \psi') = p' - n' \qquad \Omega_1 \cup \Omega_2 \tag{A.1.10}$$

$$\psi' = 0 \qquad \Gamma_{D1} \cup \Gamma_{D2} \tag{A.1.11}$$

$$\frac{\partial \psi'}{\partial \nu} = 0 \qquad \Gamma_{N1} \cup \Gamma_{N2} \tag{A.1.12}$$

$$\psi_1' = \psi_2' \qquad \Gamma \tag{A.1.13}$$

$$\epsilon_2 \left(\frac{\partial \psi_1'}{\partial \nu_1} - \frac{\partial \psi_2'}{\partial \nu_1}\right)$$
$$= \mathrm{div}_\Gamma \left[(\epsilon_1 - \epsilon_2) \nabla_\Gamma \psi_1\right] V_1$$
$$+ \frac{\partial}{\partial \nu_1} \left[(\epsilon_1 - \epsilon_2) \frac{\partial \psi_1}{\partial \nu_1}\right] V_1$$
$$+ (\epsilon_1 - \epsilon_2) \frac{\partial \psi_1}{\partial \nu_1} H_1 V_1 \qquad \Gamma \tag{A.1.14}$$

A.2 Shape sensitivity of n-equation

The boundary value problem of electron density is

$$\begin{cases} \nabla \cdot \mathbf{F}_n = 0 \\ \mathbf{F}_n = -\mu_n(\nabla n - n\nabla\psi) \end{cases} \qquad \Omega_1 \cup \Omega_2 \qquad \text{(A.2.1)}$$

$$n = n_D \qquad \Gamma_{D1} \cup \Gamma_{D2} \qquad \text{(A.2.2)}$$

$$\mathbf{F}_n \cdot \nu = 0 \qquad \Gamma_{N1} \cup \Gamma_{N2} \qquad \text{(A.2.3)}$$

$$\begin{cases} n_1 = n_2 \\ \mathbf{F}_{n1} \cdot \nu_1 + \mathbf{F}_{n2} \cdot \nu_2 = -f \end{cases} \qquad \Gamma \qquad \text{(A.2.4)}$$

Recalling the dependence of μ_n on $\nabla\psi$, we compute the shape derivative of $\mathbf{F}_n$ by the chain rule

$$\mathbf{F}_n' = -\mu_n \left(\nabla n' - n'\nabla\psi\right) + \mu_n n\nabla\psi' - \left(\nabla n - n\nabla\psi\right) \frac{\partial \mu_n}{\partial(\nabla\psi)} \cdot \nabla\psi' \qquad \text{(A.2.5)}$$

where $\frac{\partial \mu_n}{\partial(\nabla\psi)}$ denotes the gradient of μ_n with respect to $\nabla\psi$. For convenience, we will use $\mathbf{F}_n'$ for the sensitivity of electron flux in the derivation below and replace $\mathbf{F}_n'$ by A.2.5 only when necessary.

We multiply ϕ on both sides of the n-equation, apply integration by parts, and make use of A.2.4 to obtain

$$\int_{\Omega_1} (-\mathbf{F}_{n1}) \cdot \nabla\phi + \int_{\Omega_2} (-\mathbf{F}_{n2}) \cdot \nabla\phi = \int_{\Gamma} f\phi \qquad \text{(A.2.6)}$$

Note here f is a function defined only on the interface Γ. Hence, we then take

shape derivative on both sides, applying the fomulars 4.5.3, 4.5.4 and 4.5.5

$$\begin{aligned}
&\int_{\Omega_1} (-\mathbf{F}'_{n1}) \cdot \nabla\phi + \int_{\partial\Omega_1} (-\mathbf{F}_{n1}) \cdot \nabla\phi V_1 \\
&+ \int_{\Omega_2} (-\mathbf{F}'_{n2}) \cdot \nabla\phi + \int_{\partial\Omega_2} (-\mathbf{F}_{n2}) \cdot \nabla\phi V_2 \\
&= \int_\Gamma f'\phi + f\frac{\partial\phi}{\partial\nu_1}V_1 + \int_\Gamma f\phi H_1 V_1, \qquad \text{(A.2.7)}
\end{aligned}$$

where f' is given as in equation 5.3.15.

We note the identity $\mathbf{F}_n = P_\Gamma(\mathbf{F}_n) + P_{\nu_1}(\mathbf{F}_n)$ on Γ. After substituting it to the last equation and applying the boundary condition A.2.3 and A.2.4, we have

$$\begin{aligned}
&\int_{\Omega_1} (-\mathbf{F}'_{n1}) \cdot \nabla\phi + \int_{\Omega_2} (-\mathbf{F}'_{n2}) \cdot \nabla\phi \\
&+ \int_\Gamma (-P_\Gamma(\mathbf{F}_{n1}) + P_\Gamma(\mathbf{F}_{n2})) \cdot \nabla_\Gamma\phi \, V_1 \\
&= \int_\Gamma (f' + fH_1V_1)\,\phi. \qquad \text{(A.2.8)}
\end{aligned}$$

Next we apply integration by parts to the domain integral and have

$$\begin{aligned}
&\int_{\Omega_1} (\nabla \cdot \mathbf{F}'_{n1})\,\phi + \int_{\Omega_2} (\nabla \cdot \mathbf{F}'_{n2})\,\phi \\
&- \int_{\partial\Omega_1} \mathbf{F}'_{n1} \cdot \nu_1\phi - \int_{\partial\Omega_2} \mathbf{F}'_{n2} \cdot \nu_2\phi \\
&= \int_\Gamma P_\Gamma\,(\mathbf{F}_{n1} - \mathbf{F}_n 2) \cdot \nabla_\Gamma\phi \; V_1 + \int_\Gamma (f' + fH_1V_1)\,\phi. \qquad \text{(A.2.9)}
\end{aligned}$$

Then, we apply integration by parts formula 4.1.7 on Γ

$$\begin{aligned}
&\int_{\Omega_1} (\nabla \cdot \mathbf{F}'_{n1})\,\phi + \int_{\Omega_2} (\nabla \cdot \mathbf{F}'_{n2})\,\phi \\
&- \int_{\partial\Omega_1} \mathbf{F}'_{n1} \cdot \nu_1\phi - \int_{\partial\Omega_2} \mathbf{F}'_{n2} \cdot \nu_2\phi \\
&= \int_\Gamma \{-\mathrm{div}_\Gamma\,[V_1\; P_\Gamma\,(\mathbf{F}_{n1} - \mathbf{F}_{n2})] + (f' + fH_1V_1)\}\,\phi. \qquad \text{(A.2.10)}
\end{aligned}$$

Finally, we obtain the PDE by observing that ϕ was arbitrarily chosen. We summarize the shape sensitivity PDE of n-equation below

$$\nabla \cdot \mathbf{F}'_n = 0 \qquad \Omega_1 \cup \Omega_2 \qquad \text{(A.2.11)}$$

$$n' = 0 \qquad \Gamma_D \qquad \text{(A.2.12)}$$

$$\mathbf{F}'_n \cdot \nu = 0 \qquad \Gamma_N \qquad \text{(A.2.13)}$$

$$n'_1 + \frac{\partial n_1}{\partial \nu_1} V_1 = n'_2 + \frac{\partial n_2}{\partial \nu_1} V_1 \qquad \Gamma \qquad \text{(A.2.14)}$$

$$\begin{aligned} -\mathbf{F}'_{n1} \cdot \nu_1 - \mathbf{F}'_{n2} \cdot \nu_2 = &-\mathrm{div}_\Gamma \left[V_1 \, P_\Gamma \left(\mathbf{F}_{n1} - \mathbf{F}_{n2} \right) \right] \\ &+ f' + f H_1 V_1 \qquad \Gamma \qquad \text{(A.2.15)} \end{aligned}$$

A.3 Shape sensitivity of p-equation

The boundary value problem of hole density is

$$\begin{cases} \nabla \cdot \mathbf{F}_p = 0 \\ \mathbf{F}_p = -\mu_p (\nabla p + p \nabla \psi) \end{cases} \qquad \Omega_1 \cup \Omega_2 \qquad \text{(A.3.1)}$$

$$p = p_D \qquad \Gamma_{D1} \cup \Gamma_{D2} \qquad \text{(A.3.2)}$$

$$\mathbf{F}_p \cdot \nu = 0 \qquad \Gamma_{N1} \cup \Gamma_{N2} \qquad \text{(A.3.3)}$$

$$\begin{cases} p_1 = p_2 \\ \mathbf{F}_{p1} \cdot \nu_1 + \mathbf{F}_{p2} \cdot \nu_2 = -f \end{cases} \qquad \Gamma \qquad \text{(A.3.4)}$$

where μ_p is the mobility of holes.

Recalling the dependence of μ_p on $\nabla \psi$, we compute the shape derivative of $\mathbf{F}_p$

by the chain rule.

$$\mathbf{F}'_p = -\mu_p \left(\nabla p' + p' \nabla \psi\right) - \mu_p p \nabla \psi' - \left(\nabla p + p \nabla \psi\right) \frac{\partial \mu_p}{\partial (\nabla \psi)} \cdot \nabla \psi' \tag{A.3.5}$$

where $\frac{\partial \mu_p}{\partial (\nabla \psi)}$ denotes the gradient of μ_p with respect to $\nabla \psi$. For convenience, we will use $\mathbf{F}'_p$ for the sensitivity of hole flux in the derivation below and replace $\mathbf{F}'_p$ by A.3.5 only when necessary.

The derivation of the shape sensitivity of p-equation is identical to that of the n-equation; we only need to replace $\mathbf{F}_n$ with $\mathbf{F}_p$. Hence we write down the shape sensitivity of p-equation

$$\nabla \cdot \mathbf{F}'_p = 0 \qquad \Omega_1 \cup \Omega_2 \tag{A.3.6}$$

$$p' = 0 \qquad \Gamma_D \tag{A.3.7}$$

$$\mathbf{F}'_p \cdot \nu = 0 \qquad \Gamma_N \tag{A.3.8}$$

$$p'_1 + \frac{\partial p_1}{\partial \nu_1} V_1 = p'_2 + \frac{\partial p_2}{\partial \nu_1} V_1 \qquad \Gamma \tag{A.3.9}$$

$$\begin{aligned} -\mathbf{F}'_{p1} \cdot \nu_1 - \mathbf{F}'_{p2} \cdot \nu_2 = &-\mathrm{div}_\Gamma \left[V_1 \, P_\Gamma \left(\mathbf{F}_{p1} - \mathbf{F}_{p2}\right)\right] \\ &+ f' + f H_1 V_1 \qquad \Gamma \end{aligned} \tag{A.3.10}$$

A.4 Shape sensitivity of u-equation

The boundary value problem of exciton is

$$\begin{cases} \nabla \cdot \mathbf{F}_u = G - d_u u \\ \mathbf{F}_u = -\mu_u \nabla u \end{cases} \qquad \Omega_1 \cup \Omega_2 \tag{A.4.1}$$

$$u = u_D \qquad \Gamma_{D1} \cup \Gamma_{D2} \tag{A.4.2}$$

$$\mathbf{F}_u \cdot \nu = 0 \qquad \Gamma_{N1} \cup \Gamma_{N2} \tag{A.4.3}$$

$$\begin{cases} u_1 = u_2 \\ \mathbf{F}_{u1} \cdot \nu_1 + \mathbf{F}_{u2} \cdot \nu_2 = f \end{cases} \qquad \Gamma \tag{A.4.4}$$

The shape derivative of the exciton flux is very simple, since μ_u has no dependence on other unknowns. Hence we have

$$\mathbf{F}'_u = -\mu_u \nabla u' \tag{A.4.5}$$

The derivation of shape sensitivity of u-equation is not identical but similar to that of the n-equation. Let ϕ be a test function that is 0 on Dirichlet boundaries $\Gamma_D = \Gamma_{D1} \cup \Gamma_{D2}$. We multiply ϕ on both sides of the u-equation, apply integration by parts, and make use of A.4.3 and A.4.4 to obtain

$$\int_{\Omega_1} (-\mathbf{F}_{u1}) \cdot \nabla\phi + \int_{\Omega_2} (-\mathbf{F}_{u2}) \cdot \nabla\phi + \int_{\Omega} d_u u\phi = \int_{\Omega} G\phi - \int_{\Gamma} f\phi \tag{A.4.6}$$

We then take shape derivative on both sides, applying 4.5.3, 4.5.4, and 4.5.5

$$\begin{aligned}
&\int_{\Omega_1} (-\mathbf{F}'_{u1}) \cdot \nabla\phi + \int_{\partial\Omega_1} (-\mathbf{F}_{u1}) \cdot \nabla\phi V_1 \\
&+ \int_{\Omega_2} (-\mathbf{F}'_{u2}) \cdot \nabla\phi + \int_{\partial\Omega_2} (-\mathbf{F}_{u2}) \cdot \nabla\phi V_2 \\
&+ \int_{\Omega} d_u u'\phi \\
=& - \int_{\Gamma} \left(f'\phi + f\frac{\partial\phi}{\partial\nu_1} V_1 \right) - \int_{\Gamma} f H_1 V_1 \phi
\end{aligned} \tag{A.4.7}$$

where we have used the boundary condition of u across the interface and the fact that G does not depend on the shape.

What remains is again very similar to the steps of deriving the sensitivity of n-equation. Following exactly the same route map, we can obtain the sensitivity of u-equation, which is summarized below

$$\nabla \cdot \mathbf{F}'_u + d_u u' = 0 \qquad \Omega_1 \cup \Omega_2 \tag{A.4.8}$$

$$u' = 0 \qquad \Gamma_D \tag{A.4.9}$$

$$\mathbf{F}'_u \cdot \nu = 0 \qquad \Gamma_N \tag{A.4.10}$$

$$u'_1 + \frac{\partial u_1}{\partial\nu_1} V_1 = u'_2 + \frac{\partial u_2}{\partial\nu_1} V_1 \qquad \Gamma \tag{A.4.11}$$

$$\begin{aligned}
-\mathbf{F}'_{u1} \cdot \nu_1 - \mathbf{F}'_{u2} \cdot \nu_2 &= -\mathrm{div}_\Gamma \left[V_1 \, P_\Gamma \left(\mathbf{F}_{u1} - \mathbf{F}_{u2} \right) \right] \\
&\quad - \left[f' + f H_1 V_1 \right] \qquad \Gamma
\end{aligned} \tag{A.4.12}$$

Appendix B

Adjoint Equations of Shape Optimization for the First Drift-Diffusion Model

In this chapter, we derive the adjoint equations for computing the shape gradient in Section 5.4.

- **Step 1: Integration by parts for** (L_ψ, L_n, L_p, L_u)

  In this part, we apply integration by parts on each of (L_ψ, L_n, L_p, L_u). During the process of integration by parts, the boundary conditions for (ψ', n', p', u') on $\Gamma_D \cup \Gamma_N$ as well as Γ will be applied; cf. Section 5.3.5.

–

$$
\begin{aligned}
L_\psi &= \int_{\Omega_1 \cup \Omega_2} \left(-\lambda^2 \nabla \cdot (\epsilon \nabla \psi') - p' + n'\right) \xi_\psi \\
&= \int_{\Omega_1 \cup \Omega_2} \left[-\lambda^2 \nabla \cdot (\epsilon \nabla \xi_\psi)\right] + (-\xi_p) p' + \xi_\psi n' \\
&\quad + \int_{\Gamma_D} \left(-\lambda^2 \epsilon \frac{\partial \psi'}{\partial \nu}\right) \xi_\psi \\
&\quad + \int_{\Gamma_N} \lambda^2 \epsilon \psi' \frac{\partial \xi_\psi}{\partial \nu} \\
&\quad + \int_{\Gamma} \lambda^2 \left[-\epsilon_1 \frac{\partial \psi_1'}{\partial \nu_1} \xi_{\psi 1} - \epsilon_2 \frac{\partial \psi_2'}{\partial \nu_2} \xi_{\psi 2}\right] + \lambda^2 \left[\epsilon_1 \psi_1' \frac{\partial \xi_{\psi 1}}{\partial \nu_1} + \epsilon_2 \psi_2' \frac{\partial \xi_{\psi 2}}{\partial \nu_2}\right]
\end{aligned}
\tag{B.0.1}
$$

– The expression of $\mathbf{F}'_n$ from Section 5.3.5 is

$$
\begin{aligned}
\mathbf{F}'_n &= -\mu_n \left(\nabla n' - n' \nabla \psi\right) \\
&\quad + \mu_n n \nabla \psi' - \left(\nabla n - n \nabla \psi\right) \frac{\partial \mu_n}{\partial (\nabla \psi)} \cdot \nabla \psi'
\end{aligned}
\tag{B.0.2}
$$

We replace it into L_n and apply integration by parts and the boundary

conditions for $\mathbf{F}'_n$ and n':

$$
\begin{aligned}
L_n &= \int_{\Omega_1 \cup \Omega_2} (\nabla \cdot \mathbf{F}'_n)\, \xi_n \\
&= \int_{\Omega_1 \cup \Omega_2} \left[-\nabla \cdot (\mu_n \nabla \xi_n) - \mu_n \nabla \psi \cdot \nabla \xi_n \right] n' \\
&\qquad + \left[\nabla \cdot (\mu_n n \nabla \xi_n) - \nabla \cdot \left(\nabla \xi_n \cdot (\nabla n - n \nabla \psi) \frac{\partial \mu_n}{\partial (\nabla \psi)} \right) \right] \psi' \\
&\quad + \int_{\Gamma_{D1}} \mathbf{F}'_{n1} \cdot \nu_1 \xi_{n1} \\
&\quad + \int_{\Gamma_{D2}} \mathbf{F}'_{n2} \cdot \nu_2 \xi_{n2} \\
&\quad + \int_{\Gamma_N} (\mu_n \nabla \xi_n \cdot \nu)\, n' \\
&\qquad + \left[-\mu_n n \nabla \xi_n \cdot \nu + \nabla \xi_n \cdot (\nabla n - n \nabla \psi) \frac{\partial \mu_n}{\partial (\nabla \psi)} \cdot \nu \right] \psi' \\
&\quad + \int_{\Gamma} \mathbf{F}'_{n1} \cdot \nu_1\, \xi_{n1} + \mathbf{F}'_{n2} \cdot \nu_2\, \xi_{n2} \\
&\qquad + (\mu_{n1} \nabla \xi_{n1} \cdot \nu_1)\, n'_1 + (\mu_{n2} \nabla \xi_{n2} \cdot \nu_2)\, n'_2 \\
&\qquad + \left[-(\mu_{n1} n_1 \nabla \xi_{n1} \cdot \nu_1) + \nabla \xi_{n1} \cdot (\nabla n_1 - n_1 \nabla \psi_1) \frac{\partial \mu_{n1}}{\partial (\nabla \psi)} \cdot \nu_1 \right] \psi'_1 \\
&\qquad + \left[-(\mu_{n2} n_2 \nabla \xi_{n2} \cdot \nu_2) + \nabla \xi_{n2} \cdot (\nabla n_2 - n_2 \nabla \psi_2) \frac{\partial \mu_{n2}}{\partial (\nabla \psi)} \cdot \nu_2 \right] \psi'_2
\end{aligned}
\tag{B.0.3}
$$

– The expression of $\mathbf{F}'_p$ from Section 5.3.5 is

$$
\begin{aligned}
\mathbf{F}'_p &= -\mu_p \left(\nabla p' + p' \nabla \psi \right) \\
&\qquad - \mu_p p \nabla \psi' - (\nabla p + p \nabla \psi) \frac{\partial \mu_p}{\partial (\nabla \psi)} \cdot \nabla \psi'
\end{aligned}
\tag{B.0.4}
$$

We replace it to L_p and apply integration by parts and the boundary

conditions for $\mathbf{F}'_p$ and p':

$$
\begin{aligned}
L_p &= \int_{\Omega_1 \cup \Omega_2} \left(\nabla \cdot \mathbf{F}'_p\right) \xi_p \\
&= \int_{\Omega_1 \cup \Omega_2} \left[-\nabla \cdot (\mu_p \nabla \xi_p) + \mu_p \nabla \psi \cdot \nabla \xi_p\right] p' \\
&\qquad + \left[-\nabla \cdot (\mu_p p \nabla \xi_p) - \nabla \cdot \left(\nabla \xi_p \cdot (\nabla p + p \nabla \psi) \frac{\partial \mu_p}{\partial (\nabla \psi)}\right)\right] \psi' \\
&\quad + \int_{\Gamma_{D1}} \mathbf{F}'_{p1} \cdot \nu_1 \, \xi_{p1} \\
&\quad + \int_{\Gamma_{D2}} \mathbf{F}'_{p2} \cdot \nu_2 \, \xi_{p2} \\
&\quad + \int_{\Gamma_N} (\mu_p \nabla \xi_p \cdot \nu) \, p' \\
&\qquad + \left[\mu_p p \nabla \xi_p \cdot \nu + \nabla \xi_p \cdot (\nabla p + p \nabla \psi) \frac{\partial \mu_p}{\partial (\nabla \psi)} \cdot \nu\right] \psi' \\
&\quad + \int_{\Gamma} \mathbf{F}'_{p1} \cdot \nu_1 \, \xi_{p1} + \mathbf{F}'_{p2} \cdot \nu_2 \, \xi_{p2} \\
&\qquad + (\mu_{p1} \nabla \xi_{p1} \cdot \nu_1) \, p'_1 + (\mu_{p2} \nabla \xi_{p2} \cdot \nu_2) \, p'_2 \\
&\qquad + \left[(\mu_{p1} p_1 \nabla \xi_{p1} \cdot \nu_1) + \nabla \xi_{p1} \cdot (\nabla p_1 + p_1 \nabla \psi_1) \frac{\partial \mu_{p1}}{\partial (\nabla \psi)} \cdot \nu_1\right] \psi'_1 \\
&\qquad + \left[(\mu_{p2} p_2 \nabla \xi_{p2} \cdot \nu_2) + \nabla \xi_{p2} \cdot (\nabla p_2 + p_2 \nabla \psi_2) \frac{\partial \mu_{p2}}{\partial (\nabla \psi)} \cdot \nu_2\right] \psi'_2
\end{aligned}
\tag{B.0.5}
$$

–

$$
\begin{aligned}
L_u &= \int_{\Omega_1 \cup \Omega_2} \left(\nabla \cdot \mathbf{F}'_u + d_u u'\right) \xi_u \\
&= \int_{\Omega_1 \cup \Omega_2} \left[-\nabla \cdot (\mu_u \nabla \xi_u) + d_u \xi_u\right] u' \\
&\quad + \int_{\Gamma_{D1}} -\mu_{u1} \nabla u'_1 \cdot \nu_1 \xi_{u1} + \int_{\Gamma_{D2}} -\mu_{u2} \nabla u'_2 \cdot \nu_2 \xi_{u2} \\
&\quad + \int_{\Gamma_N} \mu_u \nabla \xi_u \cdot \nu u' \\
&\quad + \int_{\Gamma} \mu_{u1} \nabla \xi_{u1} \cdot \nu_1 \; u'_1 + \mu_{u2} \nabla \xi_{u2} \cdot \nu_2 \; u'_2 \\
&\qquad - \mu_{u1} \nabla u'_1 \cdot \nu_1 \; \xi_{u1} - \mu_{u2} \nabla u'_2 \cdot \nu_2 \; \xi_{u2}
\end{aligned} \tag{B.0.6}
$$

- **Step 2: group integrals on the same domain**

  In this step, we will re-arrange the terms of $L = J' + L_\psi + L_n + L_p + L_u$ so that the integrals on the same domain are put together.

  – Integration on $\Omega_1 \cup \Omega_2$

$$
\begin{aligned}
L_{\Omega_1\cup\Omega_2} = \int_{\Omega_1\cup\Omega_2} & \left[-\lambda^2\nabla\cdot(\epsilon\nabla\xi_\psi)\right]\psi' + (-\xi_\psi)\,p' + \xi_\psi\,n' \\
& + \left[-\nabla\cdot(\mu_n\nabla\xi_n) - \mu_n\nabla\psi\cdot\nabla\xi_n\right]n' \\
& + \left[\nabla\cdot(\mu_n n\nabla\xi_n) - \nabla\cdot\left(\nabla\xi_n\cdot(\nabla n - n\nabla\psi)\,\frac{\partial\mu_n}{\partial(\nabla\psi)}\right)\right]\psi' \\
& + \left[-\nabla\cdot(\mu_p\nabla\xi_p) + \mu_p\nabla\psi\cdot\nabla\xi_p\right]p' \\
& + \left[-\nabla\cdot(\mu_p p\nabla\xi_p) - \nabla\cdot\left(\nabla\xi_p\cdot(\nabla p + p\nabla\psi)\,\frac{\partial\mu_p}{\partial(\nabla\psi)}\right)\right]\psi' \\
& + \left[-\nabla\cdot(\mu_u\nabla\xi_u) + d_u\xi_u\right]u'
\end{aligned}
$$

$$
\begin{aligned}
= \int_{\Omega_1\cup\Omega_2} & \left[-\lambda^2\nabla\cdot(\epsilon\nabla\xi_\psi)\right. \\
& + \nabla\cdot(\mu_n n\nabla\xi_n) - \nabla\cdot\left(\nabla\xi_n\cdot(\nabla n - n\nabla\psi)\,\frac{\partial\mu_n}{\partial(\nabla\psi)}\right) \\
& \left.-\nabla\cdot(\mu_p p\nabla\xi_p) - \nabla\cdot\left(\nabla\xi_p\cdot(\nabla p + p\nabla\psi)\,\frac{\partial\mu_p}{\partial(\nabla\psi)}\right)\right]\psi' \\
& + \left[\,\xi_\psi - \nabla\cdot(\mu_n\nabla\xi_n) - \mu_n\nabla\psi\cdot\nabla\xi_n\,\right]n' \\
& + \left[\,-\xi_\psi - \nabla\cdot(\mu_p\nabla\xi_p) + \mu_p\nabla\psi\cdot\nabla\xi_p\,\right]p' \\
& + \left[\,-\nabla\cdot(\mu_u\nabla\xi_u) + d_u\xi_u\,\right]u' \qquad \text{(B.0.7)}
\end{aligned}
$$

– Integration on $\Gamma_{D1}\cup\Gamma_{D2}$

$$L_{\Gamma_{D1}} = \int_{\Gamma_{D1}} \left(-\mathbf{F}'_{p1} \cdot \nu_1 + \mathbf{F}'_{n1} \cdot \nu_1\right) + \int_{\Gamma_{D1}} \left[\left(-\lambda^2 \epsilon_1 \frac{\partial \psi'_1}{\partial \nu_1}\right) \xi_{\psi 1} + \left(\mathbf{F}'_{n1} \cdot \nu_1\right) \xi_{n1} + \left(\mathbf{F}'_{p1} \cdot \nu_1\right) \xi_{p1} - \left(\mu_{u1} \frac{\partial u1'}{\partial \nu_1}\right) \xi_{u1}\right] \tag{B.0.8}$$

$$L_{\Gamma_{D2}} = \int_{\Gamma_{D2}} \left[\left(-\lambda^2 \epsilon_2 \frac{\partial \psi'_2}{\partial \nu_2}\right) \xi_{\psi 2} + \left(\mathbf{F}'_{n2} \cdot \nu_2\right) \xi_{n2} + \left(\mathbf{F}'_{p2} \cdot \nu_2\right) \xi_{p2} - \left(\mu_{u2} \frac{\partial u2'}{\partial \nu_2}\right) \xi_{u2}\right] \tag{B.0.9}$$

Note that we differentiate the $L_{\Gamma_{D1}}$ and $L_{\Gamma_{D2}}$ because that the photocurrent is defined on Γ_{D1} only and therefore the expression of $L_{\Gamma_{D1}}$ differs from that of $L_{\Gamma_{D2}}$.

– Integration on Γ_N

$$
\begin{aligned}
L_{\Gamma_N} = \int_{\Gamma_N} & \left(\lambda^2\epsilon\frac{\partial\xi_\psi}{\partial\nu}\right)\ \psi' \\
& + \left(\mu_n\frac{\partial\xi_n}{\partial\nu}\right)\ n' + \left[-\mu_n n\frac{\partial\xi_n}{\partial\nu} + \nabla\xi_n\cdot(\nabla n - n\nabla\psi)\frac{\partial\mu_n}{\partial(\nabla\psi)}\cdot\nu\right]\psi' \\
& + \left(\mu_p\frac{\partial\xi_p}{\partial\nu}\right)\ p' + \left[\ \ \mu_p p\frac{\partial\xi_p}{\partial\nu} + \nabla\xi_p\cdot(\nabla p + p\nabla\psi)\frac{\partial\mu_p}{\partial(\nabla\psi)}\cdot\nu\right]\ \psi' \\
& + \left(\mu_u\frac{\xi_u}{\nu}\right)\ u'
\end{aligned}
$$

$$
\begin{aligned}
= \int_{\Gamma_N} \psi' \Bigg[& \lambda^2\epsilon\frac{\partial\xi_\psi}{\partial\nu} \\
& - \mu_n n\frac{\partial\xi_n}{\partial\nu} + \nabla\xi_n\cdot(\nabla n - n\nabla\psi)\frac{\partial\mu_n}{\partial(\nabla\psi)}\cdot\nu \\
& + \mu_p p\frac{\partial\xi_p}{\partial\nu} + \nabla\xi_p\cdot(\nabla p + p\nabla\psi)\frac{\partial\mu_p}{\partial(\nabla\psi)}\cdot\nu\Bigg] \\
& + n'\left(\mu_n\frac{\xi_n}{\nu}\right) \\
& + p'\left(\mu_p\frac{\xi_p}{\nu}\right) \\
& + u'\left(\mu_u\frac{\xi_u}{\nu}\right)
\end{aligned}
\tag{B.0.10}
$$

– Integration on interface Γ

The details of the derivation for the integral on Γ is omitted, but the major steps are outlined below:

1. First we replace all shape derivatives with subscript "2" by their counterparts with subscript "1". To achieve this, we apply the boundary conditions on the interface for the shape derivatives (ψ', n', p', u'); cf. Section 5.3.5.

2. After applying the boundary conditions of (ψ', n', p', u') on Γ, we observe the presence of integrals whose integrands contain the shape derivative of interface reaction rate f'. Therefore, we replace f' by its expression in formula 5.3.15. Also we apply the formula 4.4.8 and 4.4.9 for ν_1' and H_1'. All these operations convert the orginal integral of f' to integrals of terms containing ψ', n', p', u' and V_1.

3. Then we group integrals on Γ by their integrands. For example, we put all integrals whose integrands contain ψ_1' into one integral. The same is done for all other types of integrands.

4. Finally, we apply the tangential Green's formula 4.1.7 to obtain the form that we expected.

After going through these steps, we arrive at the formula of integral on Γ as below:

$$\begin{aligned} L_\Gamma = \quad & L_\Gamma(\psi_1') + L_\Gamma(n_1') + L_\Gamma(p_1') + L_\Gamma(u_1') \\ & + L_\Gamma(\frac{\partial \psi_1'}{\partial \nu_1}) + L_\Gamma(\mathbf{F}'_{n1}) + L_\Gamma(\mathbf{F}'_{p1}) + L_\Gamma(\frac{\partial u_1'}{\partial \nu_1}) \\ & + L_\Gamma(V_1) \end{aligned} \tag{B.0.11}$$

where

*

$$
\begin{aligned}
L_\Gamma(\psi_1') = \int_\Gamma \psi_1' \Bigg\{ & \lambda^2 \left(\epsilon_1 \frac{\partial \xi_{\psi 1}}{\partial \nu_1} + \epsilon_2 \frac{\partial \xi_{\psi 2}}{\partial \nu_2} \right) \\
& - \mu_{n1} n_1 \frac{\partial \xi_{n1}}{\partial \nu_1} - \mu_{n2} n_2 \frac{\partial \xi_{n2}}{\partial \nu_2} \\
& + \nabla \xi_{n1} \cdot (\nabla n_1 - n_1 \nabla \psi_1) \frac{\partial \mu_{n1}}{\partial (\nabla \psi)} \cdot \nu_1 \\
& + \nabla \xi_{n2} \cdot (\nabla n_2 - n_2 \nabla \psi_2) \frac{\partial \mu_{n2}}{\partial (\nabla \psi)} \cdot \nu_2 \\
& + \mu_{p1} p_1 \frac{\partial \xi_{p1}}{\partial \nu_1} + \mu_{p2} p_2 \frac{\partial \xi_{p2}}{\partial \nu_2} \\
& + \nabla \xi_{p1} \cdot (\nabla p_1 + p_1 \nabla \psi_1) \frac{\partial \mu_{p1}}{\partial (\nabla \psi)} \cdot \nu_1 \\
& + \nabla \xi_{p2} \cdot (\nabla p_2 + p_2 \nabla \psi_2) \frac{\partial \mu_{p2}}{\partial (\nabla \psi)} \cdot \nu_2 \\
& - \mathrm{div}_\Gamma \left[(\xi_{u2} - \xi_{n2} - \xi_{p2}) P_\Gamma \left(\frac{\partial f}{\partial (\nabla \psi)} \right) \right] \Bigg\}
\end{aligned}
\tag{B.0.12}
$$

*

$$
\begin{aligned}
L_\Gamma(n_1') = \int_\Gamma n_1' \Bigg\{ & \mu_{n1} \frac{\partial \xi_{n1}}{\partial \nu_1} + \mu_{n2} \frac{\partial \xi_{n2}}{\partial \nu_2} \\
& + (\xi_{u2} - \xi_{n2} - \xi_{p2}) \frac{\partial f}{\partial n} \Bigg\}
\end{aligned}
\tag{B.0.13}
$$

*

$$
\begin{aligned}
L_\Gamma(p_1') = \int_\Gamma p_1' \Bigg\{ & \mu_{p1} \frac{\partial \xi_{p1}}{\partial \nu_1} + \mu_{p2} \frac{\partial \xi_{p2}}{\partial \nu_2} \\
& + (\xi_{u2} - \xi_{n2} - \xi_{p2}) \frac{\partial f}{\partial p} \Bigg\}
\end{aligned}
\tag{B.0.14}
$$

*

$$L_\Gamma(u_1') = \int_\Gamma u_1' \left\{ \mu_{u1} \frac{\partial \xi_{u1}}{\partial \nu_1} + \mu_{u2} \frac{\partial \xi_{u2}}{\partial \nu_2} + (\xi_{u2} - \xi_{n2} - \xi_{p2}) \frac{\partial f}{\partial u} \right\} \tag{B.0.15}$$

*

$$L_\Gamma(\frac{\partial \psi_1'}{\partial \nu_1}) = \int_\Gamma \frac{\partial \psi_1'}{\partial \nu_1} \left\{ \lambda^2 \left(-\epsilon_1 \xi_{\psi 1} + \epsilon_2 \xi_{\psi 2} \right) + \left(\xi_{u2} - \xi_{n2} - \xi_{p2} \right) P_{\nu_1} \left(\frac{\partial f}{\partial (\nabla \psi)} \right) \right\} \tag{B.0.16}$$

*

$$L_\Gamma(\mathbf{F}'_{n1}) = \int_\Gamma \mathbf{F}'_{n1} \cdot \nu_1 (\xi_{n1} - \xi_{n2}) \tag{B.0.17}$$

*

$$L_\Gamma(\mathbf{F}'_{p1}) = \int_\Gamma \mathbf{F}'_{p1} \cdot \nu_1 (\xi_{p1} - \xi_{p2}) \tag{B.0.18}$$

*

$$L_\Gamma(\frac{\partial u_1'}{\partial \nu_1}) = \int_\Gamma \frac{\partial u_1'}{\partial \nu_1} \, \mu_{u1} (\xi_{u2} - \xi_{u1}) \tag{B.0.19}$$

*

$$L_\Gamma(V_1) = \int_\Gamma G \, V_1 \tag{B.0.20}$$

and

$$
\begin{aligned}
G = (-\lambda^2)\xi_{\psi 2} \Bigg\{ & \operatorname{div}_\Gamma \left[(\epsilon_1 \epsilon_2) \nabla_\Gamma \psi_1 \right] + \frac{\partial}{\partial \nu_1} \left[(\epsilon_1 - \epsilon_2) \frac{\partial \psi_1}{\partial \nu_1} \right] + (\epsilon_1 - \epsilon_2) \frac{\partial \psi_1}{\partial \nu_1} H_1 \Bigg\} \\
& - \mu_{n2} \frac{\partial \xi_{n2}}{\partial \nu_1} \left(\frac{\partial n_1}{\partial \nu_1} - \frac{\partial n_2}{\partial \nu_1} \right) \\
& - \nabla_\Gamma \xi_{n2} \cdot P_\Gamma \left(\mathbf{F}_{n1} - \mathbf{F}_{n2} \right) \\
& - \mu_{p2} \frac{\partial \xi_{p2}}{\partial \nu_1} \left(\frac{\partial p_1}{\partial \nu_1} - \frac{\partial p_2}{\partial \nu_1} \right) \\
& - \nabla_\Gamma \xi_{p2} \cdot P_\Gamma \left(\mathbf{F}_{p1} - \mathbf{F}_{p2} \right) \\
& - \mu_{u2} \frac{\partial \xi_{u2}}{\partial \nu_1} \left(\frac{\partial u_1}{\partial \nu_1} - \frac{\partial u_2}{\partial \nu_1} \right) \\
& - \nabla_\Gamma \xi_{u2} \cdot P_\Gamma \left(\mathbf{F}_{u1} - \mathbf{F}_{u2} \right) \\
& + \operatorname{div}_\Gamma \left[(\xi_{u2} - \xi_{n2} - \xi_{p2}) P_\Gamma \left(\frac{\partial f}{\partial \mathbf{y}} \right) \right] \\
& - \triangle_\Gamma \left[(\xi_{u2} - \xi_{n2} - \xi_{p2}) \frac{\partial f}{\partial H_1} \right] \\
& + (\xi_{u2} - \xi_{n2} - \xi_{p2}) \left[\frac{\partial f}{\partial n} \frac{\partial n_1}{\partial \nu_1} + \frac{\partial f}{\partial p} \frac{\partial p_1}{\partial \nu_1} + \frac{\partial f}{\partial u} \frac{\partial u_1}{\partial \nu_1} \right] \\
& + (\xi_{u2} - \xi_{n2} - \xi_{p2}) \left(\frac{\partial f}{\partial (\nabla \psi)} \cdot D^2 \psi \cdot \nu_1 + \frac{\partial f}{\partial H_1} \frac{\partial H_1}{\partial \nu_1} + f H_1 \right)
\end{aligned}
\tag{B.0.21}
$$

- **Step 3: Derive the adjoint equations and the shape gradient**

  To summarize the results of previous steps, we re-write the Lagrangian functional L in the following way:

$$
\begin{aligned}
L &= J' + L_\psi + L_n + L_p + L_u \\
&= L_{\Omega_1 \cup \Omega_2} + L_{\Gamma_{D1}} + L_{\Gamma_{D2}} + L_{\Gamma_N} + L_\Gamma
\end{aligned}
\tag{B.0.22}
$$

Thus the adjoint equations is obtained by letting the integrals that contain ψ', n', p', u' be 0. Hence we have the system of adjoint equations for the adjoint variables $\Xi = (\xi_\psi, \xi_n, \xi_p, \xi_u)$:

– **In** $\Omega_1 \cup \Omega_2$

$$\begin{aligned} &-\lambda^2 \nabla \cdot (\epsilon \nabla \xi_\psi) \\ &+ \nabla \cdot (\mu_n n \nabla \xi_n) - \nabla \cdot \left(\nabla \xi_n \cdot (\nabla n - n \nabla \psi) \frac{\partial \mu_n}{\partial (\nabla \psi)} \right) \\ &- \nabla \cdot (\mu_p p \nabla \xi_p) - \nabla \cdot \left(\nabla \xi_p \cdot (\nabla p + p \nabla \psi) \frac{\partial \mu_p}{\partial (\nabla \psi)} \right) \quad = 0 \end{aligned} \tag{B.0.23}$$

$$\xi_\psi - \nabla \cdot (\mu_n \nabla \xi_n) - \mu_n \nabla \psi \cdot \nabla \xi_n \quad = 0 \tag{B.0.24}$$

$$-\xi_\psi - \nabla \cdot (\mu_p \nabla \xi_p) + \mu_p \nabla \psi \cdot \nabla \xi_p \quad = 0 \tag{B.0.25}$$

$$-\nabla \cdot (\mu_u \nabla \xi_u) + d_u \xi_u \quad = 0 \tag{B.0.26}$$

– **On** Γ_{D1}

$$\xi_{\psi 1} = 0 \tag{B.0.27}$$

$$\xi_{n1} = 1 \tag{B.0.28}$$

$$\xi_{p1} = -1 \tag{B.0.29}$$

$$\xi_{u1} = 0 \tag{B.0.30}$$

– **On** Γ_{D2}

$$\xi_{\psi 2} = 0 \tag{B.0.31}$$

$$\xi_{n2} = 0 \tag{B.0.32}$$

$$\xi_{p2} = 0 \tag{B.0.33}$$

$$\xi_{u2} = 0 \tag{B.0.34}$$

– **On** Γ_N

$$\begin{aligned} &\lambda^2 \epsilon \frac{\partial \xi_\psi}{\partial \nu} \\ &+ \nabla \xi_n \cdot (\nabla n - n \nabla \psi) \frac{\partial \mu_n}{\partial (\nabla \psi)} \cdot \nu \\ &+ \nabla \xi_p \cdot (\nabla p + p \nabla \psi) \frac{\partial \mu_p}{\partial (\nabla \psi)} \cdot \nu = 0 \end{aligned} \tag{B.0.35}$$

$$\frac{\partial \xi_n}{\partial \nu} = 0 \tag{B.0.36}$$

$$\frac{\partial \xi_p}{\partial \nu} = 0 \tag{B.0.37}$$

$$\frac{\partial \xi_u}{\partial \nu} = 0 \tag{B.0.38}$$

– **On** Γ

We have 8 boundary conditions on Γ for the adjoint equations:

*

$$
\begin{aligned}
&\lambda^2 \left(\epsilon_1 \frac{\partial \xi_{\psi 1}}{\partial \nu_1} + \epsilon_2 \frac{\partial \xi_{\psi 2}}{\partial \nu_2} \right) \\
&- \mu_{n1} n_1 \frac{\partial \xi_{n1}}{\partial \nu_1} - \mu_{n2} n_2 \frac{\partial \xi_{n2}}{\partial \nu_2} \\
&+ \nabla \xi_{n1} \cdot (\nabla n_1 - n_1 \nabla \psi_1) \frac{\partial \mu_{n1}}{\partial (\nabla \psi)} \cdot \nu_1 \\
&+ \nabla \xi_{n2} \cdot (\nabla n_2 - n_2 \nabla \psi_2) \frac{\partial \mu_{n2}}{\partial (\nabla \psi)} \cdot \nu_2 \\
&+ \mu_{p1} p_1 \frac{\partial \xi_{p1}}{\partial \nu_1} + \mu_{p2} p_2 \frac{\partial \xi_{p2}}{\partial \nu_2} \\
&+ \nabla \xi_{p1} \cdot (\nabla p_1 + p_1 \nabla \psi_1) \frac{\partial \mu_{p1}}{\partial (\nabla \psi)} \cdot \nu_1 \\
&+ \nabla \xi_{p2} \cdot (\nabla p_2 + p_2 \nabla \psi_2) \frac{\partial \mu_{p2}}{\partial (\nabla \psi)} \cdot \nu_2 \\
&- \operatorname{div}_\Gamma \left[(\xi_{u2} - \xi_{n2} - \xi_{p2}) P_\Gamma \left(\frac{\partial f}{\partial (\nabla \psi)} \right) \right] \qquad = 0
\end{aligned}
\tag{B.0.39}
$$

*

$$
\mu_{n1} \frac{\partial \xi_{n1}}{\partial \nu_1} + \mu_{n2} \frac{\partial \xi_{n2}}{\partial \nu_2} + (\xi_{u2} - \xi_{n2} - \xi_{p2}) \frac{\partial f}{\partial n} \qquad = 0 \tag{B.0.40}
$$

*

$$
\mu_{p1} \frac{\partial \xi_{p1}}{\partial \nu_1} + \mu_{p2} \frac{\partial \xi_{p2}}{\partial \nu_2} + (\xi_{u2} - \xi_{n2} - \xi_{p2}) \frac{\partial f}{\partial p} \qquad = 0 \tag{B.0.41}
$$

*

$$
\mu_{u1} \frac{\partial \xi_{u1}}{\partial \nu_1} + \mu_{u2} \frac{\partial \xi_{u2}}{\partial \nu_2} + (\xi_{u2} - \xi_{n2} - \xi_{p2}) \frac{\partial f}{\partial u} \qquad = 0 \tag{B.0.42}
$$

*

$$
\lambda^2 \left(-\epsilon_1 \xi_{\psi 1} + \epsilon_2 \xi_{\psi 2} \right) + (\xi_{u2} - \xi_{n2} - \xi_{p2}) P_{\nu_1} \left(\frac{\partial f}{\partial (\nabla \psi)} \right) \qquad = 0 \tag{B.0.43}
$$

*

$$\xi_{n1} - \xi_{n2} = 0 \tag{B.0.44}$$

*

$$\xi_{p1} - \xi_{p2} = 0 \tag{B.0.45}$$

*

$$\xi_{u2} - \xi_{u1} = 0 \tag{B.0.46}$$

Once the adjoint equations are solved, most terms in the formula of Lagrangian (B.0.22) vanish except for $L_\Gamma(V_1)$. Therefore, one can compute the shape derivative of photocurrent formally

$$\begin{aligned} J'(\mathbf{V}) &= L \\ &= L_\Gamma(V_1) \\ &= \int_\Gamma G\, V_1 \end{aligned} \tag{B.0.47}$$

where G is the shape gradient given in formula B.0.21.

Appendix C

Sensitivity Analysis of Phase-Field Drift-Diffusion Model

In this section, we derive the sensitivity analysis in Section 6.3. For any function b, we let b' denote its directional derivative with respect to the phase field function ϕ in some valid direction ϕ_1, i.e. $b' = b'(\phi; \phi_1)$.

We also recall that we defined δb in Section 6.3 to be its **partial** directional derivative through its explicit dependence on ϕ and $\nabla\phi$. In particular, if b is a physical parameter (such as the mobilities and reaction rates) that depends on the ϕ, $\delta b \neq 0$. On contrast, if b is any of the unknowns $\{\psi, n, p, u\}$, then $\delta b = 0$, since they have no explicit dependence on ϕ; rather their directional derivative is determined by analyzing the sensitivity of drift-diffusion equations, which is the goal in this Appendix.

As in Appendix A, a common observation for all the unknowns in the drift-diffusion model is that $\psi' = n' = p' = u' = 0$ on Γ_D, since the Dirichlet boundary condition is invariant with respect to the change in phase field function. What remains to show is the PDE's for ψ', n', p', u' on Ω and their boundary conditions on Γ_N.

In what follows, we let ξ be an arbitrarily chosen smooth function over Ω such that $\xi = 0$ on Γ_D.

C.1 Shape Sensitivity of ψ-equation

The weak form of equation (6.2.1) is

$$\int_\Omega -\lambda^2 \nabla \cdot (\epsilon \nabla \psi)\, \xi = \int_\Omega (p - n)\, \xi \tag{C.1.1}$$

After applying integration by parts and boundary conditions, we obtain

$$\int_\Omega \lambda^2 \epsilon \nabla \psi \cdot \nabla \xi = \int_\Omega (p - n)\, \xi \tag{C.1.2}$$

We then take derivative of both sides with respect to ϕ

$$\int_\Omega \lambda^2 \epsilon \nabla \psi' \cdot \nabla \xi - \int_\Omega (p' - n')\, \xi = -\int_\Omega \lambda^2 (\delta\epsilon) \nabla \psi \cdot \nabla \xi \tag{C.1.3}$$

Another integration by parts on both sides gives us

$$\int_\Omega \left[-\lambda^2 \nabla \cdot (\epsilon \nabla \psi') - p' + n'\right] \xi + \int_{\Gamma_N} \lambda^2 \epsilon \frac{\partial \psi'}{\partial \nu} \xi = \int_\Omega \lambda^2 \nabla \cdot [(\delta\epsilon) \nabla \psi] \tag{C.1.4}$$

Recalling that ξ is an arbitrarily chosen smooth function, we obtain the sensitivity of ψ-equation

$$-\lambda^2\nabla\cdot(\epsilon\nabla\psi') - p' + n' = \lambda^2\nabla\cdot[(\delta\epsilon)\nabla\psi] \qquad \Omega \qquad \text{(C.1.5)}$$

$$\psi' = 0 \qquad \Gamma_D \qquad \text{(C.1.6)}$$

$$\frac{\partial\psi'}{\partial\nu} = 0 \qquad \Gamma_N \qquad \text{(C.1.7)}$$

C.2 Shape Sensitivity of n-equation

The weak form of n-equation is

$$\int_\Omega \nabla\cdot[-\mu_n(\nabla n - n\nabla\psi)]\,\xi = \int_\Omega [ku - \gamma np]\,\xi \qquad \text{(C.2.1)}$$

We then apply integration by parts and the boundary conditions of n and ψ, we have

$$\int_\Omega \mu_n(\nabla n - n\nabla\psi)\cdot\nabla\xi = \int_\Omega [ku - \gamma np]\,\xi \qquad \text{(C.2.2)}$$

Then we take derivative of both sides with respect to ϕ and obtain

$$\begin{aligned}
&\int_\Omega \left\{(\nabla n - n\nabla\psi)\cdot\nabla\xi\frac{\partial\mu_n}{\partial(\nabla\psi)} - \mu_n n\nabla\xi - \xi\left(u\frac{\partial k}{\partial(\nabla\psi)} - np\frac{\partial\gamma}{\partial(\nabla\psi)}\right)\right\}\cdot\nabla\psi' \\
&+\int_\Omega \{\mu_n(\nabla n' - n'\nabla\psi)\cdot\nabla\xi + \gamma p\xi n'\} \\
&+\int_\Omega \xi\gamma np' \\
&-\int_\Omega \xi k u' \\
&= -\int_\Omega (\delta\mu_n)(\nabla n - n\nabla\psi)\cdot\nabla\xi + \int_\Omega [(\delta k)u - (\delta\gamma)np]\,\xi
\end{aligned} \qquad \text{(C.2.3)}$$

We apply another integration by parts and the boundary conditions of ψ and n, and make use of the fact that ξ is arbitrarily chosen, and finally we have the sensitivity of n-equation

$$
\begin{aligned}
&-\nabla\cdot\left[\frac{\partial\mu_n}{\partial(\nabla\psi)}\cdot\nabla\psi'\left(\nabla n-n\nabla\psi\right)-\mu_n n\nabla\psi'\right]\\
&-\left(u\frac{\partial k}{\partial(\nabla\psi)}-np\frac{\partial\gamma}{\partial(\nabla\psi)}\right)\cdot\nabla\psi'\\
&-\nabla\cdot\left[\mu_n\left(\nabla n'-n'\nabla\psi\right)\right]+\gamma n'p\\
&+\gamma np'\\
&-ku'\\
&=\nabla\cdot\left[(\delta\mu_n)\left(\nabla n-n\nabla\psi\right)\right]+\left[(\delta k)u-(\delta\gamma)np\right] \qquad \Omega \qquad \text{(C.2.4)}
\end{aligned}
$$

$$
n'=0 \qquad \Gamma_D \qquad \text{(C.2.5)}
$$

$$
\frac{\partial n'}{\partial\nu}=0 \qquad \Gamma_N \qquad \text{(C.2.6)}
$$

C.3 Shape Sensitivity of p-equation

The weak form of the p-equation is

$$
\int_\Omega\nabla\cdot\left[-\mu_p\left(\nabla p+p\nabla\psi\right)\right]\xi=\int_\Omega\left[ku-\gamma np\right]\xi \qquad \text{(C.3.1)}
$$

We then apply integration-by-parts and the boundary conditions of ψ and p to obtain

$$
\int_\Omega\mu_p\left(\nabla p+p\nabla\psi\right)\cdot\nabla\xi=\int_\Omega\left[ku-\gamma np\right]\xi \qquad \text{(C.3.2)}
$$

We then take derivative of both sides with respect to ϕ and have

$$\begin{aligned}
&\int_\Omega \left\{ (\nabla p + p\nabla\psi)\cdot\nabla\xi \frac{\partial \mu_p}{\partial(\nabla\psi)} + \mu_p p \nabla\xi - \xi\left(u\frac{\partial k}{\partial(\nabla\psi)} - np\frac{\partial\gamma}{\partial(\nabla\psi)}\right)\right\}\cdot\nabla\psi' \\
&+ \int_\Omega \xi\gamma n' p \\
&+ \int_\Omega \left\{ \mu_p \left(\nabla p' + p'\nabla\psi\right)\cdot\nabla\xi + \xi\gamma n p'\right\} \\
&- \int_\Omega \xi k u' \\
&= -\int_\Omega (\delta\mu_p)\left(\nabla p + p\nabla\psi\right)\cdot\nabla\xi + \int_\Omega \left[(\delta k)u - (\delta\gamma)np\right]\xi
\end{aligned} \tag{C.3.3}$$

We then apply integration-by-parts again as well as the boundary conditions of ψ and p to the formula above. Finally, recalling that ξ is an arbitrary smooth function, we obtain the sensitivity of the p-equation

$$\begin{aligned}
&-\nabla\cdot\left[\frac{\partial\mu_p}{\partial(\nabla\psi)}\cdot\nabla\psi'\left(\nabla p + p\nabla\psi\right) + \mu_p p\nabla\psi'\right] \\
&-\left(u\frac{\partial k}{\partial(\nabla\psi)} - np\frac{\partial\gamma}{\partial(\nabla\psi)}\right)\cdot\nabla\psi' \\
&+\gamma n' p \\
&-\nabla\cdot\left[\mu_p\left(\nabla p' + p'\nabla\psi\right)\right] + \gamma n p' \\
&-ku' \\
&= \nabla\cdot\left[(\delta\mu_p)\left(\nabla p + p\nabla\psi\right)\right] + \left[(\delta k)u - (\delta\gamma)np\right] \qquad \Omega
\end{aligned} \tag{C.3.4}$$

$$p' = 0 \qquad \Gamma_D \tag{C.3.5}$$

$$\frac{\partial p'}{\partial\nu} = 0 \qquad \Gamma_N \tag{C.3.6}$$

C.4 Shape Sensitivity of u-equation

The weak form of the u-equation is

$$\int_\Omega \nabla \cdot (-\mu_u \nabla u)\, \xi + \int_\Omega d_u u \xi = \int_\Omega Q\xi - (ku - \gamma np)\, \xi \tag{C.4.1}$$

We then apply integration-by-parts and the boundary conditions of u to obtain

$$\int_\Omega \mu_u \nabla u \cdot \nabla \xi + \int_\Omega d_u u \xi + \int_\Omega (ku - \gamma np)\, \xi = \int_\Omega Q\xi \tag{C.4.2}$$

We then take derivative of both sides with respect to ϕ and have

$$\begin{aligned}
&\int_\Omega \xi \left(u \frac{\partial k}{\partial(\nabla\psi)} - np \frac{\partial \gamma}{\partial(\nabla\psi)} \right) \cdot \nabla\psi' \\
&- \int_\Omega \xi\gamma n' p \\
&- \int_\Omega \xi\gamma n p' \\
&+ \int_\Omega \mu_u \nabla u' \cdot \nabla\xi + d_u u'\xi + ku'\xi \\
&= - \int_\Omega (\delta\mu_u) \nabla u \cdot \nabla\xi - \int_\Omega (\delta d_u) u\xi - \int_\Omega [(\delta k)u - (\delta\gamma)np]\, \xi
\end{aligned} \tag{C.4.3}$$

We note that the integral of $Q\xi$ is insensitive to ϕ, and therefore its derivative with respective to ϕ is 0.

Finally, we apply integration-by-parts again, noting the boundary conditions of u, and make use of the fact that ξ is an arbitrary smooth function to obtain the

sensitivity of the u-equation

$$\left(u\frac{\partial k}{\partial(\nabla\psi)} - np\frac{\partial\gamma}{\partial(\nabla\psi)}\right)\cdot\nabla\psi'$$

$$-\gamma n'p$$

$$-\gamma np'$$

$$-\nabla\cdot(\mu_u\nabla u') + (d_u + k)u'$$

$$= \nabla\cdot[(\delta\mu_u)\nabla u] - (\delta d_u)u - [(\delta k)u - (\delta\gamma)np] \qquad \Omega \qquad \text{(C.4.4)}$$

$$u' = 0 \qquad \Gamma_D \qquad \text{(C.4.5)}$$

$$\frac{\partial u'}{\partial\nu} = 0 \qquad \Gamma_N \qquad \text{(C.4.6)}$$

Bibliography

[1] J.A. Barker, C.M. Ramsdale, and N.C. Greenham. Modeling the current-voltage characteristics of bilayer polymer photovoltaic devices. *Physical Review B.*, 67:075205, 2003.

[2] Elie Bretin and Valerie Perrier. Phase field method for mean curvature flow with boundary constraints. *ESAIM: Mathematical Modelling and Numerical Analysis*, 46:1509–1526, 2012.

[3] Daniel Brinkman, Klemens Fellner, and Peter A. Markowich. A drift-diffusion-reaction model for excitonic photovoltaic bilayers: Asymptotic analysis and a 2-d hdg finite-element scheme. *Mathematical Models and Methods in Applied Sciences*, 23(5):839, 2013.

[4] M. Burger and R. Pinnau. Fast optimal design for semiconductor devices. *SIAM J. Appl. Math.*, 64:108, 2003.

[5] Gavin A. Buxton and Nigel Clarke. Predicting structure and property relations in polymeric photovoltaic devices. *Physical Review B*, 74:085207.

[6] Gavin A. Buxton and Nigel Clarke. Computer simulation of polymer solar cells. *Modelling Simul. Mater. Sci. Eng.*, 15:13, 2007.

[7] M.C. Delfour and J.-P. Zolesio. *Shapes and Geometries – analysis, differential calculus, and optimization.* Society for Industrial and Applied Mathematics, 2001.

[8] G. Doğan, P. Morin, R.H. Nochetto, and M. Verani. Discrete gradient flows for shape optimization and applications. *Computer Methods Appl. Mech. Engrg.*, 196:3898–3914, 2007.

[9] Günay Doğan and Ricardo H. Nochetto. First variation of the general curvature-dependent surface energy. *ESAIM: Mathematical Modelling and Numerical Analysis*, 46(01):59–79, 2012.

[10] Qiang Du. Phase field calculus, curvature-dependent energies, and vesicle membranes. *Philosophical Magazine*, 91:1:165–181, 2011.

[11] Carlo de Falco, Matteo Porro, Riccardo Sacco, and Maurizio Verri. Multiscale modeling and simulation of organic solar cells. *Comput. Methods Appl. Mech. Engrg.*, 245.

[12] Carlo de Falco, Riccardo Sacco, and Maurizio Verri. Analytical and numerical study of photocurrent transients in organic polymer solar cells.

[13] J. Haslinger and R.A.E. Mäkinen. *Introduction to Shape Optimization:theory, approximation, and computation*. Society for Industrial and Applied Mathematics, 2003.

[14] Michael Hintermüller and Wolfgang Ring. A second order shape optimization approach for image segmentation. *SIAM J. APPL. MATH.*, 64(2):442–467, 2003.

[15] Michael Hinze and René Pinnau. An optimal control approach to semiconductor design. *Mathematical Models and Methods in Applied Sciences*, 12:89–107, 2002.

[16] Michael Hinze and René Pinnau. Mathematical tools in optimal semiconductor design. *Bulletin of the Institute of Mathematics, Academia Sinica (New Series)*, 2(2):569–586, 2007.

[17] Joseph W. Jerome. *Analysis of Charge Transport*. Springer-Verlag, Berlin, Heidelberg, 1996.

[18] Ansgar Jüngel. *Transport Equations for Semiconductors*. Spring-Verlag, Berlin Heidelberg.

[19] L.J.A. Koster, E.C.P. Smits, V.D. Mihailetchi, and P.W.M. Blom. Device model for the operation of polymer/fullerene bulk heterojunction solar cells. *Physical Review B.*, 72:085205.

[20] Jacques Louis Lions. *Optimal control of systems governed by partial differential equations*. Springer-Verlag, 1971.

[21] Peter A. Markowich. *The Stationary Semiconductor Device Equations*. Springer-Verlag, Wien.

[22] Peter A Markowich, Christian A. Ringhofer, and Christian Schmeiser. *Semiconductor Equations*. Springer-Verlag, Wien.

[23] Olivier Pironneau. *Optimal Shape Design for Elliptic Systems*. Springer-Verlag, New York, 1984.

[24] Jan Sokolowski and Jean-Paul Zolesio. *Introduction to Shape Optimization*. Springer-Verlag, 1992.

[25] Akihiro Takezawa, Shinji Nishiwaki, and Mitsuru Kitamura. Shape and topology optimization based on the phase field method and sensitivity analysis. *Journal of Computational Physics*, 229:2697–2718, 2010.

[26] Fredi Tröltzsch. *Optimal control of partial differential equations: theory, methods and applications*, volume 112 of *Graduate studies in mathematics*. American Mathematical Society, 2010.

[27] A. Unterreiter and S. Volkwein. Optimal control of the stationary quantum drift-diffusion model. *COMMUN. MATH. SCI.*, 5(1):85, 2007.

[28] Wikipedia. Solar cell efficiency — Wikipedia, the free encyclopedia, 2013. [Online; accessed 28-Dec-2013].

[29] Jinchao Xu and Ludmil Zikatanov. A monotone finite element scheme for convectiondiffusion equations. *Mathematics of Computation*, 68(228):1429–1446, 1999.

[30] K.G. van der Zee. Introduction to shape differential calculus. *an ECCAM advanced school on* Isogeometric Analysis: Fundamentals and Applications, 2012.